MARINE ECOSYSTEMS THROUGH THE LENS OF SOUNDSCAPE ECOLOGY: HOW BIOLOGICAL PROCESSES, LANDSCAPE STRUCTURE, AND ANTHROPOGENIC ACTIVITY AFFECT SPATIOTEMPORAL SOUNDSCAPE PATTERNS

Rebecca Vick Van Hoeck

A dissertation submitted to the faculty at the University of North Carolina at Chapel Hill in partial fulfillment of the requirements for the degree of Doctor of Philosophy in the Ecology, Evolution, and Organismal Biology Program of the Biology Department.

Chapel Hill
2022

Approved by:

F. Joel Fodrie

Allen Hurlbert

Kenneth Lohman

DelWayne Bohnenstiehl

Sofie Van Parijs

ABSTRACT

REBECCA VICK VAN HOECK: Marine ecosystems through the lens of soundscape ecology:
How biological processes, landscape structure, and anthropogenic activity affect spatiotemporal
soundscape patterns
(Under the direction of F. Joel Fodrie)

Marine soundscapes, or the collection of all sounds across a landscape, consist of

dynamic patterns resulting from natural and anthropogenic sound-producing processes.

Soundscape ecology is focused on understanding how these processes interact with

environmental variables and landscape structure to create dynamic soundscape patterns across

space and time. As the field develops, there has been rising interest in using soundscapes as a

tool to assess biodiversity and inform conservation and management decisions. However,

understanding spatiotemporal soundscape patterns and their associations with ecological and

environmental covariates is needed for passive acoustic monitoring to be informative.

My dissertation addresses this need through two focal questions: (1) how do soundscapes

vary across marine landscapes and is this variation explained by ecological metrics; and (2) how

can soundscapes, or passive acoustic monitoring, be used to inform conservation and

management priorities? To understand soundscape variation, I first compared the soundscapes of

natural and artificial offshore reefs, finding that their temporal patterns were similar but spectral

content differed. Following these results, I evaluated soundscape spatial variation across a range

of estuarine habitat mosaics to explore whether soundscape differences between habitat types

were associated with environmental metrics. I observed four distinct soundscape types that were

associated with patch- and landscape-scale habitat metrics. Variation in all soundscape metrics

summarized was explained by landscape-scale habitat metrics, while patch-scale metrics also explained sound levels, and abiotic metrics explained species-specific call rates.

To evaluate how passive acoustic monitoring can be applied to conservation and management questions, I assessed whether soundscape monitoring was a useful complement to traditional video monitoring for tracking community development following deployment of an artificial reef. Comparing the soundscape of a newly deployed artificial reef to that of a nearby established reef revealed the colonization of multiple cryptic species that were not available from video monitoring. Lastly, I used multiple passive acoustic monitoring technologies to assess the spawning-associated grunt dynamics of Atlantic cod in a region with imminent offshore wind energy development. Elucidating the peak spawning period and aggregation site revealed that interactions between Atlantic cod spawning and offshore wind energy construction are likely.

This dissertation advances understanding of soundscape variability in multiple ecosystems and demonstrates the benefit of passive acoustic monitoring for addressing applied ecological questions. By focusing on periods of peak acoustic activity and exploring variation across marine landscapes, my research explained previously undescribed soundscape variation and identified the relevance of landscape context in understanding marine soundscape variability. In applied contexts, my findings demonstrate that species-specific results are the most ecologically informative, but the current application of passive acoustic monitoring is limited by a lack of reliable identification of species-specific call types and associated call detectors. Advances in call detection will facilitate more nuanced ecological questions to be asked of marine soundscape and expand its relevance for addressing conservation and management priorities.

To Ezra, may you grow to love the ocean as I do and know that you can accomplish anything you set your mind to.

ACKNOWLEDGEMENTS

My PhD journey has been an incredibly rewarding and challenging experience that would not be possible without the support and guidance of my family, friends, and colleagues. I would first like to thank my advisor, Joel Fodrie, for giving me the opportunity to continue my academic career at UNC and the independence to explore my own research and extracurricular interests. I especially valued your willingness to learn about marine soundscapes, advocacy in support of my career goals, and reminders to return to the broader ecological context when I got lost in the details of acoustic analysis. Thank you to my committee members, Del Bohnenstiehl, Sofie Van Parijs, Allen Hurlbert, and Ken Lohmann, for providing their feedback on my research, encouraging me to step outside my area of expertise, and supporting me throughout the process. I am especially grateful for the mentorship of Del Bohnenstiehl, who generously invested time in teaching me how to analyze acoustic data, and Sofie Van Parijs, who gave me the opportunity to work on my dream research project. This dissertation simply would not be possible without your support and guidance, and I thoroughly enjoyed collaborating with you.

Thank you to Avery Paxton who first introduced me to acoustics, took a chance on me by inviting me to work at UNC as a research technician, was a generous collaborator, and taught me the ropes of academia. Your mentorship and friendship were critical to my success at UNC. Thank you to the many friends and lab members who helped with field work, you made my research not only possible, but a lot more fun! I would especially like to thank Claire Rosemond for her friendship and collaboration, your curiosity and knowledge inspires me. Thank you also

to the many current and former Fodrie lab members and technicians who shared their time and knowledge of estuarine environments, especially Abigail Poray, Grace Roskar, and Cori Lopanzanski.

Grad school looked a lot different the last few years because of the pandemic, but the distance from colleagues was made a lot easier by the friendships formed early on. Thank you to Grace Di Cecco, Zofia Anchando, and Jeff Plumlee for your friendships, I miss being able to walk to your offices for a quick-chat, coffee break, or to troubleshoot a research problem. Thank you also to John Bruno and all Bruno lab members, especially Catie Alves, Erin Spencer, Kate Gould and Laura Mudge, for sharing their lab space with me as well as the rest of the Wilson 3rd Floor Ecology Group for welcoming me into a wonderful community of ecologists. An extra thank you to my fellow marine scientist moms, Catie Alves and Shannon Ricci. It has been a joy sharing our experiences through marine science and motherhood.

To my entire family, thank you for your endless support. To my parents, thank you for raising me to work hard for what I want, to always see the silver lining, and for giving me the space to follow my dreams. To my siblings, thank you for always being only a phone call away, for listening, for your advice, and more than anything else your unconditional friendship. Lastly, to my husband, Matt, words cannot express how grateful I am for your partnership in life. From getting married the summer after my first year to welcoming our first baby before my last year, I am so proud of the life we have built together while I've been in grad school. Thank you for encouraging me through the challenges and celebrating me during the accomplishments. I would not be where I am today without your incredible support and teamwork.

TABLE OF CONTENTS

LIST OF TABLES

LIST OF FIGURES

LIST OF ABBREVIATIONS

AIC	Akaike Information Criterion
ANOSIM	Analysis of Similarity
ANOVA	Analysis of Variance
AR	Artificial Reef
CNN	Convolutional Neural Network
CPUE	Catch Per Unit Effort
dbRDA	distance-based Redundancy Analysis
DMF	Division of Marine Fisheries
DMON	Digital acoustic Monitoring instrument
EDT	Eastern Daylight Time
FFT	Fast Fourier Transform
GB	George's Bank
GLMM	Generalized Linear Mixed Models
HSD	Honest Significant Difference
IQR	Inter Quartile Range
MARU	Marine Autonomous Recording Unit
NC	North Carolina
NFFT	Non-uniform Fast Fourier Transform
NMDS	Non-metric Multidimensional Scaling
PAM	Passive Acoustic Monitoring
PSD	Power Spectral Density
RL	Received Level

RMS	Root Mean Square
SD	Standard Deviation
SL	Source Level
SNE	Southern New England
SNR	Signal to Noise Ratio
TL	Transmission Loss
US	United States
USA	United States of America
USS	United States Ship

CHAPTER 1: INTRODUCTION

The soundscape is an intrinsic component of an ecosystem, directly resulting from biological, geological, and anthropogenic sound-producing processes. Soundscape ecology, rooted in the theory of landscape ecology, uses passive acoustic monitoring (PAM) to understand how these processes interact with environmental variables and landscape structure to form dynamic soundscape patterns across space, time, and spectral composition (Pijanowski et al. 2011). For example, the likelihood a certain biological sound is present is defined by the species' distribution, which is modulated by abiotic factors, while its presence in a community is further shaped by habitat associations, dispersal ability, and biotic interactions (Holt 2009). On temporal scales, the timing of biological sound production is often tied to life-history events such as reproduction, while the frequency spectrum is dependent on the sound sources and their relative contribution to the total sound power. Ultimately, these patterns can create feedback loops where soundscapes, used as a sensory cue by individuals, maintain or alter animal behavior (Putland et al. 2018) and can drive evolution of biological sound signals and hearing (Luczkovich & Sprague 2011). Taken together, soundscapes offer a lens through which we can ask a variety of ecological questions that span the range of biological hierarchy from individuals to ecosystems and can be used to understand interactions with anthropogenic activity.

At the population level, species-specific acoustic activity has been used to identify spawning phenology (Monczak et al. 2020) and habitat use of vocal-spawning fishes (Luczkovich et al. 2008; Ricci et al. 2017) as well as prevent vessel strikes of endangered marine mammals (Van Parijs et al. 2009). At the community and ecosystem levels, soundscapes have

been associated with habitat configuration (Tucker et al. 2014; Freeman and Freeman 2016; Gottesman et al. 2020), restoration status (Butler et al. 2016), as well as biodiversity of avian (Depraetere et al. 2012) and fish (Kennedy et al. 2010; Kaplan et al. 2015) communities in a variety of terrestrial and marine ecosystems. Passive acoustic monitoring of marine soundscapes is a non-invasive method that provides long-term sampling independent of light availability and oceanographic conditions (Mooney et al. 2020). Moreover, PAM can be used in difficult to sample habitats, such as those with complex benthic structures or areas where vessels and fishing are restricted due to protection status or ocean industry. As a result, marine soundscapes offer a novel method to understand associations between marine communities and the seascape as well as address conservation and management concerns. Despite the successes and advantages of PAM, currently available acoustic indices to summarize soundscape patterns have had equivocal results in marine systems (Bohnenstiehl et al. 2018; Bolgan et al. 2018; Mooney et al. 2020; Dimoff et al. 2021), suggesting further research is needed to understand soundscape spatiotemporal variability before soundscape monitoring can be broadly applied.

The processes that underly marine soundscape temporal patterns are largely known, though their contribution varies widely among regions, habitats, and species (Pijanowski et al. 2011; Staaterman et al. 2014; Ricci et al. 2017). For example, sound levels frequently increase on diel, lunar, and seasonal scales associated with spawning phenology and behavior of acoustically active species (Rountree et al. 2006; Luczkovich et al. 2008; Bohnenstiehl et al. 2016). Beyond bioacoustic activity, temporal patterns are also associated with geophysical processes, including rain and wind events (Wenz 1962; Hildebrand 2009), and anthropogenic activity, such as commercial shipping (Duarte et al. 2021). In contrast, relatively little agreement exists regarding soundscape spatial variation. Different habitat types (Radford et al. 2010; Lillis

2

et al. 2014), and even adjacent habitats patches (Radford et al. 2014; Lillis and Mooney 2018) are known to have distinct soundscapes; however, studies that attempt to explain this variability have identified different relationships across marine ecosystems (Nedelec et al. 2015; Ricci et al. 2017; Elise et al. 2019; Pieretti and Danovaro 2020). The current understanding of soundscape spatial variation is limited by the fact that previous studies have often focused on a single habitat type, most commonly tropical coral reefs, or over small spatial scales. Expanding understanding of spatiotemporal variation in marine soundscapes could facilitate broader application to conservation and management priorities. This task is made more urgent as marine ecosystems continue to experience global declines in coastal habitats and rising anthropogenic noise pollution due to rapidly expanding ocean industry (Orth et al. 2006; Bruno and Selig 2007; Beck et al. 2011; Duarte et al. 2021).

In this dissertation I address two focal research questions: (1) how do soundscapes vary across marine landscapes and is this variation explained by ecological metrics; and (2) how can soundscapes, or passive acoustic monitoring, be used to inform conservation and management priorities? To understand how soundscapes vary across habitat types, I first evaluated whether the soundscapes of shipwreck artificial reefs differed from that of natural reefs and found that temporal patterns were similar between the reef types, but spectral content differed (Chapter 1). Following these results, I explored whether soundscape differences between habitat types were associated with underlying environmental and seascape variability. To this end, I summarized the soundscapes of 24 estuarine habitat mosaics across the scale of an estuary and evaluated whether soundscape variation was explained by habitat, community, or abiotic metrics (Chapter 2). My study identified that soundscape differences between habitat types were explained by habitat metrics at multiple scales, variation across the continuum of habitat complexity was best

explained by landscape-scale habitat metrics, and seasonal patterns in fish chorusing were explained by abiotic metrics.

To address the question of how soundscapes can inform conservation and management priorities, I first compared the soundscapes of a newly deployed artificial reef and an established reef over the course of one year and compared the results to that of visual surveys for monitoring community assembly (Chapter 3). This passive acoustic monitoring revealed colonization of the new reef by multiple cryptic species that were not available from traditional visual surveys. Lastly, I used a combination of fixed-station and glider-based passive acoustic methods to evaluate the spatiotemporal spawning dynamics of Atlantic cod in Southern New England and assess their potential interactions with offshore wind energy (Chapter 4). I found evidence of cod spawning within the wind energy lease and that, like other cod stocks in the northwest Atlantic, spawning-associated grunt activity peaks in late November to early December, near the full moon. These results revealed that spatial and temporal overlap between Atlantic cod spawning and offshore wind energy is likely.

This dissertation spans a broad scope of ecosystems and ecological questions that when taken together reveals common trends in and expands understanding of the temporal, spatial, and spectral variability of marine soundscapes. Similar to the soundscapes of other marine systems, I identified temporal patterns at diel, lunar, and seasonal scales. Diel cycles typically peaked during crepuscular periods and were elevated at night associated with increased bioacoustic activity, while seasonal patterns were associated with water temperature, spawning phenology of soniferous fishes, and tracked community development following introduction of an artificial reef. When focused on a single species, passive acoustic monitoring provided detailed assessment of temporal patterns in spawning-associated call rates. This information was

successfully communicated to managers to inform potential interactions between fisheries and offshore wind energy.

By focusing on periods of peak acoustic activity, my research elucidates how soundscape spatial variation relates to seascape structure of nearshore estuarine habitats and offshore hardbottom reefs. My findings suggest that temporal patterns tend to be similar among habitat types, but spectral content, species-specific call rates, and band-limited sound levels differ. When investigated further, I found that differences between habitat types were correlated with patch- and landscape-scale habitat metrics as well as abiotic metrics and were explained by acoustic activity in specific low frequency bands. Previous studies that evaluated the relationship between soundscape and environmental metrics typically focused on patch-scale habitat metrics within a single habitat type. By investigating the effect of seascape structure at a broader scale of estuarine habitat complexity than previously described the role of landscape-scale habitat metrics in explaining soundscape spatial variation was revealed. My results suggest that the strength and direction of the relationship between soundscape and environmental metrics varies depending on the soundscape metric used, the habitat types included, and the spatial scale sampled. As such, extrapolating these results to other systems is unlikely and future research should carefully consider the research questions asked when designing observational studies.

A common theme of this dissertation is that differences between habitat-associated soundscapes were effectively identified using the power spectrum. Because species-specific sounds have unique frequency signatures, the power spectrum summarizes the acoustic community of a site. Comparison of the power spectrum among sites facilitated the analysis and visualization of spatial and temporal variation in marine soundscape spectral content. Specifically, differences between artificial and natural reefs were associated with acoustic

activity in two low frequency bands, while spectral differences between estuarine soundscape types were explained by patch- and landscape-scale habitat metrics as well as the presence of silver perch chorusing. Lastly, the power spectrum revealed the colonization trajectory and community development on a newly deployed artificial reef. Multivariate ordination methods are commonly used in community ecology to explore variation in community structure and its correlation with environmental metrics. My application of these methods to acoustic communities has contributed to advancing the field of soundscape ecology from simply describing differences between habitat-associated soundscapes to a more thorough evaluation of what drivers underly these differences.

Multiple chapters of this dissertation leverage the use of multi-method approaches for sampling marine soundscape and communities. For example, the simultaneous use of fixed and glider-based passive acoustic monitoring methods provided fine-scale spatial and temporal information on Atlantic cod spawning, while balancing trade-offs between the two methods. The combination of passive acoustic monitoring with visual surveys provided a more complete understanding of community development following habitat enhancement than a single method alone. Lastly, pairing soundscape summaries with traditional habitat and community sampling in estuarine systems identified unvegetated mudflats as potential spawning grounds for silver perch as well as expanded understanding of how soundscape metrics vary across a continuum of habitat complexity. Overall, these results emphasize that passive acoustic monitoring of bioacoustic activity, and soundscapes more generally, is a valuable complement to traditional sampling methods that can be directly applied to conservation and management contexts.

Throughout all chapters, I summarized the soundscape using aggregate indices and species-specific call rates. While SPL is an effective measure of sound level, it can only be

summarized within specified frequency bands that often include many different sound sources. This broad summary makes SPL difficult to interpret and compare between studies. In contrast, results related to species-specific acoustic activity, such as call rates and high frequency SPL with isolated snapping shrimp activity, were the most informative and ecologically interpretable. Diel and seasonal periods of elevated low frequency SPL were explained by fish chorusing patterns, while call rates revealed spawning dynamics and their correlations with habitat and abiotic metrics. However, due to a lack of reliable references and for many species, I was unable to identify multiple fish calls. There is a need to invest in research focused on documenting fish call types, such as *in-situ* optic-acoustic identification, and developing automatic call detectors. Moreover, the field would benefit from establishing common reporting standards for publication of documented calls (i.e., all published species IDs should include raw audio files of a call). Combined, these advances would facilitate more thorough description of acoustic communities and the ability use soundscapes to ask more nuanced questions related to community ecology.

REFERENCES

Beck, M. W., R. D. Brumbaugh, L. Airoldi, A. Carranza, loRen D. Coen, C. Crawford, Om. Defeo, gRahaM J. Edgar, and B. Hancock. 2011. Oyster reefs at risk and recommendations for conservation, restoration, and management. BioScience 61(2).

Bohnenstiehl, D. R. D., R. P. Lyon, O. N. Caretti, S. W. Ricci, and D. B. Eggleston. 2018. Investigating the utility of ecoacoustic metrics in marine soundscapes. Journal of Ecoacoustics 2(#R1156L).

Bohnenstiehl, D. R., A. Lillis, and D. B. Eggleston. 2016. The Curious Acoustic Behavior of Estuarine Snapping Shrimp: Temporal Patterns of Snapping Shrimp Sound in Sub-Tidal Oyster Reef Habitat. PloS one 11(1):e0143691.

Bolgan, M., M. C. P. Amorim, P. J. Fonseca, L. Di Iorio, and E. Parmentier. 2018. Acoustic complexity of vocal fish communities: A field and controlled validation. Scientific Reports.

Bruno, J. F., and E. R. Selig. 2007. Regional decline of coral cover in the Indo-Pacific: Timing, extent, and subregional comparisons. PLoS ONE 2(8).

Butler, J., J. A. Stanley, and M. J. I. Butler. 2016. Underwater soundscapes in near-shore tropical habitats and the effects of environmental degradation and habitat restoration. Journal of Experimental Marine Biology and Ecology 479:89–96. Elsevier B.V.

Depraetere, M., S. Pavoine, F. Jiguet, A. Gasc, S. Duvail, and J. Sueur. 2012. Monitoring animal diversity using acoustic indices: Implementation in a temperate woodland. Ecological Indicators 13:46–54.

Dimoff, S. A., W. D. Halliday, M. K. Pine, K. L. Tietjen, F. Juanes, and J. K. Baum. 2021. The utility of different acoustic indicators to describe biological sounds of a coral reef soundscape. Ecological Indicators 124:107435. Elsevier Ltd.

Duarte, C. M., L. Chapuis, S. P. Collin, D. P. Costa, R. P. Devassy, V. M. Eguiluz, C. Erbe, T. A. C. Gordon, B. S. Halpern, H. R. Harding, M. N. Havlik, M. Meekan, N. D. Merchant, J. L. Miksis-Olds, M. Parsons, M. Predragovic, A. N. Radford, C. A. Radford, S. D. Simpson, H. Slabbekoorn, E. Staaterman, I. C. Van Opzeeland, J. Winderen, X. Zhang, and F. Juanes. 2021. The soundscape of the Anthropocene ocean. Science 371(6529):eaba4658.

Elise, S., I. Urbina-Barreto, R. Pinel, V. Mahamadaly, S. Bureau, L. Penin, M. Adjeroud, M. Kulbicki, and J. H. Bruggemann. 2019. Assessing key ecosystem functions through soundscapes: A new perspective from coral reefs. Ecological Indicators 107:105623.

Freeman, L. A., and S. E. Freeman. 2016. Rapidly obtained ecosystem indicators from coral reef soundscapes. Marine Ecology Progress Series 561:69–82.

Gottesman, B. L., J. Sprague, D. J. Kushner, K. Bellisario, D. Savage, M. F. McKenna, D. L. Conlin, E. DiDonato, M. J. Barkaszi, M. B. Halvorsen, and B. C. Pijanowski. 2020. Soundscapes indicate kelp forest condition. Marine Ecology Progress Series

654(November):35–52. Inter-Research Science Center.

Hildebrand, J. 2009. Anthropogenic and natural sources of ambient noise in the ocean. Marine Ecology Progress Series 395:5–20.

Kaplan, M. B., T. A. Mooney, J. Partan, and A. R. Solow. 2015. Coral reef species assemblages are associated with ambient soundscapes. Marine Ecology Progress Series.

Kennedy, E. V., M. W. Holderied, J. M. Mair, H. M. Guzman, and S. D. Simpson. 2010. Spatial patterns in reef-generated noise relate to habitats and communities: Evidence from a Panamanian case study. Journal of Experimental Marine Biology and Ecology 395:85–92.

Lillis, A., D. Eggleston, and D. Bohnenstiehl. 2014. Estuarine soundscapes: distinct acoustic characteristics of oyster reefs compared to soft-bottom habitats. Marine Ecology Progress Series 505:1–17.

Lillis, A., and T. A. Mooney. 2018. Snapping shrimp sound production patterns on Caribbean coral reefs: relationships with celestial cycles and environmental variables. Coral Reefs 37:597–607.

Luczkovich, J. J., R. C. Pullinger, S. E. Johnson, and M. W. Sprague. 2008. Identifying Sciaenid Critical Spawning Habitats by the Use of Passive Acoustics. Transactions of the American Fisheries Society 137(2):576–605.

Monczak, A., B. McKinney, C. Mueller, and E. W. Montie. 2020. What's all that racket! Soundscapes, phenology, and biodiversity in estuaries. PLoS ONE 15(9 September):1–18.

Mooney, T. A., L. Di Iorio, M. Lammers, T. Lin, S. L. Nedelec, M. Parsons, C. Radford, E. Urban, and J. Stanley. 2020. Listening forward: approaching marine biodiversity assessments using acoustic methods. Royal Society Open Science 7:201287.

Nedelec, S. L., S. D. Simpson, M. W. Holderied, A. N. Radford, G. Lecellier, C. Radford, and D. Lecchini. 2015. Soundscapes and living communities in coral reefs: temporal and spatial variation. Marine Ecology Progress Series 524:125–135.

Orth, R. J., T. J. B. Carruthers, W. C. Dennison, C. M. Duarte, J. W. Fourqurean, K. L. Heck, A. R. Hughes, G. A. Kendrick, W. J. Kenworthy, S. Olyarnik, F. T. Short, M. Waycott, and S. L. Williams. 2006. A global crisis for seagrass ecosystems. BioScience 56(12):987–996.

Van Parijs, S. M., C. W. Clark, R. S. Sousa-Lima, S. E. Parks, S. Rankin, D. Risch, and I. C. Van Opzeeland. 2009. Management and research applications of real-time and archival passive acoustic sensors over varying temporal and spatial scales. Marine Ecology Progress Series 395:21–36.

Pieretti, N., and R. Danovaro. 2020. Acoustic indexes for marine biodiversity trends and ecosystem health: Acoustic indexes in marine environments. Philosophical Transactions of the Royal Society B 375:20190447. Royal Society Publishing.

Pijanowski, B. C., A. Farina, S. H. Gage, S. L. Dumyahn, and B. L. Krause. 2011. What is soundscape ecology? An introduction and overview of an emerging new science. Landscape Ecology 26(9):1213–1232.

Radford, C. A., J. A. Stanley, and A. G. Jeffs. 2014. Adjacent coral reef habitats produce different underwater sound signatures. Marine Ecology Progress Series 505:19–28.

Radford, C. A., J. A. Stanley, C. T. Tindle, J. C. Montgomery, and A. G. Jeffs. 2010. Localised coastal habitats have distinct underwater sound signatures. Marine Ecology Progress Series 401:21–29.

Ricci, S. W., D. B. Eggleston, and D. W. R. Bohnenstiehl. 2017. Use of passive acoustic monitoring to characterize fish spawning behavior and habitat use within a complex mosaic of estuarine habitats.

Rountree, R. A., R. G. Gilmore, C. A. Goudey, A. D. Hawkins, J. J. Luczkovich, and D. . Mann. 2006. Listening to fish: Applications of passive acoustics to fisheries science. Fisheries 31(9):433–446.

Staaterman, E., C. Paris, H. DeFerrari, D. Mann, an Rice, and E. D'Alessandro. 2014. Celestial patterns in marine soundscapes. Marine Ecology Progress Series 508:17–32.

Tucker, D., S. H. Gage, I. Williamson, and S. Fuller. 2014. Linking ecological condition and the soundscape in fragmented Australian forests. Landscape Ecology 29:745–758.

Wenz, G. M. 1962. Acoustic Ambient Noise in the Ocean: Spectra and Sources. The Journal of the Acoustical Society of America 34(12):1936–1956.

CHAPTER 2: SOUNDSCAPES OF NATURAL AND ARTIFICIAL REEFS: SIMILAR TEMPORAL PATTERNS BUT DISTINCT SPECTRAL CONTENT[1]

Introduction

The ways in which animals make and perceive sounds play an important role in the ecology of many species. Individuals use sound to communicate and interpret a wide array of social and ecological cues, including territorial aggression, group cohesion, mate attraction, gamete release synchronization, navigation, and settlement (Suthers et al. 2004, Popper & Hawkins 2019). Among the more than 30,000 extant fishes, over 800 teleost fish species, representing 30 families, are known to produce species-specific calls for communication (Rountree et al. 2006). Moreover, all fishes possess the morphological capability to perceive acoustic particle motion and many species have specialized hearing due to connections between the inner ear and gas-filled sacs, such as swim bladders (Ladich 2014). These connections can facilitate lower hearing thresholds, broader frequency sensitivity, and detection of sound pressure (Popper & Fay 2011).

The collection of biological sounds, in combination with geological and anthropogenic sounds, across a landscape form the soundscape (Pijanowski et al. 2011). Early research in marine soundscape ecology identified that ambient acoustic levels are elevated at structured habitats compared to adjacent unstructured benthos (Radford et al. 2011, Lillis et al. 2014).

Furthermore, different habitat types have been documented to have different soundscape characteristics, even when situated within a few kilometers of one another. For example, the soundscape of sea urchin dominated reefs in New Zealand contain a greater number of snapping shrimp snaps and increased acoustic activity in an 800 – 2500 Hz frequency band compared to macro-algae dominated reefs and beach habitats (Radford et al. 2010). Additionally, Radford et al. (2014) documented distinct temporal and spectral characteristics at adjacent fringing reefs, back reefs, and lagoon sites.

Across numerous taxa and life stages, marine organisms respond to underwater sound. For example, many species of coral reef fish larvae (Tolimieri et al. 2000, Tolimieri et al. 2004, Leis & Lockett, 2005) and crab post-larvae (Radford et al. 2007) exhibit a directional swimming response to broadcasted reef sounds, and juvenile and adult coral reef fish use sound to guide nocturnal migrations (Radford et al. 2011). Similarly, among the planktonic larvae of sessile invertebrates, oyster (Lillis et al. 2013) and coral (Vermeij et al. 2010) settlement increases in response to reef sound. As a result of the broad use of sound as a navigational and settlement cue among marine organisms, differences in broadcasted soundscapes among distinct habitats and habitat types may affect recruitment processes, community structure, and habitat function.

Artificial reefs are frequently introduced to marine environments to increase habitat availability and enhance fishery productivity (Pickering & Whitmarsh 1997). To understand the success of artificial reef deployment for conservation and management goals, comparisons with natural reefs are required (Carr & Hixon 1997). Following colonization by fish, artificial reefs often support different community compositions and greater biomass than natural reefs. This pattern of increased biomass is especially pronounced in planktivorous species, leading to an altered trophic structure of artificial reef communities compared to natural reef communities

(Arena et al. 2007, Simon et al. 2013, Paxton et al. 2017). Differences in community composition between artificial and natural reefs may produce distinct soundscapes on each reef type, especially in terms of biophony. If marine organisms are using sound to navigate their environment and make habitat selections, differences in the soundscapes of natural and artificial reefs could lead to recruitment of different species, thereby affecting the function of artificial reefs. A few studies have explored soundscape characteristics at artificial patch reefs, frequently constructed out of cinder blocks (Ghazali et al. 2013, Lyon et al. 2019) though, to our knowledge, the soundscape characteristics of artificial reefs have not been compared to natural reefs.

In the present analysis, we evaluate whether temperate marine soundscapes differ between natural and artificial reefs. Specifically, we document the fish vocalizers that exhibited seasonal chorusing behavior as well as describe and compare the temporal and spectral soundscape characteristics of four temperate reefs offshore of North Carolina – two natural and two artificial. Lastly, we discuss the potential ecological implications of distinct soundscapes broadcasted on natural and artificial reefs and on individual habitats more broadly.

Methods

Study sites

Two natural and two artificial reefs in Onslow Bay, North Carolina (NC), USA, were selected for soundscape description and comparison (Fig. 1a). Onslow Bay has a heterogeneous seafloor consisting of sandy benthic substrates, hardbottom formed by rocky reef ledges and pavements, as well as numerous artificial reefs, including historic shipwrecks, intentionally scuttled ships, and other human-made structures (Department of the Navy, 2009). The reefs

included in this study range from 41.5 – 50.4 km from Beaufort Inlet, and 35.4 – 42.4 km from the shelf break. The natural reefs include two rocky reef ledges: 210 Rock (34° 14.448' N, 76° 35.538' W) and West Rock (34° 19.368' N, 76° 36.396' W), located at 32 m and 30 m depths, respectively. The artificial reefs include a 55.8 m U.S. Coast Guard Buoy Tender at 34 m depth, *Spar* (34° 16.626' N, 76° 38.730' W), and a 133.8 m U.S. Navy Cable Layer at 35 m depth, *Aeolus* (34° 16.698' N, 76° 38.592' W). Both artificial reefs were intentionally scuttled as part of the North Carolina Division of Marine Fisheries Artificial Reef Program (AR-305; N. C. Department of Natural Resources & Fisheries 1988). The *Spar* was sunk in June 2004 and is fully intact. The *Aeolus* was sunk in July 1988 and consists of an intact bow and stern with a region of rubble in the middle.

Acoustic data collection

Underwater sound was recorded concurrently on each site during up to five, approximately week-long deployments between November 2015 and August 2016 (Table S1). Both natural reefs and the *Spar* were sampled during all five deployments. We intended to sample two artificial reefs during all deployments; however, strong current and sediment movement at an initially selected artificial reef site impeded data collection. As a result, the *Aeolus* was selected as a contingency site during the third through the fifth deployments. Continuous recordings were made using calibrated, omni-directional hydrophones (SoundTrap 202 STD, Ocean Instruments, New Zealand) mounted 0.5 m above the seafloor on a weighted, metal conical frame which was placed approximately 5 m from the habitat structure (Fig. 1b). The positions of the hydrophones and frames were fixed across all deployments.

Sound pressure was recorded continuously at a rate of 96 kHz, with instruments producing a flat (±3 dB) frequency response between 0.020 – 43.0 kHz. To reduce computational challenges associated with continuous recordings and facilitate rapid visual screening of acoustic activity via spectrogram, the audio was initially subsampled to two-minute recordings every 15 minutes for the duration of the deployments. These subsamples mimic the typical duty cycle employed in many marine soundscape ecology studies (e.g., Bohnenstiehl et al. 2018). All acoustic processing was conducted in MATLAB using purpose-written code (MATLAB R2019b). Each file was demeaned, and response corrected to µPa using the hydrophone specific calibration value.

Time-series and spectral analysis of the two-minute subsamples identified sporadic, anomalously large amplitude impulsive signals that drastically altered the sound pressure level (SPL) time-series and power spectra (Fig. 2, Fig. S1). These impulsive signals may be produced when a swimming animal collides with the instrument frame or hydrophone (i.e., fish bumps; e.g. Buskirk et al. 1981, Bowman & Wilcock 2014). To remove the effect of the impulsive signals and reduce the intrusion of anthropogenic noise, each two-minute recording was further subsampled by extracting the eight quietest five-second duration, non-overlapping time windows within the file. This resulted in a summary of 40 seconds of recorded audio every 15 minutes. To accomplish this subsampling, a Fast Fourier Transform was applied to the full two-minute file (NFFT = 2^{15} points, 0% overlap, and Hanning window). Next, the average root-mean-square (RMS) bandwidth power of every five-second, non-overlapping time window within the two-minute file was summarized and sorted from quietest to loudest. The average acoustic spectra for each file were then calculated by summarizing only the eight quietest five-second windows (Fig. 2; see supplement for further explanation). Across a deployment, this acoustic summary resulted

in a matrix where each column represented the mean spectra of a recording and each row

contained the power at a given frequency (frequency resolution, $\Delta f = 2.92$ Hz). Band-limited

SPLs were then calculated by integrating the acoustic power over the appropriate rows in this

matrix. All SPL values are RMS and reported in units of dB referenced to 1 μPa.

Statistical analyses

Fish chorusing

Spectrograms and acoustic spectra of individual recordings were visually

inspected to identify dominant fish vocalizations and chorusing as well as rapidly screen for

anthropogenic noise. The source of frequently observed sounds (biological, anthropological, or

unknown) and the species identity of biological vocalizers were confirmed by both aural and

visual inspection of the recording when possible. Observed vocalizations were compared to

described fish calls in bioacoustic catalogues (Fish & Mowbray 1970) and the peer-reviewed

literature in attempt to identify the species (Lobel et al. 2010, Staaterman et al. 2014, Mooney et

al. 2016). Representative calls and daily calling pattern of each type of dominant fish

vocalization were documented via spectrogram with an appropriate time and frequency

resolution for each call type. Average acoustic features of each call type were summarized using

purpose-written code by extracting call samples from all sites and deployments when calls were

observed.

Temporal patterns

To evaluate acoustic activity in an ecologically relevant manner, data were separated into

a low- and high-frequency band. The low-frequency band, from 0.1 – 2.0 kHz, was selected to

isolate sounds from fishes and minimize ambient noise from geologic origins, such as rain or wind at the surface (Urick 1983, Hildebrand 2009). The high-frequency band, $7 - 20$ kHz, was selected to isolate invertebrate sounds, predominantly snapping shrimp (Everest et al. 1948). The gap between selected frequency bands intentionally excludes intermediate frequencies, which contain overlaps between fish and invertebrate sounds.

Temporal variation in SPL was examined on daily and seasonal scales. As week-long recordings were made at up to five time points over the course of ten months, we refer to each deployment by the month it occurred in and among deployment variation as seasonal variation. To evaluate differences in observed SPLs among the reef-types, sites, and deployments we conducted a two-way ANOVA for each frequency band. To identify which sites and deployments were contributing to significant differences we conducted pairwise comparisons using Tukey's honest significant difference tests. Due to observed diurnal patterns in SPLs and their relation to the photoperiod, we isolated the recordings between sunset and astronomical twilight (henceforth called dusk) when daily SPLs peaked across all sites and deployments, for comparison. To account for temporal autocorrelation among the acoustic files, dusk SPLs were averaged for each day within a deployment. As a result, the number of replicates included for each site and deployment combination was equal to the number of days in a deployment. For each frequency band, we evaluated the differences between reef types and among sites separately for a total of four ANOVAs (low frequency by reef type, low frequency by site, high frequency by reef type, high frequency by site). We first investigated differences in dusk SPL aggregated by reef-type. The full model for each frequency band included dusk SPL as the response variable and reef-type, deployment, and an interaction between reef-type and deployment as predictor variables. The site-level model also included site, deployment, and an

17

interaction between site and deployment as predictor variables for each frequency band. For all

models (reef-type level and site level, for high- and low-frequency bands) removal of the

interaction term significantly worsened the fit of the model and inspection of normal Q-Q plots

demonstrated that the assumptions of normality were met; therefore, we proceeded with the full

model and Gaussian distributions for both frequency bands. All statistical analysis was

conducted using the programming software R version 3.6.0 (R Core Team, 2019).

Spectral content

To evaluate dissimilarity in soundscape spectral content at each site, we used distance-

based redundancy analysis (dbRDA) – a multivariate method that uses pairwise ecological

distances to map variables in reduced dimensional space allowing visual assessment of patterns

in the data. DbRDA was conducted on each deployment individually, resulting in five

ordinations. The distance between pairwise samples was calculated using the spectral

dissimilarity index developed by Sueur et al., (2008). The spectral dissimilarity is calculated as

[Eq. 1]:

$$[\text{Eq. 1}] \qquad D_f = \frac{1}{2} \sum_{f=1}^{N} |S_1(f) - S_2(f)|, \text{ with } D_f \in [0,1]$$

where D_f represents the dissimilarity between two samples on a scale from 0 to 1, f represents the

frequency bins over which the index is evaluated and $S_1(f)$ and $S_2(f)$ represent the probability

mass functions of the two spectra being compared. In our study, $S_n(f)$ and D_f were evaluated

over the low-frequency band (0.1-2.0 kHz) using the mean hourly spectra recorded during

nighttime hours. Only nighttime recordings were included because this was an observed period

of increased biological activity and reduced anthropogenic noise.

To identify what acoustic activity was driving sample separation, the proportion of total acoustic power within select frequency bands was calculated for each sample. These frequency bands were determined by viewing the spectra and identifying common peak frequencies (e.g. 0.1 – 0.3 kHz, 0.3 – 0.5 kHz, 0.5 – 0.8 kHz, and 0.8 – 2 kHz). The formula for each dbRDA was the spectral dissimilarity distance matrix constrained by the proportion of acoustic power contained within these smaller frequency bands. As such, the frequency bands driving sample separation are indicated by the loading vectors and the eigenvalues of each ordination dimension represent the amount of variability explained by the loading constraints.

To evaluate whether spectral content varied by reef-type, a multivariate Analysis of Similarity (ANOSIM) was conducted on the spectral dissimilarity matrix from each deployment. ANOSIM is a nonparametric test that evaluates the null hypothesis that there are no differences in dissimilarity within and between groups. To evaluate this hypothesis, ANOSIM ranks all pairwise dissimilarities from a distance matrix, summarizes the mean ranks between and within groups, calculates a test statistic, and evaluates significance via Monte Carlo permutations (n = 1000). The test statistic, R, is expected to be 0 under the null hypothesis and 1 when all pairs between groups are more dissimilar than pairs within groups (Clarke 1993). All multivariate analyses were conducted using the "vegan" package in R (Oksanen et al. 2019).

Results

Fish chorusing

The dominant fish vocalizers that exhibited seasonal chorusing patterns consisted of toadfish boatwhistles (*Opsanus* spp.), and three unidentified vocalizers described as a knock, creak, and growl. (Fig. 3). Though the unidentified calls were compared to similar calls reported

in various fish call databases, there were not close enough matches to confidently report a species identity. To facilitate future identification, temporal and spectral features of each call type were summarized (Table 1).

Fish choruses were observed in November, April, and June and all chorusing species were observed on both natural and artificial reefs. Toadfish chorusing was observed in April and June but was most abundant in April. During April, toadfish calls were observed on all sites at all times throughout the day, with the onset of chorusing usually observed at 20:00 EDT and lasting until 06:00 EDT (Fig. 4a). The daily patterns in SPL in the low-frequency band in April can be attributed largely to this calling behavior of toadfish across all sites (Fig. 5). Toadfish choruses also were observed on all sites except West Rock in June, with chorus onset around 21:00 EDT lasting until 05:00 EDT.

The unidentified knock was an impulsive sound frequently in sets of multiple knocks (Fig. 3b). Choruses of the knocks were observed on all sites during April, while occasional knocks were observed in all deployments. During April, the daily pattern consisted of a rapid onset of a dusk chorus at 20:00 EDT that was maintained for approximately one hour with occasional knocks continuing for up to four hours (Fig. 4a).

The unidentified creak was observed on the *Spar* and West Rock in November from approximately 19:00 EDT – 06:00 EDT, with periods of most intense chorusing during crepuscular periods (Fig. 4b). This call consisted of multiple pulse sets in a pulse train. Each pulse set consisted of three pulses alternating in frequency (Fig. 3c). The first and third pulses had a peak frequency of 1669.4 ± 101.7 Hz on average while the second pulse peaked at 2728.7 ± 156.1 Hz. Each pulse varied in duration, lasting 1.7 ± 0.8 ms, ms, and 2.1 ± 1.0 ms,

respectively. The first and second pulse were separated by 5.0 ± 1.6 ms and the second and third were separated by 4.9 ± 1.5 ms.

Choruses of the unidentified growl, a low frequency sound with a 90-500 Hz bandwidth, were also observed on all sites in November and January (Fig. 3d). The chorus had a rapid onset at 19:00 EDT, lasted one hour with occasional growls observed until 07:00 EDT (Fig. 4b). Similar to the creaking sound, the growl consisted of multiple pulse sets in a pulse train. Each pulse set contained two pulses alternating in frequency with 26.5 ± 11.8 ms between the center of each pulse. The first pulse had an average duration of 40.1 ± 11.7 ms and peak frequency of 100.8 ± 22.9 Hz, while the second pulse was 19.5 ± 4.9 ms long with a 160.9 ± 57.3 Hz peak frequency.

Temporal patterns

In general, the temporal patterns of biological sound production were similar across all reefs. Within the low-frequency band ($0.1 - 2$ kHz), dominated by fish sounds, daily patterns across all sites consisted of increased SPL at dusk and generally greater SPLs at night than during the day (Fig. 5). Seasonally, the intensity of the dusk peak varied, corresponding with the presence of fish chorusing. During November, there was also a peak in acoustic activity on the *Spar* and West Rock at dawn that can be attributed to chorusing by the unidentified creaking species.

Within the low frequency band, dusk SPL did not differ between natural and artificial reefs (ANOVA, $F_{\text{reef type }(1,113)} = 2.63$, $p = 0.108$). All sites broadly exhibited similar seasonal trends; however, dusk SPL significantly differed among sites (ANOVA, $F_{\text{site }(3,105)} = 3.37$, $p < 0.021$), deployment (ANOVA, $F_{\text{deployment}(4,105)} = 63.56$, $p < 0.001$), and an interaction between site

and deployment (ANOVA, $F_{site*deployment(10,105)} = 2.00$, $p = 0.040$). Post-hoc Tukey's HSD tests revealed that differences in dusk SPL were driven largely by seasonal variation as there were no significant differences among sites within a deployment (Fig. 6). Overall, dusk SPL decreased significantly from November to January, increased drastically to a maximum in April, then decreased to a minimum in August (Fig. 7). The April deployment, which coincided with the most abundant fish chorusing, was significantly louder than all others. Lastly, SPLs between the sites across the entire sampling period only significantly differed between two sites, with the *Spar* supporting greater levels than West Rock (Tukey HSD, p = 0.015).

Within the invertebrate dominated high-frequency band (7 – 20 kHz), crepuscular peaks in SPL and elevated SPL at night were observed in all sites and seasons (Fig. 8). Investigation of dusk SPLs identified significant differences between the reef types, with artificial reefs supporting louder high-frequency soundscapes (ANOVA, $F_{reef type (1,113)} = 99.55$, p <0.001). SPLs also varied by deployment (ANOVA, $F_{deployment (4,113)} = 19.89$, p <0.001) and an interaction between reef type and deployment (ANOVA, $F_{reef type*deployment(4,113)} = 8.73$, p <0.001). Post-hoc Tukey's HSD test revealed that artificial reef SPLs were significantly higher than natural reefs in November (p < 0.001), January (p < 0.001), and April (p < 0.001), but not in June (p = 0.587) or August (p = 0.998; Fig. 9).

Comparisons of dusk SPLs at the site level revealed significant differences among sites (ANOVA, $F_{site(3,105)} = 342.85$, p < 0.001), deployments (ANOVA, $F_{deployment(4,105)} = 124.17$, p < 0.001), and their interaction ($F_{site*deployment(10,105)} = 13.45$, p < 0.001). Pairwise comparisons among the deployments revealed that seasonal variation was mostly driven by reduced SPLs during January (Tukey HSD, Fig. 10a). While, variation among the sites was driven by increased SPLs on the *Spar* and reduced SPLs at West Rock (Tukey HSD, Fig. 10b). Pairwise comparisons

among sites within deployment revealed many significant differences. Notably, dusk SPLs were always higher on the *Spar* than the *Aeolus* (Tukey HSD, Apr. p < 0.001; Jun. p < 0.001; Aug. p < 0.001) and tended to be higher on 210 Rock than West Rock (Tukey HSD, Jan. p < 0.001; Apr. p < 0.001; Aug. p < 0.001).

Spectral content

During seasons with increased SPLs and fish chorusing events, specifically April and June, the spectral content of each reef's soundscape became more distinct. This is shown by tighter grouping of samples within site and greater separation between sites (Fig. 11). Moreover, as each sample represents an hour, temporal trends in spectral activity can be observed over the course of the night. Pairwise D_f values for each ordination ranged from 0.1 to 0.8 suggesting that there were substantial differences between some pairwise spectral probability mass functions.

Evaluating low-frequency spectral differences using dbRDA allowed the ordinations to be described in terms of the acoustic activity driving the differences between sites. The smaller frequency bands used to constrain each ordination generally represented a unique dominant fish caller in the average spectra. Activity in the 100-300 Hz range was usually attributed to miscellaneous low-frequency sounds, and in some deployments a toadfish peak. The 300-500 Hz band was indicative of toadfish, the 500-800 Hz band of the unidentified knock, and the 800-2000 Hz band of the unidentified creaking call.

Comparison of spectral dissimilarities between natural and artificial reefs revealed that spectral content significantly varied by reef type in all deployments except November (ANOSIM, R = 0.06, p = 0.19). The separation between reef types was greatest during April (ANOSIM, 0.64, p = 0.001), with artificial reef position driven by activity in the 300-500 Hz

band while natural reefs were driven by 100-300 Hz activity. Separation between the reef types was also significant in January (ANOSIM, R = 0.39, p = 0.001), June (ANOSIM, R = 0.40, p = 0.001), and August (ANOSIM, R = 0.38, p = 0.001).

Analysis of November showed that activity within the 100-300 Hz band was driving the separation of 210 Rock from the other sites, while the overlap in *Spar* and West Rock samples was driven by activity in the 800-2000 Hz band (Fig 11a). This 800-2000 Hz activity, on both a natural and artificial reef, aligns with the timing of the unidentified creaking chorus and explains the lack of significant difference between the reef types during November (Fig. 11b). Overall, the loading vectors explained 93.8% of the variation among the samples, with 58.3% captured on axis 1 and 35.5% captured on axis 2.

In January 2016, the average spectra of each site contain a unique peak that drove its loading (Fig. 11d). The *Spar* and West Rock samples were each tightly clumped suggesting minimal spectral change throughout the night, with the *Spar* being driven by the 300-500 Hz band and West Rock the 800-2000 Hz band. The majority of 210 Rock samples plotted between the *Spar* and West Rock; however, an increase in activity in the 500-800 Hz band from 2-6 hours after sunset drove some separation of the samples (Fig. 11c, d). Overall, the loading vectors explained 86.0% of the variation among the samples, with 60.0% captured on axis 1 and 26.0% captured on axis 2.

Within April, each site showed distinct spectral separation from the other sites, although a consistent temporal trend was observed among all sites (Fig. 11e). This temporal trend was driven by an increase in activity in the 500-800 Hz band, attributed to the knocking chorus, ranging from 1-4 hours after sunset, with the duration of the increase varying across sites (Fig.

11f). Overall, the loading vectors explained 84.7% of the variation among the samples in April, with 48.4% of the variation captured on axis 1 and 36.3% captured on axis 2.

Within June, natural reef samples each ordinate closely within site, with the loadings of 210 Rock driven by activity in the 100-300 Hz band and West Rock driven by the 500-800 Hz and 800-2000 Hz bands (Fig. 11g). Although within site grouping was apparent for the artificial reefs, their samples broadly ordinated similarly with their loadings driven by minimal activity in the 300-500 Hz, 500-800 Hz, and 800-2000 bands (Fig. 11g, h). Overall, the loading vectors explained 91.2% of the variation among the samples in June, with 58.1% of the variation captured on axis 1 and 33.1% captured on axis 2.

In August, the samples within each site clumped tightly together with minimal separation among the sites (Fig. 11i). The loadings of West Rock were driven by a broad peak between 1500 and 1750 Hz and align strongly with the 800-2000 Hz vector (Fig. 11i, j). Among the other three sites, the average spectra showed that there were few to no distinct spectral peaks associated with a specific caller (Fig. 11j). Overall, the loading vectors explained 87.6% of the variation among the samples in August, with 75.2% and 12.4% of the variation captured on axis 1 and 2, respectively.

Discussion

Our research demonstrates that soundscape characterization is a novel approach towards testing whether artificial reefs mimic natural reefs. We documented the soundscapes of four temperate reefs, two natural and two artificial, during five sampling periods across a 10-month period. Although the broad temporal patterns were consistent across all reefs regardless of reef type, these patterns were driven largely by the timing of dominant sound sources. Further

analyses of finer details available in the spectral content revealed distinct soundscapes on each site, with spectral differences generally greater between natural and artificial reefs than within reef type. This separation between natural and artificial reefs was especially pronounced during time periods with increased acoustic activity and higher SPLs. These spectral differences may be the result of differing community compositions and trophic structures on natural and artificial reefs. Moreover, consistent soundscape differences across reef types could affect artificial reef function through species behavior and interactions in response to sound.

Comparison between reef types

While the general pattern of crepuscular peaks in SPL aligning with the seasonal photoperiod was similar between the reef types, high frequency dusk SPLs were significantly higher on artificial reefs than natural reefs during three out of five deployments. More complex habitat structures, such as those of healthy sponge-dominated reefs, are known to host higher densities of snapping shrimp and are associated with higher observed snap rates and high-frequency SPLs (Butler et al. 2016). One possible explanation for elevated SPLs on artificial reefs is that the higher vertical relief and resulting habitat complexity of shipwrecks (Paxton et al. 2017) could support higher densities of snapping shrimp than the comparatively diffuse habitat structure of a natural rocky reef ledge.

Many marine soundscape studies have evaluated differences among sites or habitat types; however, few have employed multivariate analyses such as dbRDA. The strong consistency between the observed average spectra and separation of samples according to the ordination loading vectors suggest that this method is appropriate and informative for evaluating differences in soundscape spectral composition. Across most deployments, the samples grouped most

similarly within their site and were separated from samples of other sites, demonstrating that each site exhibited a unique spectral composition. This is notable especially for the two artificial reefs which are situated only 250 m from one another.

The April deployment, which consisted of the highest SPLs and most abundant low-frequency acoustic activity, provided the most interesting result. During April, the night soundscape of all sites contained choruses of toadfish and unidentified knocks. Despite the presence of the same chorusing species on each reef, there was still substantial spectral separation of the sites. The soundscapes also were separated by reef type, with the artificial reefs exhibiting similar spectral content in the 300-500 Hz band and the natural reefs in the 100-300 Hz band.

Within our study system in Onslow Bay, NC, comparative surveys of natural and artificial reefs have found that artificial reefs and specifically ships support greater fish biomass than natural reefs, whereas other metrics such as species richness are similar between reef types (Paxton et al. 2017, Paxton et al. 2019). Moreover, differences in community composition by reef type are driven by greater abundances of large piscivores and water column planktivores, such as jacks and scad respectively, on artificial reefs, leading to an altered trophic structure (Paxton et al. 2017). Given the presence of the same dominant vocalizers across all reefs, the spectral separation between the reef types is likely a result of differences in the proportion of the total soundscape that the dominant vocalizers occupy, as well as differences in miscellaneous acoustic activity, including less dominant calls and sounds associated with feeding, that are not currently attributable to a certain vocalizer or behavior. As artificial and natural reefs frequently support communities that differ in trophic structure (Arena et al. 2007, Simon et al. 2013, Paxton et al. 2017), it is plausible that there would be differences in sounds associated with feeding on

natural and artificial reefs. It would be valuable to explore whether these non-vocalization sounds can be attributed to specific sources or behaviors, possibly through the use of combined visual surveys and multi-hydrophone localization arrays.

The differences in spectral composition documented on the temperate hardbottom reefs included in this study may have important ecological implications. Multiple studies have shown that different habitats and specifically different reef types broadcast distinct soundscapes (Radford et al. 2010, 2014, Lillis et al. 2014a). We provide initial evidence that shipwreck reefs may broadcast distinct soundscape from natural reefs, as well. Given the ability of fishes to localize a sound source (Sand & Bleckmann 2008, Hawkins & Popper 2018) and marine organisms' attraction to habitat-associated soundscapes, soundscape differences between habitats may play a role in facilitating recruitment to reef habitats and could perpetuate differences among reef types or benthic habitats more broadly. Models of sound propagation away from reefs suggest that habitat-associated sounds, and specifically chorusing events, can be detected on the order of kilometers away from a reef. (Radford et al. 2011b, Lillis et al. 2014b). We propose that if a migrating individual encountered competing acoustic cues from adjacent habitats and the soundscape of one reef has a dominant signal in a preferred frequency band, such as one associated with conspecifics, the individual may be more likely to settle at that reef. As different species of fishes have unique auditory sensitivities, these behavioral patterns could ultimately support distinct communities on separate reefs. Future research on whether marine animals are able to perceive small differences in acoustic signals and whether they are attracted to acoustic activity in specific frequency ranges would facilitate a better understanding of whether the spectral differences we observed across multiple reefs have a meaningful ecological effect.

<u>Comparisons among sites</u>

We documented strong diurnal patterns in biological acoustic activity, with tight ties to the photoperiod. Within the fish-dominated, low-frequency band these patterns were similar to those documented in other marine soundscape studies with SPLs quietest during the day, loudest at dusk, and remaining elevated through the night. While there were not significant differences between the reef types, the diurnal pattern was generally consistent across all sites and seasons with the level of the dusk peak varying seasonally accordant with the amount of fish chorusing observed. Across all sites, the daily pattern was least apparent during January and August, coinciding with the deployment with the quietest dusk SPLs. During these deployments, few distinct fish calls were observed and there was no presence of fish chorusing. Alternatively, the diurnal patterns in acoustic activity were most apparent in April and can largely be attributed to frequent calling and chorusing by toadfish (*Opsanus spp.*) and the dusk chorus of the unidentified knock.

Investigation of low-frequency spectral content identified distinct soundscapes on all reefs, with separation among the sites most pronounced during April and June. As previously summarized, the April soundscape consisted of choruses of toadfish and the unidentified knock. The onset of the knock chorus, with a peak frequency around 650 Hz, occurred immediately after sunset and continued most intensely for one hour, with occasional knocks observed until approximately 4 hours after sunset. This pattern is clearly visible in the corresponding ordination, with a temporal shift away from activity in the 500-800 Hz band as the night progressed. This common temporal pattern among the dominant vocalizer yet maintained spectral separation among the sites and reef types most clearly summarizes the finding of similar temporal patterns but distinct spectral content on temperate reefs.

Within the invertebrate-dominated, high-frequency band, acoustic levels were consistently lowest during the day, peaked at dawn and dusk, and were elevated at night. Similar to the low-frequency band, the strength of this daily pattern exhibited strong seasonal variation with the quietest SPLs observed across all sites sampled in January. Snapping shrimp acoustic activity in shallow-water estuarine systems varies with abiotic variables, such as temperature (Bohnenstiehl et al. 2016). The coldest temperatures in Onslow Bay, NC, are generally around January, which may explain the decrease in acoustic activity during that deployment (Whitfield et al. 2014). Additionally, comparisons among the sites revealed that dusk SPLs were always higher on the *Spar* and 210 Rock than the *Aeolus* and West Rock, respectively. This relationship between sites was also mirrored in the low-frequency band during multiple deployments.

It is interesting to consider whether there are site-level traits that could explain the consistent pattern of higher SPLs on specific reefs within a reef type. Research in a variety of other marine systems have identified correlations between habitat and community metrics, such as density, abundance, species diversity, and coral cover, and increased SPLs in specific frequency bands (Kennedy et al. 2010, Freeman & Freeman 2016, Staaterman et al. 2017). A few possible mechanisms to explain the elevated SPLs on the *Spar* and 210 Rock are differences in community composition, abundance, or trophic structure that relate to differences in habitat traits such as complexity, vertical relief, size of the reef, or proximity to other reefs. Additionally, reef location and context, such as proximity to the shelf break, prevailing current speed and direction, or level of anthropogenic noise disturbance, could affect the community composition and associated soundscape.

Overall, this consistent pattern in relative SPLs among sites in addition to the documented spectral differences among the soundscapes of each reef warrants further

exploration of the relationship between habitat and community traits and the soundscape of temperate natural and artificial reefs. As there are known differences in habitat metrics and community composition on each reef we sampled, our findings provide further support that marine soundscapes may be indicative of habitat and community metrics and could be a valuable remote sensing tool to index fish communities. To gain a deeper understanding of whether the documented soundscape differences are correlated with specific habitat or community features further exploration, with a larger sample size, of soundscape characteristics paired with habitat and community traits across multiple reefs within each reef type are needed.

Fish chorusing

Animal vocalizations serve numerous social and ecological roles, and fish vocalizations are frequently associated with reproductive or agonistic behaviors. For example, fish chorusing, or periods of frequent to constant calling, are almost always associated with reproductive behaviors and spawning (Bass & Rice 2010). The acoustic signature of spawning activity makes passive acoustic monitoring and soundscape description a useful method for studying the spatial and temporal variability of marine population dynamics, as well as evaluating habitat utilization. Because our sampling events were spread across multiple seasons throughout the year, we were able to capture some of the temporal variability potentially related to spawning activity on or near the habitats studied. For a thorough understanding of temporal dynamics, long-term recordings with minimal gaps are required.

The sonic behaviors of toadfish are among the most well-studied for any fish species. Toadfish make their characteristic boatwhistle call, associated with mating and nest defense, by rapid contraction of muscles lining the swim bladder (Fine & Lenhardt 1983). The oyster

toadfish, *Opsanus tau*, is the only documented toadfish in the inshore waters of North Carolina and is known to make seasonal migrations from offshore wintering locations to inshore and estuarine habitats for spawning in spring (Shwartz 1974). The late spring onset of toadfish chorusing we observed on temperate offshore reefs matches seasonal chorusing onset documented in a Chesapeake Bay oyster reef system, as well as on offshore reefs in Georgia and Florida (Ricci et al. 2017, Rice et al. 2017). It is unclear whether the toadfish calls we documented are from a resident offshore population that foregoes seasonal migrations inshore, or if they are a species other than *O. tau,* such as the leopard toadfish, *Opsanus pardus*, which inhabits deeper rocky reefs year-round in the Gulf of Mexico or an analogous undescribed *Opsanus* species.

In attempt to identify the specific source of the unidentified choruses, the call features were compared to documented vocalizers in other soundscape studies and soniferous fish collections in the Western North Atlantic. The observed knock vocalization is similar in pulse duration and frequency range to known pomacentrid calls, such has the dusky and bicolor damselfish (*Stegastes adusus and S. partitus*), both of which are present on the studied reefs (Spanier 1979). However, pomacentrids are generally more acoustically active during the day, while the knock chorus was observed at dusk (Lobel et al. 2010). In laboratory recordings, tomtate (*Haemulon aurolineatum*) which are abundant on the studied reefs and have a spring spawning season, have also been documented making a similar impulsive vocalization. However, tomtate vocalizations have a longer pulse duration (40-130 ms) and more of a grunt quality than a knock.

The unidentified creak was compared to vocalizations of the striped cusk eel (*Ophidion marginatum*), but inspection of the frequency spectrum revealed the cusk eel pulse is centered on

only one frequency (Mooney et al. 2016), while the creak pulses alternate between two frequencies. For the unidentified growl, gray snapper (*Lutjanus griseus*) adult and larvae make a similar low frequency growl (Staaterman et al. 2014), though to our knowledge there has not been documentation of gray snapper choruses in field or laboratory settings. As a result, visual confirmation of the growl source is required to confidently assign a species identity. While it would be ideal to identify each vocalizer to species, or even family, to enhance understanding of the ecological role of marine soundscapes and their interaction with individuals, it is still possible to explore these interactions without specific identification. Moreover, documentation of the unidentified vocalizations in the literature is critical to facilitating future identification.

Caveats

In the current study, we did not evaluate how the soundscapes varied in response to abiotic factors, such as lunar phase, temperature, wind, or sea state. As the sites included in this study are geographically close to one another and range in depth from 30-37m, it is unlikely that wind is a substantial contributor to the soundscape differences documented. Future research investigating how these abiotic factors affect the soundscape of temperate reefs would help to infer whether differences in acoustic levels are site-level differences that can be attributed to ecological differences among the habitats. Additionally, it is important to note that the distance between the sound source and the hydrophone will affect observed SPL, and due to the unique geometries of each reef we were unable to fully standardize the position of the hydrophone relative to the extent, quantity or characteristics of each reef habitat.

Lastly, we acknowledge that the sample size of the present study limits our ability to generalize how the soundscapes of artificial reefs relate to that of natural reefs more broadly.

However, the consistent spectral differences we observed between the reef types, as well as among all sites warrants further exploration. To date, research on how marine soundscapes vary across habitat and community traits has resulted in promising, but equivocal results. Artificial reefs vary greatly and measurably in area, vertical relief, and heterogeneity, with documented differences in the communities they support. With appropriately designed studies, artificial reefs could be a useful system to better understand the mechanistic relationships between soundscape variation and habitat and community traits.

REFERENCES

Arena PT, Jordan LKB, Spieler RE (2007) Fish assemblages on sunken vessels and natural reefs in southeast Florida, USA. Hydrobiologia 580:157–171.

Bass AH, Rice AN (2010) Vocal-Acoustic Communication in Fishes: Neuroethology. In: *In: Encyclopedia of animal behavior. Oxford: Academic Press*. p 558–567

Bohnenstiehl DR, Lillis A, Eggleston DB (2016) The Curious Acoustic Behavior of Estuarine Snapping Shrimp: Temporal Patterns of Snapping Shrimp Sound in Sub-Tidal Oyster Reef Habitat. PLoS One 11:e0143691.

Bohnenstiehl DRD, Lyon RP, Caretti ON, Ricci SW, Eggleston DB (2018) Investigating the utility of ecoacoustic metrics in marine soundscapes. J Ecoacoustics 2: #R1156L.

Bowman DC, Wilcock WSD (2014) Unusual signals recorded by ocean bottom seismometers in the flooded caldera of Deception Island volcano: volcanic gases or biological activity? Antarct Sci 26:267–275.

Buskirk RE, Frohlich C, Latham G V., Chen AT, Lawton J (1981) Evidence that biological activity affects Ocean Bottom Seismograph recordings. Mar Geophys Res 5:189–205.

Butler J, Stanley JA, Iv MJB, Butler MJ (2016) Underwater soundscapes in near-shore tropical habitats and the effects of environmental degradation and habitat restoration. J Exp Mar Bio Ecol 479:89–96.

Carr MH, Hixon MA (1997) Artificial Reefs: The Importance of Comparisons with Natural Reefs. Fisheries 22:28–33.

Clarke K (1993) Non☐parametric multivariate analyses of changes in community structure. Aust J Ecol 18:117–143.

Department of the Navy (2009) Essential Fish Habitat Assessment for the Environmental Impact Statement/Overseas Environmental Impact Statement

Everest FA, Young RW, Johnson MW (1948) Acoustical Characteristics of Noise Produced by Snapping Shrimp. J Acoust Soc Am 20:137–142.

Fine ML, Lenhardt ML (1983) Shallow-water propagation of the toadfish mating call Sonic system of deep-sea cusk-eels (Ophidiidae) View project SHALLOW-WATER PROPAGATION OF THE TOADFISH MATING CALL " Artic Comp Biochem Physiol Part A Physiol Camp Eiochmz Ph~sroi 76:2–231.

Fish MP, Mowbray WH (1970) Sounds of Western North Atlantic Fishes: A Reference File of Biological Underwater Sounds. Johns Hopkins Press, Baltimore, MD.

Freeman LA, Freeman SE (2016) Rapidly obtained ecosystem indicators from coral reef soundscapes. Mar Ecol Prog Ser 561:69–82.

Ghazali SM, Montgomery JC, Jeffs AG, Ibrahim Z, Radford CA (2013) The diel variation and spatial extent of the underwater sound around a fish aggregation device (FAD). Fish Res 148:9–17.

Hawkins AD, Popper AN (2018) Directional hearing and sound source localization by fishes. Cit J Acoust Soc Am 144:3329.

Hildebrand J (2009) Anthropogenic and natural sources of ambient noise in the ocean. Mar Ecol Prog Ser 395:5–20.

Kennedy E V., Holderied MW, Mair JM, Guzman HM, Simpson SD (2010) Spatial patterns in reef-generated noise relate to habitats and communities: Evidence from a Panamanian case study. J Exp Mar Bio Ecol 395:85–92.

Ladich F (2014) Fish bioacoustics. Curr Opin Neurobiol 28:121–127.

Leis JM, Lockett MM (2005) Localization of reef sounds by settlement-stage larvae of coral-reef fishes (Pomacentridae). Bull Mar Sci 76:715–724.

Lillis A, Eggleston D, Bohnenstiehl D (2014a) Estuarine soundscapes: distinct acoustic characteristics of oyster reefs compared to soft-bottom habitats. Mar Ecol Prog Ser 505:1–17.

Lillis A, Eggleston DB, Bohnenstiehl DR (2013) Oyster Larvae Settle in Response to Habitat-Associated Underwater Sounds. PLoS One 8:e79337.

Lillis A, Eggleston DBD, Bohnenstiehl DRD (2014b) Soundscape variation from a larval perspective: the case for habitat-associated sound as a settlement cue for weakly swimming estuarine larvae. Mar Ecol Prog Ser 509:57–70.

Lobel PS, Kaatz IM, Rice AN (2010) Acoustical Behavior of Coral Reef Fishes. In: *Reproduction and Sexuality in Marine Fishes: Patterns and Processes*. Cole KS (ed) University of California Press, p 307–348

Lyon RP, Eggleston DB, Bohnenstiehl DR, Layman CA, Ricci SW, Allgeier JB (2019) Fish community structure, habitat complexity, and soundscape characteristics of patch reefs in a tropical, back-reef system. Mar Ecol Prog Ser 609:33–48.

MATLAB (2019) version 9.1.0.441655 (R2019a). Natick, Massachusetts: The MathWorks Inc.

Mooney TA, Kaplan MB, Izzi A, Lamoni L, Sayigh L (2016) Temporal trends in cusk eel sound production at a proposed US wind farm site. Mar Ecol Prog Ser 24:201–210.

North Carolina Department of Natural Resources & Community Development (1988) North Carolina Artificial Reef Master Plan

Oksanen J, Blanchet FG, Friendly M, Kindt R, Legendre P, McGlinn D, Minchin PR, O'Hara RB, Simpson GL, Solymos P, Stevens MHH, Szoecs E, Wagner H (2019) Vegan:

Community Ecology Package.

Paxton AB, Peterson CH, Taylor JC, Adler AM, Pickering EA, Silliman BR (2019) Artificial reefs facilitate tropical fish at their range edge. Commun Biol 2:https://doi.org/10.1038/s42003-019-0398-2.

Paxton AB, Pickering EA, Adler AM, Taylor JC, Peterson CH (2017) Flat and complex temperate reefs provide similar support for fish: Evidence for a unimodal species-habitat relationship. PLoS One 12:e0183906.

Pickering H, Whitmarsh D (1997) Artificial reefs and fisheries exploitation: A review of the 'attraction versus production' debate, the influence of design and its significance for policy. Fish Res 31:39–59.

Pijanowski BC, Villanueva-Rivera LJ, Dumyahn SL, Farina A, Krause BL, Napoletano BM, Gage SH, Pieretti N (2011) Soundscape Ecology: The Science of Sound in the Landscape. Bioscience 61:203–216.

Popper AN, Fay RR (2011) Rethinking sound detection by fishes. Hear Res 273:25–36.

Popper AN, Hawkins AD (2019) An overview of fish bioacoustics and the impacts of anthropogenic sounds on fishes. J Fish Biol 94:692–713.

R Core Team (2019) R: A language and environment for statistical computing. Version 3.6.0.

Radford CA, Jeffs AG, Montgomery JC (2007) Directional swimming behavior by five species of crab postlarvae in response to reef sound. Bull Mar Sci 80:369–378.

Radford CA, Stanley JA, Jeffs AG (2014) Adjacent coral reef habitats produce different underwater sound signatures. Mar Ecol Prog Ser 505:19–28.

Radford CA, Stanley JA, Simpson SD, Jeffs AG (2011a) Juvenile coral reef fish use sound to locate habitats. Coral Reefs 30:295–305.

Radford CA, Stanley JA, Tindle CT, Montgomery JC, Jeffs AG (2010) Localised coastal habitats have distinct underwater sound signatures. Mar Ecol Prog Ser 401:21–29.

Radford CA, Tindle CT, Montgomery JC, Jeffs AG (2011b) Modelling a reef as an extended sound source increases the predicted range at which reef noise may be heard by fish larvae. Mar Ecol Prog Ser 438:167–174.

Ricci SW, Bohnenstiehl DR, Eggleston DB, Kellogg ML, Lyon RP (2017) Oyster toadfish (Opsanus tau) boatwhistle call detection and patterns within a large-scale oyster restoration site. PLoS One 12:e0182757.

Rice AN, Soldevilla MS, Quinlan JA (2017) Nocturnal patterns in fsh chorusing off the coasts of Georgia and eastern Florida. Bull Mar Sci 93:455–474.

Rountree RA, Gilmore RG, Goudey CA, Hawkins AD, Luczkovich JJ, Mann D. (2006) Listening to fish: Applications of passive acoustics to fisheries science. Fisheries 31:433–446.

Sand O, Bleckmann H (2008) Orientation to auditory and lateral line stimuli. In: *Fish Bioacoustics*. Springer New York, p 192–240

Shwartz FJ (1974) Movements of the Oyster Toadfish (Pisces: Batrachoididade) about Solomons, Maryland. Chesap Sci 15:155–159.

Simon T, Joyeux J-C, Pinheiro HT (2013) Fish assemblages on shipwrecks and natural rocky reefs strongly differ in trophic structure. Mar Environ Res 90:55–65.

Spanier E (1979) Aspects of Species Recognition by Sound in Four Species of Damselfishes, Genus Eupomacentrus (Pisces: Pomacentridae). J Comp Ethol 51:301–316.

Staaterman E, Ogburn MB, Altieri AH, Brandl SJ, Whippo R, Seemann J, Goodison M, Duffy JE (2017) Bioacoustic measurements complement visual biodiversity surveys: Preliminary evidence from four shallow marine habitats. Mar Ecol Prog Ser 575:207–215.

Staaterman E, Paris CB, Kough AS (2014) First evidence of fish larvae producing sounds. Biol Lett 10:2–6.

Sueur J, Pavoine S, Hamerlynck O, Duvail S (2008) Rapid acoustic survey for biodiversity appraisal. PLoS One 3:1–9.

Suthers RA, Fitch WT, Fay RR, Popper AN (2004) Vertebrate sound production and acoustic communication. In (Fay RR & Popper AN (ed) Springer Handbook of Auditory Research. Springer, Switzerland.

Tolimieri N, Haine O, Jeffs A, McCauley R, Montgomery J (2004) Directional orientation of pomacentrid larvae to ambient reef sound. Coral Reefs 23:184–191.

Tolimieri N, Jeffs A, Montgomery JC (2000) Ambient sound as a cue for navigation by the pelagic larvae of reel fishes. Mar Ecol Prog Ser 207:219–224.

Urick RJ (1983) Principles of Underwater Sound. McGraw-Hill Inc., New York, NY.

Vermeij MJA, Marhaver KL, Huijbers CM, Nagelkerken I, Simpson SD (2010) Coral larvae move toward reef sounds. PLoS One 5:e10660.

Whitfield PE, Muñoz RC, Buckel CA, Degan BP, Freshwater DW, Hare JA (2014) Native fish community structure and Indo-Pacific lionfish Pterois volitans densities along a depth-temperature gradient in Onslow Bay, North Carolina, USA. Mar Ecol Prog Ser 509:241–254.

Table 2. 1 Acoustic features of fish calls that exhibited seasonal chorusing. Sample calls and pulses were extracted from each site and deployment chorusing was observed. The distribution of toadfish fundamental frequency was bimodal as such the mean and standard deviation of each mode is reported. The multiple values of bandwidth and peak frequency for the creak and growl describe each pulse in a pulse set.

Features	Toadfish	Knock	Creak	Growl
Duration (ms)	508.3 ± 106.4	7.7 ± 6.3	2281.1 ± 488.5	3350.1 ± 229.5
Fundamental Frequency (Hz)	147.9 ± 13.7 256.3 ± 6.7	--	--	--
No. Harmonics	2 (1 − 4)	--	--	--
Bandwidth (Hz)	--	553.4 ± 138.1	326.8 ± 100.6 420.2 ± 137.7	146.5 ± 24.7 367.8 ± 96.0
Peak Frequency (Hz)	--	653.4 ± 153.2	1669.4 ± 101.7 2728.7 ± 156.1	100.8 ± 22.9 160.9 ± 57.3
No. pulses in set	--	6.7 ± 4.0	56.3 ± 11.8	111.0 ± 7.8
Pulses per second	--	7.8 ± 8.9	24.8 ± 1.4	33.2 ± 1.1
No. calls summarized	161	399 pulses, 10 sets	646 pulse sets, 75 pulse trains	94 pulse sets, 23 growl trains
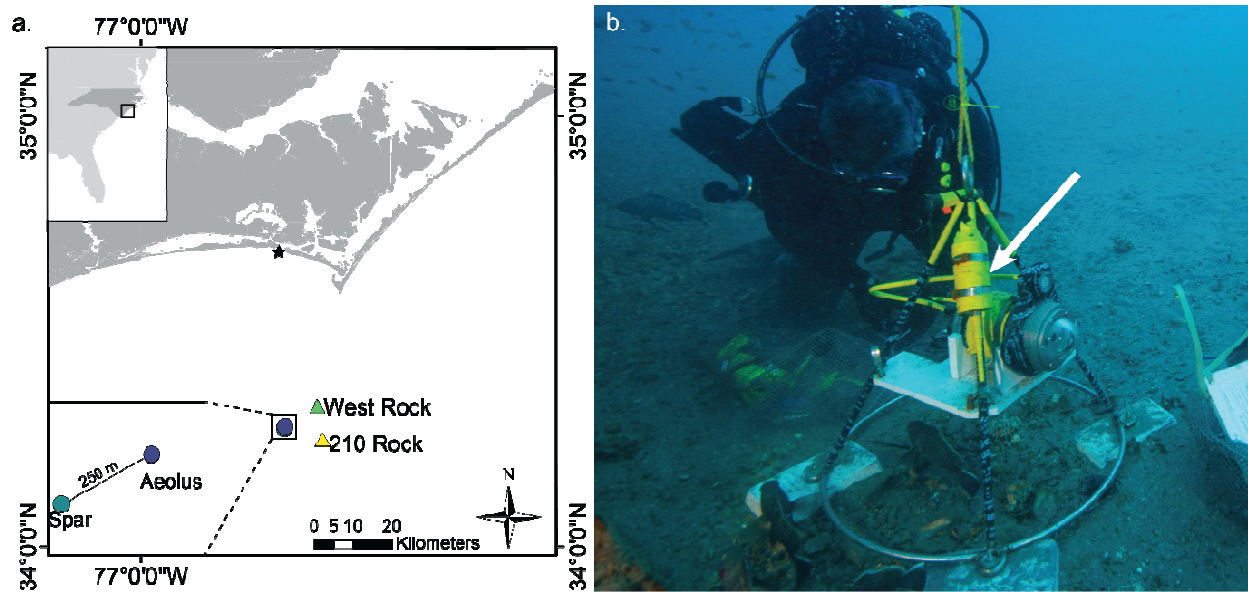
Figure 2. 1 Map of reef sites and hydrophone deployment setup. a. Reef sites offshore of Onslow Bay, NC. Triangles are natural reefs, circles are artificial reefs, and Beaufort Inlet is indicated by the star. b. Image of hydrophone deployment set-up, the arrow indicates the position of the SoundTrap. Photo credit: J. McCord / CSI
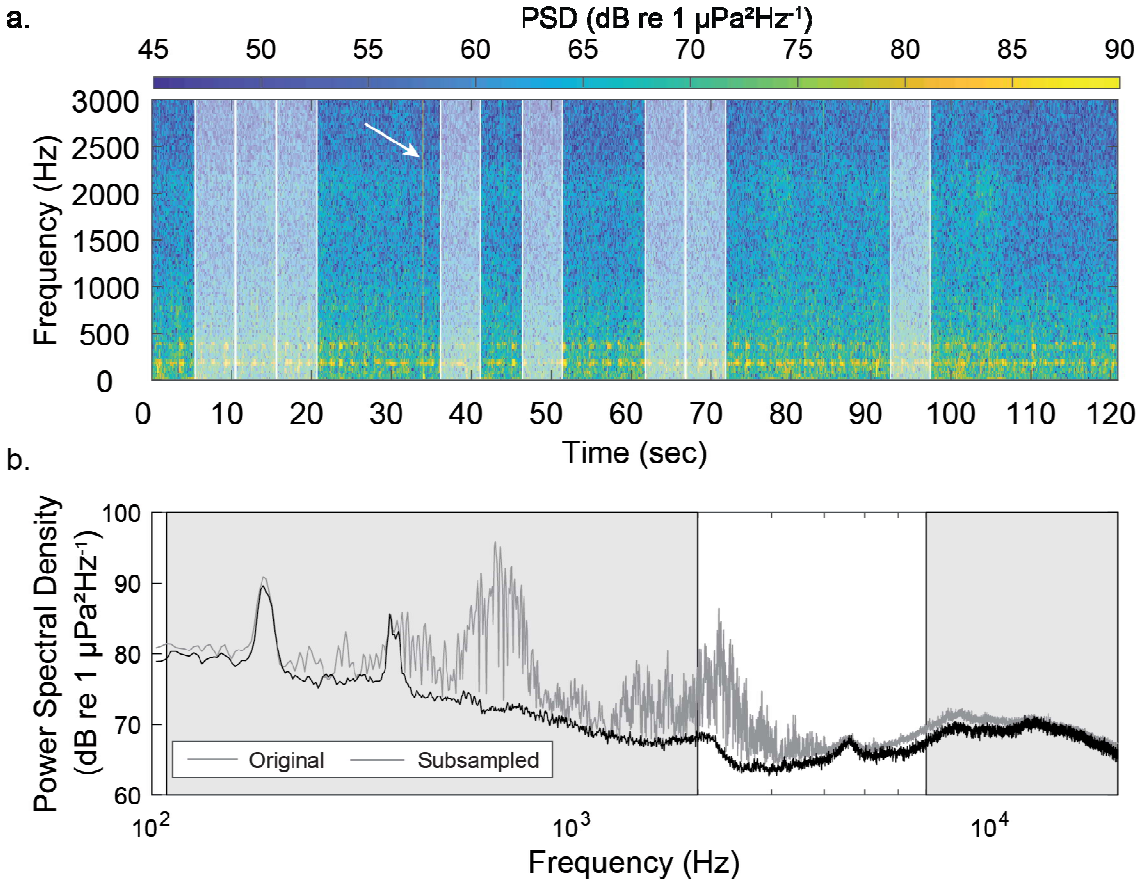
Figure 2. 2 Demonstration of the effect of a "fish bump" on the average power spectral density of a two-minute audio file. (a) Spectrogram of a representative file recorded on 210 Rock in April 2016. The arrow points to an impulsive signal likely the result of an animal collision with the hydrophone. The white shaded boxes indicate the eight quietest, five-second subsamples extracted to remove the effect of the fish bump. (b) Plot of power spectral density demonstrating that the subsampling methodology preserves the toadfish peaks while removing the noise due to the fish bump. The gray shaded boxes indicate the frequencies summarized in each frequency band.
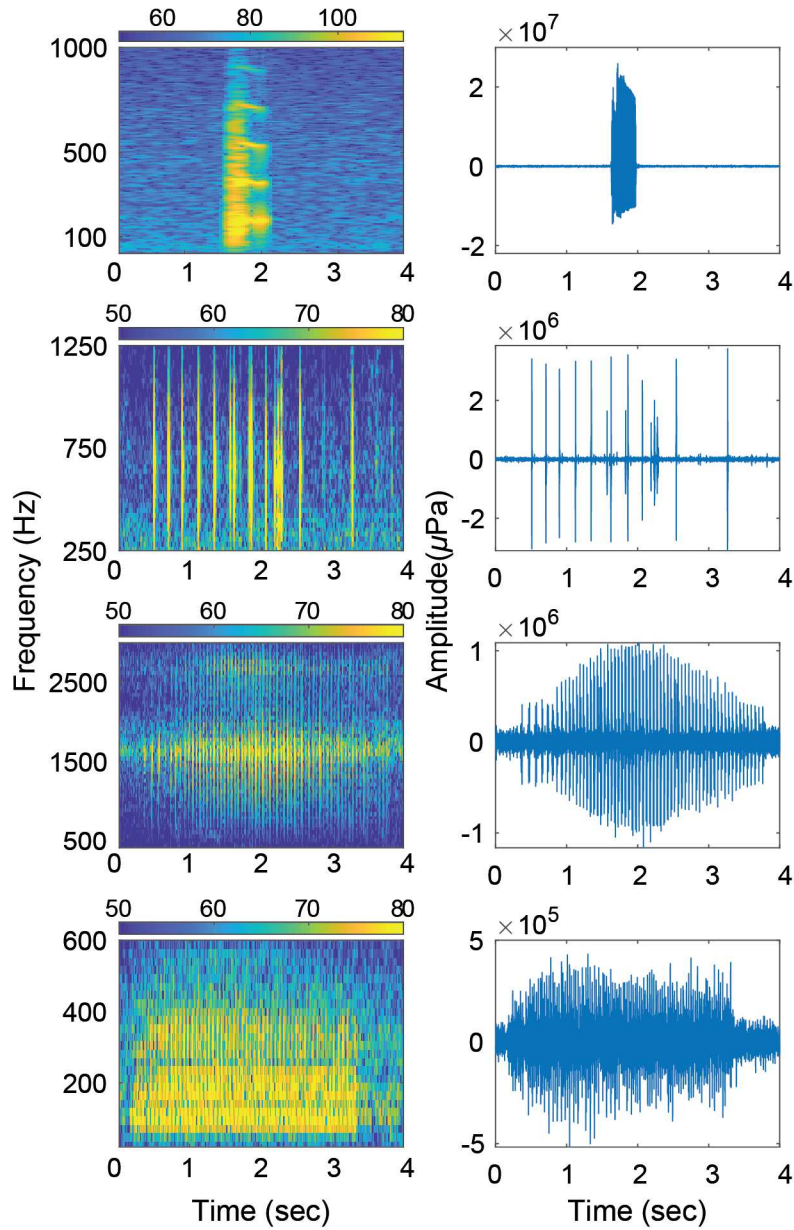
Figure 2. 3 Spectrogram (left panel) and waveform (right panel) of dominant fish calls observed. Note variations in y-axes scales. The colorbar is power spectral density (dB re 1 $\mu Pa^2 Hz^{-1}$) (a.) Toadfish boatwhistle (spectrogram NFFT = 2^{15}, 90% overlap); (b) unidentified knocks (spectrogram NFFT = 2^{12}, 90% overlap); (c) unidentified creak (spectrogram NFFT = 2^{11}, 90% overlap); (d) unidentified growl (spectrogram NFFT = 2^{12}, 90% overlap).
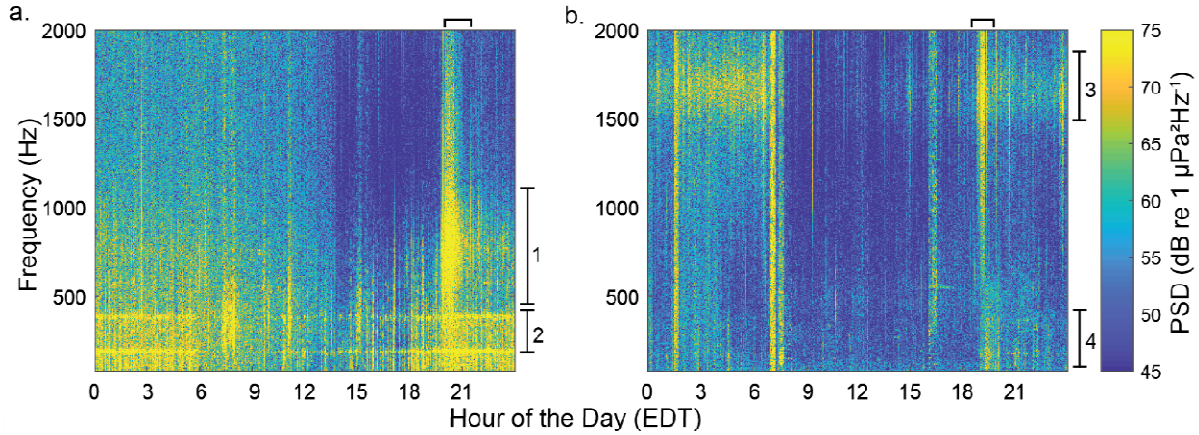
Figure 2. 4 Daily patterns of fish chorusing events during April and November. Each figure is a stacked spectrogram of all two-minute subsamples from a single day with representative fish chorusing events (NFFT = 2^{15}). The bracket on top of each panel identifies dusk and the numbered brackets on the right side identify the frequency bands of interest for each vocalizer. (1) knock, (2) toadfish, (3) creak, (4) growl. (a) Knock and toadfish choruses recorded during April on 210 Rock. Toadfish vocalizations were present throughout the day but peak during dusk, while the unidentified knock chorus was only present at dusk. (b) Creak and growl choruses recorded during November on West Rock. The creak chorus peaked during crepuscular periods while the growl chorus was only present at dusk.
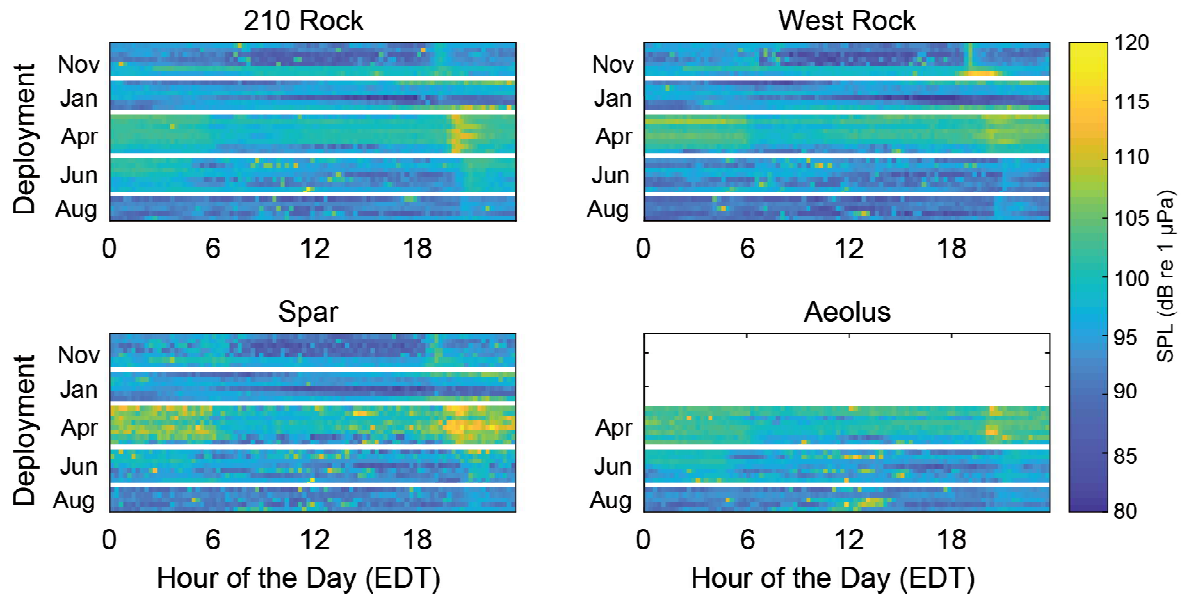
Figure 2. 5 Daily patterns in acoustic activity in the low-frequency band. Peak SPLs were observed at dusk on all sites and deployments, and are especially pronounced during November, April, and June when fish chorusing was observed. Each pixel represents the average SPL within one 40 second subsample and each row of pixels is the SPL variation over a single 24hr period. The white rows separate the deployments. All recordings within each deployment were concurrent on each reef.
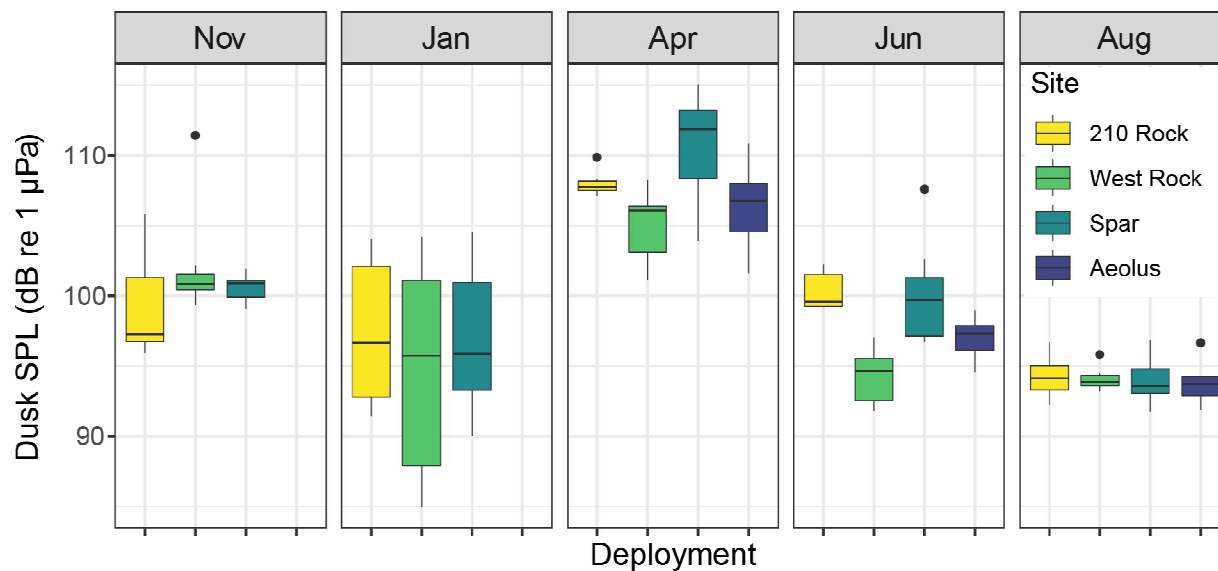
Figure 2. 6 Boxplots of average SPLs at dusk within the low-frequency band (0.1-2 kHz) highlight that variations in SPL are driven by seasonal variability rather than differences among the sites. The black bar is the median while the lower and upper edges of the box are the first and third quartiles. The whiskers extend to either the most extreme value or to 1.5 times the interquartile range and any outliers are plotted individually.
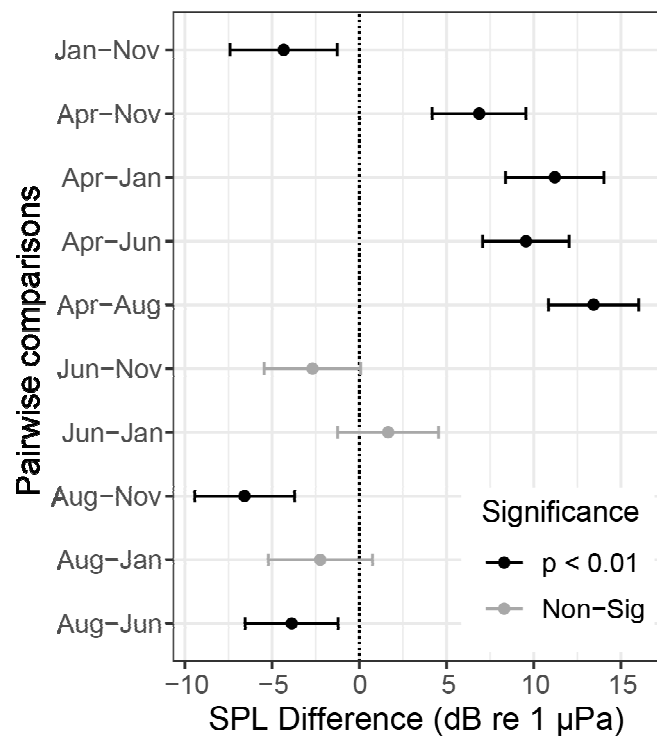
Figure 2. 7 Tukeys HSD 95% confidence intervals of pairwise comparisons between deployments for low frequency (0.1 – 2 kHz) dusk SPLs. This demonstrates that dusk SPLs during April were significantly higher than all other deployments and are driving the variability among the deployments.
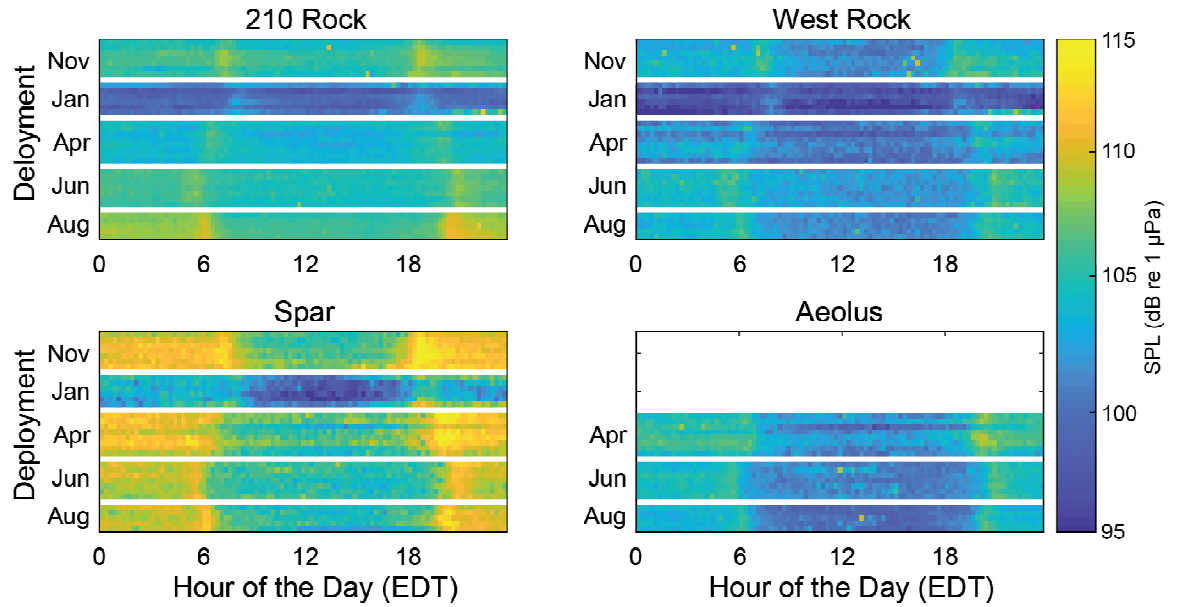
Figure 2. 8 Diurnal patterns in acoustic activity within the high-frequency band (7-20 kHz). Crepuscular peaks in SPL, attributed to snapping shrimp, are persistent across seasons and track the seasonal photoperiod. All sites exhibited the minimum SPLs in January. Each pixel represents the average SPL within one 40 second subsample and each row of pixels is the SPL variation over a single 24hr period. The white rows separate the deployments. All recordings within each deployment were concurrent on each reef.
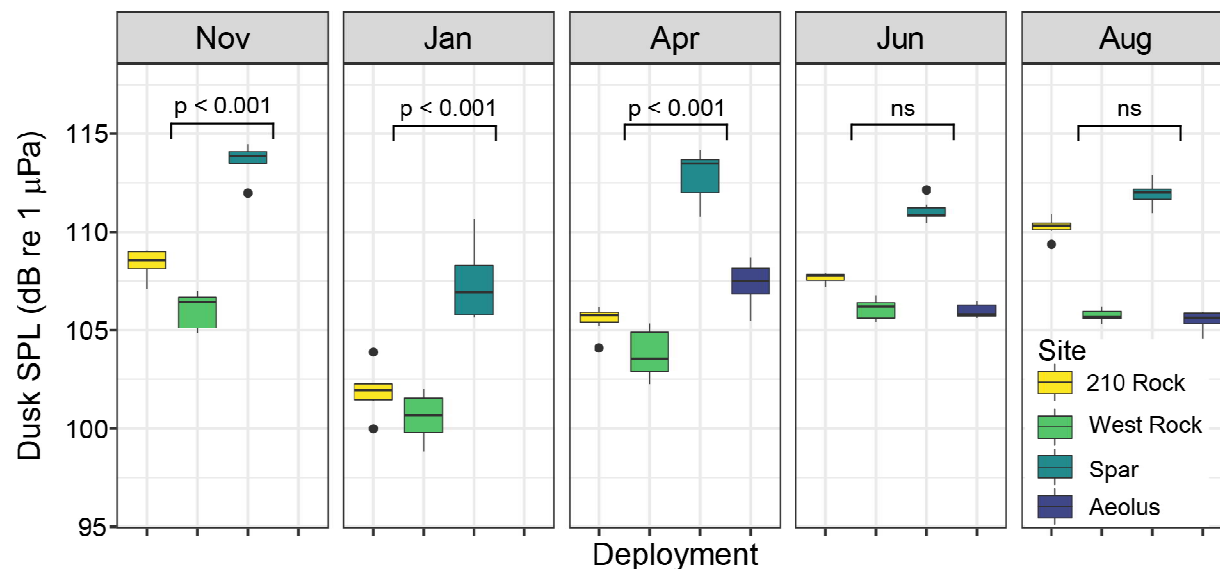
Figure 2. 9 Boxplots of average daily SPLs at dusk in the high-frequency band (7-20 kHz). During the first three deployments dusk SPLs were significantly higher on artificial reefs than natural reefs, while variation among the sites is driven by increased SPLs on the *Spar*. The p-values are the result of Tukeys HSD test of pairwise comparisons between the reef types. For the boxplots, the black bar is the median while the lower and upper edges of the box are the first and third quartiles. The whiskers extend to either the most extreme value or to 1.5 times the interquartile range and any outliers are plotted individually.
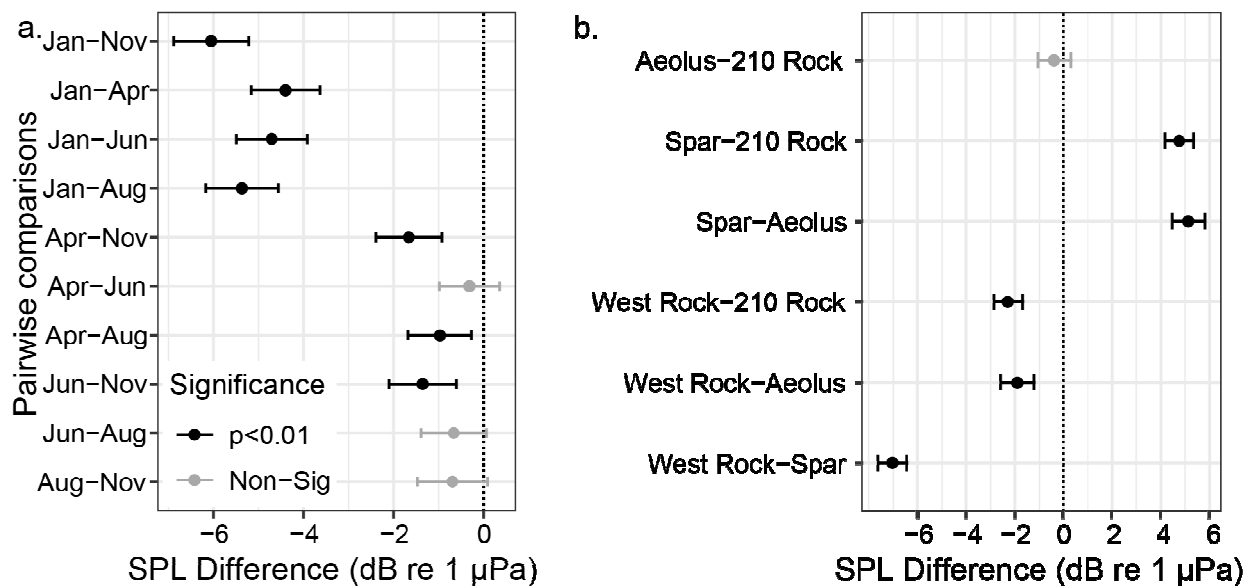
Figure 2. 10 Tukeys HSD 95% confidence interval of pairwise comparisons between (a) deployments and (b) sites for the high frequency (7 – 20kHz) dusk SPLs. The results demonstrate seasonal variation is driven by reduced SPLs during January (Deployment 2), while variation among the sites is driven by elevated SPLs on the *Spar* and reduced SPLs on West Rock. Moreover, within reef type the *Spar* and 210 Rock are louder than the *Aeolus* and West Rock, respectively.
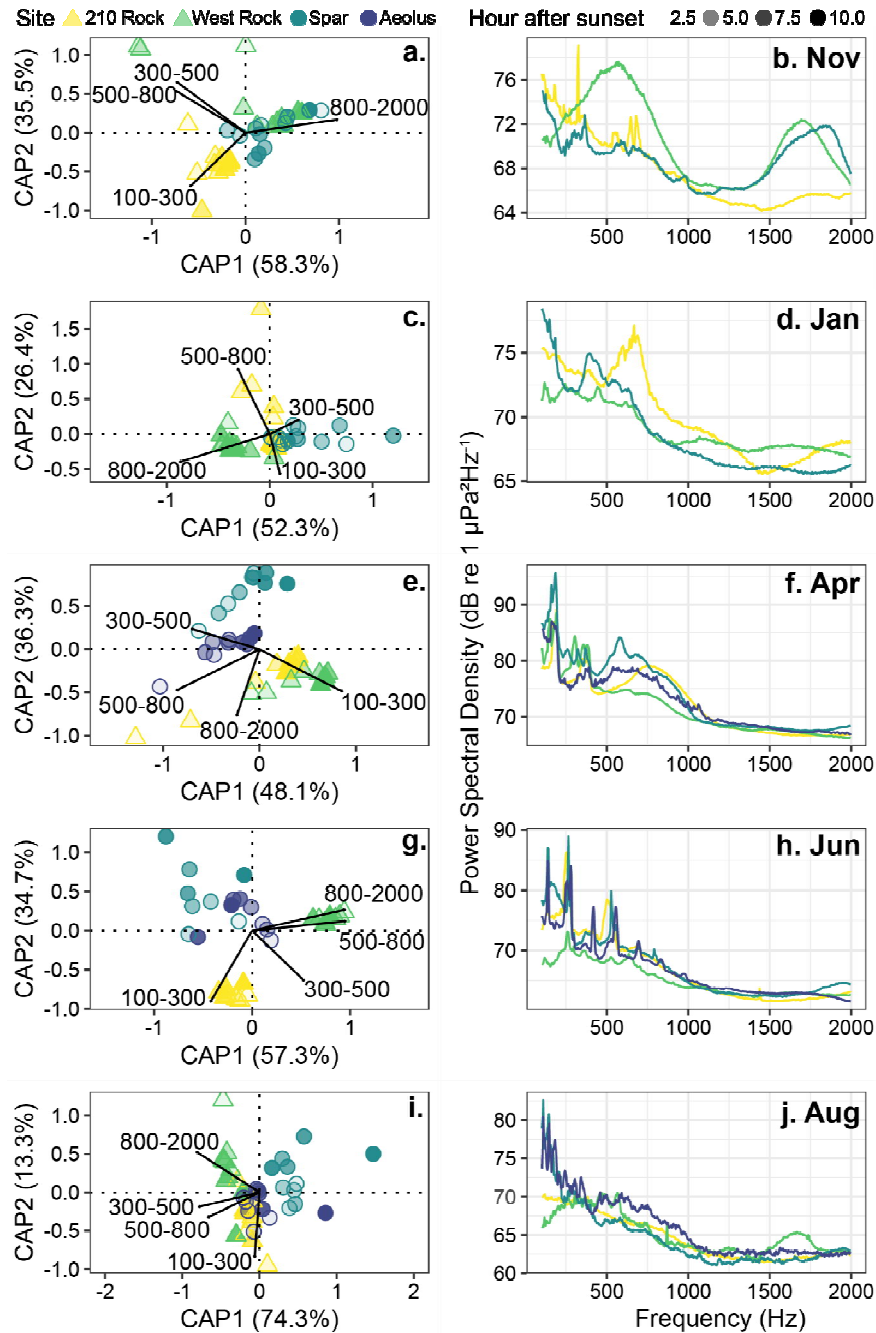
Figure 2. 11 Multivariate analyses on the spectral dissimilarity index suggest that during deployments with increased acoustic activity in the low-frequency band (0.1-2 kHz) there is distinct separation of the spectral content at each reef, with increased separation between the reef types. This difference between natural and artificial reef was especially pronounced during April. As each reef type contains the same dominant vocalizers, differences between natural and artificial reefs are likely the result of less dominant vocalizations and miscellaneous acoustic activity. The left column contains the dbRDA ordinations of the spectral dissimilarity index for each deployment, while the right column contains the average spectra for each site within each deployment (note change in PSD scale).

CHAPTER 3: EAVESDROPPING ON ESTUARIES: SOUNDSCAPE SPATIAL VARIATION EXPLAINED BY ABIOTIC METRICS AND HABITAT METRICS AT MULTIPLE SCALES

Introduction

Understanding spatial heterogeneity and its consequences for ecological patterns and processes is a foundational goal of landscape ecology that also informs conservation and management practices (Turner 2005; Boström et al. 2011). For example, a landscape approach revealed how interactions between spatial heterogeneity and animal behavior affect how animals move within and among habitat patches (Wiens et al. 1997). Studying the effect of heterogeneity on ecological communities has identified associations with increased diversity and stability of grassland birds (Hovick et al. 2015), as well as the density and richness of fish communities in mangrove systems (Pittman et al. 2007). More recently, the developing field of soundscape ecology has drawn from this body of research to explore how the sounds produced across a landscape, referred to as the soundscape, relate to the underlying landscape and ecological patterns (Villanueva-Rivera et al. 2011; Farina et al. 2014).

A conceptual framework of soundscape ecology posits that the diverse temporal, spatial, and spectral patterns observed among soundscapes are the result of interactions between biological communities, landscape structure, and anthropogenic activities (Pijanowski et al. 2011). As such, many studies across terrestrial and marine ecosystems have attempted to describe the relationship between soundscape patterns and environmental heterogeneity (Gasc et al. 2017; Lindseth and Lobel 2018), often through the use of acoustic metrics (Sueur et al. 2008).

These methods have been applied with some success in terrestrial communities, for example, relative sound power of biophony in an Australian forest was positively correlated with patch size and connectivity to adjacent remnant patches (Tucker et al. 2014), and multiple acoustic indices effectively tracked recovery of island seabird populations in the years after removal of an invasive predator (Borker et al. 2020). In marine systems, soundscape studies have produced varied results with evidence of positive correlations between low frequency sounds and benthic complexity and density of benthic invertebrates (Freeman and Freeman 2016), as well as fish density and diversity (Kennedy et al. 2010) in coral reef systems. Meanwhile, other studies have found limited support for the use of currently available acoustic indices as indicators of habitat or community variables (Bohnenstiehl et al. 2018; Bolgan et al. 2018; Lyon et al. 2019; Mooney et al. 2020; Dimoff et al. 2021). Given that acoustic signals generally propagate independently of light and oceanographic conditions and passive acoustic monitoring is a non-invasive, cost-effective sampling method, the goal of understanding soundscape variation is often to evaluate whether soundscape monitoring could be applied to conservation and management contexts.

Passive acoustic monitoring of marine soundscapes and species-specific call rates have been used to identify essential habitats (Luczkovich et al. 2008; Ricci et al. 2017b), evaluate restoration success (Butler et al. 2016), and assess interactions with anthropogenic activity (Kline et al. 2020). However, for soundscape monitoring to be successfully applied in management contexts, a more detailed understanding of soundscape heterogeneity is required. Although temporal patterns differ among habitat types and biogeographic regions, these patterns are well understood and are often associated with known environmental cycles and the phenology of soniferous species (Staaterman et al. 2014; Bohnenstiehl et al. 2016; Monczak et al. 2019). In contrast, there is comparatively little agreement on the drivers of soundscape spatial variation.

Many early assessments of spatial variation identified that different habitat types have unique soundscape signatures, such as oyster reefs compared to unvegetated sand flats (Lillis et al. 2014), and urchin-dominated reefs compared to macroalgae-dominated reefs (Radford et al. 2010). More recent studies have evaluated the soundscape variability across a range of habitat complexity (Ricci et al. 2017b; Lyon et al. 2019; Elise et al. 2019), though these previous studies have frequently only captured variation across a small spatial scale or within a single habitat type (Nedelec et al. 2015).

Because estuaries typically consist of a mosaic of habitat types, it is necessary to explore how spatial heterogeneity in the seascape, biodiversity, and abiotic factors affect observed estuarine soundscape patterns. Moreover, there is a rich body of research focused on both understanding the relationship between faunal communities and the seascape (Yarnall et al. 2022), and on the soundscape of estuarine habitats (Ricci et al. 2016; Monczak et al. 2020; Luczkovich and Sprague 2022). Beyond their utility as a study system, estuarine habitats provide numerous beneficial functions for ecosystems and society. For example, they serve as critical nursery habitats for marine animals (Beck et al. 2001), buffer against shoreline erosion (Scyphers et al. 2011), and sequester carbon (Duarte and Krause-Jensen 2017). Despite the fundamental role of estuarine habitats for healthy coastal ecosystems and economies, they have experienced substantial global declines in recent decades (Orth et al. 2006; Beck et al. 2011). Taken together, this makes even more compelling the possibility of using soundscape monitoring to address questions of estuarine biodiversity and habitat conservation.

To expand understanding of soundscape spatial variation across the scale of an estuary, the present study pairs soundscape metrics with habitat and biodiversity sampling at two dozen habitat patches with unique configurations of estuarine habitat mosaics. We ask two research

questions: (1) Is soundscape variation among the sampled patches clustered in common soundscape "types" and (2) Do patch-scale habitat, landscape-scale habitat, community, and/or abiotic metrics explain the observed variation in soundscape metrics. We summarized the soundscape with both aggregate indices, such as sound pressure level and the spectral dissimilarity index, as well as species-specific call rates and employed multivariate analyses, linear regression, and variance partitioning to address these questions. Lastly, following unexpected results during preliminary analyses, we conducted a playback experiment to quantify the effect of seagrass cover on acoustic transmission loss to aid interpretation of our results.

Methods

To evaluate whether spatial variation in estuarine soundscapes is correlated with habitat, community, and abiotic metrics we sampled 24 habitat patches in Back and Core sounds, North Carolina (NC), during six sampling periods from May to August 2019 (Fig. 1). Back and Core sounds are shallow well-mixed estuaries with salinities ranging from 24 – 36 ppt and a complex mosaic of seagrass, saltmarsh, and mudflat habitats (Kenworthy et al. 1982). Back Sound extends east to west and meets the northeast to southwest oriented Core Sound at Cape Lookout, NC. Situated at a temperate-subtropical boundary, the seagrass beds sampled exhibit co-dominance of the temperate species *Zostera marina* and subtropical species *Halodule wrightii*, with some presence of *Ruppia maritma.* The saltmarshes consisted of complex configurations dominated by *Spartina alterniflora* with tidal creeks and adjacent oyster reefs of *Crassostrea virginica*, while the mudflats consisted of expanses of unvegetated, sandy bottom separated from structured habitat by at least 200 m.

To facilitate pairing of community data with habitat and soundscape data, all sites were randomly selected from a collection of 18 seagrass beds, 9 saltmarsh creeks, and 9 mudflats in Back Sound, NC, that have been sampled monthly since 2010 (Baillie et al. 2015). Each sampling period consisted of an approximately week-long hydrophone deployment at either one saltmarsh creek, two seagrass beds, and one mudflat, or two saltmarsh creeks and two seagrass beds. Due to the greater number of seagrass meadows available and to capture greater variability among habitat patches with structured biogenic habitat, more seagrass and saltmarsh creek sites were sampled than mudflats. All hydrophones were deployed near low tide to ensure that the hydrophone would remain submerged throughout the deployment. The hydrophone position was haphazardly selected within a habitat patch of interest where low-tide water depth was > 0.7 m. The hydrophones were mounted approximately 0.15 m above the seafloor and secured to a metal garden stake.

Acoustic Analysis

All hydrophones were SoundTrap ST200s (Ocean Instruments, NZ) that recorded audio for two minutes every 15 minutes at a 48kHz sampling rate and measured water temperature every 60 s while recording. This recording duty cycle extended battery life of the hydrophone while retaining natural soundscape variability in the dataset (Bohnenstiehl et al. 2018). The power spectrum of each retained two-minute audio file was summarized using a Fast Fourier Transform (NFFT = 2^{15}, 0% overlap, Hanning window). During this summary each two-minute file was further subsampled to reduce the impact of anthropogenic noise and "fish bumps", which are anomalously high-amplitude impulsive signals caused by an animal colliding with the hydrophone that distort the sound level and power spectrum of an audio file, on the acoustic timeseries. This subsampling was accomplished by dividing the file into non-overlapping five-

second segments and averaging the eight quietest segments. This summary method was demonstrated to reduce the impact of impulsive noise while retaining the PSD of all other signals in Van Hoeck et al. (2020).

In addition to the acoustic spectrum, the soundscape of each site was summarized by its average sound pressure level (SPL). To separate the contribution of fish and invertebrates to the soundscape, SPLs were calculated for the fish-dominated low frequency band from $0.1 - 2$ kHz and the snapping shrimp dominated high frequency band from $7 - 15$ kHz. All SPLs are root-mean-square SPLs and are reported in decibels referenced to 1 µPa. Because the observed SPL in shallow water is affected by tidal inundation and marine bioacoustic activity tends to increase at night, only audio files that were ± 2 hours around a nighttime high tide were retained for SPL analyses. This subsampling standardized the effective sampling radius across tidal inundation, while simultaneously reducing the presence of anthropogenic noise and improving the ability to interpret bioacoustic activity.

Manual spectrogram inspection of each site identified at least six unique fish call types, including oyster toadfish (*Opsanus tau*), silver perch (*Bairdiella chrysoura*), spotted seatrout (*Cynoscion nebulosus*), multiple unidentified knocks, and an unidentified growl. Due to a lack of existing automatic call detectors and multiple call types occurring simultaneously within the same frequency range, only oyster toadfish and silver perch call rates could be reliably quantified. Fish calls were identified using species-specific call detectors on the full two-minute audio files. Average call rates for each species were calculated for nighttime files when calling was present.

Oyster toadfish boatwhistles were enumerated with a multi-kernel spectral correlation detector adapted from Ricci et al. 2017a. The method searches for the first two harmonic tones of

the boatwhistle, using template kernels frequency constrained by the previously established relationship between call frequency and water temperature (Fine 1978; Ricci et al. 2017a). A correlation threshold of 0.25 was used for detection. To suppress false positive detections, files with a <6 calls per minute were masked in the analysis, and any call with a fundamental frequency that differed by more than 20% from the deployment median was excluded. Lastly, a scatter plot of the median fundamental frequency of toadfish boatwhistles in a file versus water temperature was viewed for each site and any sites without a linear relationship were manually inspected and false positives removed.

Silver perch call rates were summarized using a two-stage process of detection and classification (Bohnenstiehl in prep). In the detection stage, candidate calls were identified based on the kurtosis and signal to noise ratio (SNR) calculated in 10-ms duration sliding windows operating in the 2 – 3.5 kHz frequency band, where silver perch are the dominant sound producers. When peaks in SNR and the derivative of kurtosis co-occurred, a 30 ms window of data was extracted and used to generate a wavelet scalogram image. Next, the images were fed into the convolutional neural network (CNN) ResNet50. The activations from the connected layer (fc1000) of ResNet50 were used as features for a support vector machine classifier that identified the scalograms as "perch" or "other".

The model was trained using 10,000 labeled scalograms (5,000 "perch" and 5,000 "other") from soundscape data in the Pamlico Sound, NC. To confirm detector functionality, the model was tested on 4,374 labeled scalograms from the present dataset (2,273 "perch", 2,101 "other") and an overall false positive rate of 1.37% was identified. For a given file, if the number of perch calls detected was lower than the estimated number of misclassified images, then the number of perch calls was set to zero. Because silver perch calls have a known temporal pattern,

with call rates increasing after sunset to a maximum around midnight, the call rate timeseries for each site were visualized and any unexpected patterns were inspected (Mok and Gilmore 1983; Monczak et al. 2017; Ricci et al. 2017b). Based on this inspection, any remaining false positives were manually removed.

Ecological metrics

Patch-scale habitat characteristics were summarized via quadrat sampling along three 50 m transects centered on the hydrophone. The percent cover of each species was visually estimated within a 0.125-m^2 quadrat every 5 m along the transect. If seagrass was present, then shoot density was counted and canopy height was summarized at every other quadrat. Canopy height was measured by randomly collecting 10 shoots from each quadrat for measurement at the lab. Each patch-scale habitat metric was averaged across all quadrats and transects for a site average. In addition to percent cover, alpha diversity metrics of patch-scale habitat variables were summarized (i.e., species richness, evenness).

Landscape-scale habitat characteristics, defined as a 500-m radius around the hydrophone, were summarized in ArcMap version 10.8.1 (ESRI, California, USA) from 4-band orthoimagery with 6 in pixel resolution that was collected in early 2020 by NC OneMap. After isolating the landscape area for each site, the types of habitat present were classified using the interactive supervised classification algorithm in ArcMap. The habitat-classified raster images were then exported with a 1-m pixel resolution and landscape metrics, including total area, indices of shape, and perimeter-to-area ratios were calculated for each habitat type using the SDMTools package in R (VanDerWal et al. 2014). Additionally, total area of habitat-forming species and nearest neighbor ratios were calculated for each site at the landscape scale. Lastly, alpha diversity metrics were summarized using the total area of each habitat-forming species.

The community at each site was summarized via two benthic trawls on the last day of the hydrophone sampling period. Trawls were conducted near high tide using a 5-m wide otter trawl without a tickler chain (5-m head rope, 2-cm mesh, 0.6-cm cod-end mesh). Each trawl was towed for 2.1 ± 0.3 min (mean $\pm$ 1 SD) at a speed of 3.8 ± 0.5 km/hr. During the trawl tow, the water temperature and salinity were recorded. The number of each species caught was counted on the boat and all organisms were released after the second trawl was completed. The catch per unit effort (CPUE) of each species was calculated by adding the two trawls together and standardizing to the number of individuals per 200-m trawled. Community metrics summarized for each site included total CPUE, silver perch CPUE, alpha diversity metrics, and the richness of soniferous species. Silver perch CPUE was retained for future analyses because they were among the most common species caught and their call rates were summarized in soundscape analyses. Depth and salinity recorded during the trawls were retained as abiotic metrics for future analyses. Additionally, the average water temperature for each site was calculated from the hydrophone measurements and included as an abiotic metric.

Statistical analysis

Non-metric multidimensional scaling (NMDS) was used to evaluate whether variation in soundscape spectral content among the sites was correlated with the habitat, community, or environmental metrics calculated. The spectral content was summarized by calculating the average low-frequency (0.01 – 2 kHz) power spectral density (PSD) during the nighttime high tide for each site, then pairwise dissimilarities were calculated using the spectral dissimilarity index (Sueur et al. 2008) resulting in a distance matrix. The variation among the soundscapes was visualized with an ordination plot, where each point represents the average soundscape of a single site. Next, the candidate ecological metrics were fit to the ordination and metrics with

59

significant correlations with the ordination axes were visualized as vectors. Significance was determined by permutation of the environmental variables using an alpha value of 0.05. All ordination methods were conducted using the "vegan" package (Oksanen et al. 2019) in R studio version 4.0.3 (R Core Team 2020).

To explore whether the sites were grouped into "soundscape types", cluster analysis was performed on the spectral dissimilarity matrix using the R package "cluster" (Maechler et al. 2019). The number of clusters retained was selected based on inspection of the cluster dendrogram and the average spectra of the sites within each cluster. The retained clusters were visualized in the ordination using 95% confidence ellipses. Lastly, the soundscape type represented by each cluster was described by the average acoustic spectrum and the 5 - 95 quantile PSD of all sites within the cluster.

Once all soundscape, habitat, community, and abiotic metrics were calculated, pairwise Pearson's correlation matrices between all metrics were investigated for each soundscape response variable. When two metrics had a correlation coefficient magnitude greater than 0.7, only the metric with a stronger correlation with the soundscape response variable was retained for future analyses. Next, a candidate metric set for each soundscape response variable was identified by retaining all ecological metrics that had a correlation greater than $\pm$ 0.3 with the soundscape metric.

To investigate whether soundscape variation was explained by the ecological metrics, the relationship between each soundscape metric and its candidate ecological metric set was evaluated using multi-model inference on linear least squares regressions and a variance partitioning analysis. To prevent spurious correlations, all candidate metrics were grouped by their metric type (ie., patch-scale habitat, landscape-scale habitat, community, and abiotic). Next,

models with all possible combinations of ecological metric categories were evaluated and the

model with the best fit to the data was identified using AICc. Lastly, a variance partitioning

analysis was conducted to quantify the unique variation in the soundscape response variable

explained by each ecological metric category.

<u>Transmission loss experiment</u>

During preliminary analysis of the relationships between ecological and soundscape

metrics we identified negative correlations between multiple soundscape metrics and seagrass

metrics at both patch and landscape scales. Based on current understanding regarding the

positive effect of seagrass cover and area on fish abundance and species richness (Yeager et al.

2016), we hypothesized that the relationship between seagrass cover and sound levels or call

rates would be positive. To facilitate interpretation of whether the observed negative trend was a

true ecological pattern or a result of the physics of sound propagation in shallow, vegetated water

we conducted a playback experiment to measure transmission loss.

The playback experiment consisted of ten repeated trials at two sites, one contiguous

seagrass bed and one unvegetated mudflat. The playback audio included a series of 0.5-s tones at

eight frequencies ranging from 0.1 – 10 kHz, capturing the full range of relevant bioacoustic

activity. The experiment was conducted using an underwater speaker (Lubbel Labs UW-30) that

was suspended 0.5-m above the seafloor and oriented towards a transect of hydrophones. A

hydrophone was placed 1-m in front of the speaker to record the source level (SL) of the tones.

The received sound level (RL) was recorded at seven points ranging from 2 – 64-m away from

the speaker, with the distance to next hydrophone doubling at each point. All hydrophones were

mounted approximately 0.5-m above the seafloor. Due to the limited number of hydrophones, the

experiment was conducted in two phases. First, hydrophones were placed 2-, 4-, and 8-m away

from the speaker. Then, they were placed at 16-, 32-, and 64-m away from the speaker. The reference hydrophone at the 1-m mark was kept in place for the entire experiment, to ensure consistency between the two phases. The source and received sound levels were summarized by isolating each tone using the signal analyzer app in MATLAB. Transmission loss (TL) was calculated following the equation, $TL = SL - RL$.

Results

Ecological metrics

At the patch-scale, total biogenic habitat cover ranged from 0 – 80%, with all mudflats lacking vegetation and the highest total cover observed at seagrass beds. Among the seagrass beds sampled, one site had oysters present otherwise they consisted solely of seagrass. *Halodule wrightii* was the most common species observed, followed by *Zostera marina*, then *Ruppia maritma*. The saltmarsh creeks sampled consisted of varying combinations of saltmarsh grasses and oyster reefs, except for one creek where oysters were absent, and seagrass was observed (Fig. 2A). At the landscape scale, total area of biogenic habitat ranged from 0 – 350,000 m^2, with 16 out of 24 landscapes containing all 3 habitat types quantified and one landscape lacking biogenic habitat completely (Fig. 2B).

Catch rates of the nektonic community at each site ranged from 0 – 868 CPUE, with seagrass beds having the highest catch rates and species richness (Fig. 2C). Silver perch were collected at 10 of the sites sampled, including nine seagrass beds and one saltmarsh creek. Salinities and depths recorded at the time of trawling ranged from 32 – 37 ppt and 0.4 – 1.5 m, with an average of 35.1 ppt and 0.9 m, respectively. Nighttime temperatures ranged from 18.5 – 34.4ºC, with a mean of 25.7ºC. Temperature exhibited a seasonal pattern, increasing to a

maximum during the fourth deployment in mid-July, then decreasing slightly through the final deployment in late August (Fig. 3).

Multivariate analysis

Ordination of the spectral dissimilarity index captured soundscape variation among the sites as well as trends among the habitat types. In general, the soundscapes of saltmarsh creeks and mudflats tended to be more similar to each other and were separated from seagrass soundscapes along NMDS axis 1 (Fig. 4). Specifically, axis 1 was positively correlated with patch-scale *Halodule wrightii* cover ($r^2 = 0.45$, $p = 0.004$) and was negatively correlated with landscape-scale oyster perimeter ($r^2 = 0.27$, $p = .03$). This pattern was also reflected in the cluster analysis. Following inspection of the cluster dendrogram and associated acoustic spectra, four distinct clusters plus a single site outlier were retained for description of the soundscape types. These consisted of two saltmarsh-like soundscapes and two seagrass-like soundscapes. Of which, the average acoustic spectra of each cluster suggests that the primary difference between the two clusters within a habitat type was the intensity of silver perch calls (Fig. 5).

Both saltmarsh-like clusters were associated with landscape-scale oyster perimeter. The average acoustic spectra of each cluster suggests that the primary difference between the two saltmarsh soundscapes was the presence or absence of silver perch chorusing. Cluster A included two saltmarsh creeks and three mudflats. The average acoustic spectra of the cluster showed that the soundscapes consisted of oyster toadfish and multiple unknown fish callers in the $100 - 800$ Hz bandwidth but were dominated by silver perch choruses (Fig. 5A). Conversely, cluster B included three saltmarsh creeks and one seagrass bed with soundscapes consisting of oyster toadfish, multiple unknown fish calls between $300 - 800$ Hz, and snapping shrimp (Fig. 5B). An exception to this pattern was occasional silver perch calls at two creek sites in Cluster B.

The two seagrass-like clusters were associated with patch-scale *Halodule* cover and variation within the clusters was associated with increased seagrass core area at the landscape scale ($r^2 = 0.51$, $p = 0.001$) and silver perch CPUE ($r^2 = 0.27$, $p = 0.04$). Cluster C included three seagrass beds and one saltmarsh creek, and the average acoustic spectra showed that the soundscape contained multiple callers within the 100 – 500 Hz band and silver perch (Fig. 5C). Cluster D encompassed the most soundscape variation of the clusters, including seven seagrass beds, two saltmarsh creeks, and one mudflat. The average acoustic spectra showed that this soundscape type consisted of oyster toadfish, occasional silver perch calls, multiple unknown callers between 100 – 1400 Hz, and snapping shrimp (Fig. 5D).

Soundscape and ecological metric correlation

Average low frequency SPL during nighttime high tides ranged from 90.15 - 115.94 dB re 1 μPa. Seagrass beds tended to be the quietest sites and mudflats the loudest. After removing redundant ecological metrics, 24 candidate ecological metrics across all four metrics categories were identified for correlation with low frequently SPLs. At the patch-scale, low frequency SPL was negatively correlated with *Ruppia maritma* ($r = -0.31$), habitat species richness ($r = -0.59$), and maximum seagrass canopy height ($r = -0.52$). At the landscape-scale, low frequency SPL was negatively correlated with seagrass core area ($r = -0.39$), but positively correlated with seagrass perimeter area ratio ($r = 0.32$) and oyster perimeter (0.48). Low frequency SPL was also negatively correlated with silver perch CPUE ($r = -0.38$), and average temperature ($r = -0.49$) (Fig. 6).

Model selection identified the model with patch- and landscape-scale habitat, and abiotic metrics as the model with the best support for the variation in low frequency SPLs. The model of low-frequency SPL captured 75.80% of the total variance, with landscape-scale habitat variables

explaining the most unique variance at 31.29%. Patch-scale habitat variables uniquely explained 25.36% and abiotic variables explained 9.88% of the variance (Table 1).

Average high frequency SPLs during nighttime high tides ranged from 85.30 – 112.72 dB re 1 µPa and tended to be lower at mudflats. Of the 22 candidate ecological metrics, high frequency SPL was correlated with metrics from all four categories including, positive correlations with habitat species evenness (r = 0.32), habitat type richness (r = 0.33), and total cover (r = 0.54) at the patch scale, oyster perimeter (r = 0.55) at the landscape scale, and soniferous species richness (r = 0.34). Among abiotic metrics summarized, deployment number (r = 0.56), temperature (r = 0.45), and depth (r = 0.42) were positively correlated with high frequency SPLs, while salinity was negatively correlated (r = -0.43; Fig. 7).

Model selection by AICc identified two models with similar support for the observed high frequency SPLs, one with patch-scale habitat, landscape-scale habitat, and community metrics and one with only patch- and landscape-scale habitat metrics. Variance partitioning was conducted using the more complex model to more fully quantify the variance explained by each metric type. The total variance explained was 72.15% with most of the unique variance explained by patch- and landscape-scale habitat variables at 38.47% and 36.75%, respectively. Community variables uniquely explained 2.90% of the variance (Table 1).

Toadfish boatwhistles were observed during the first five deployments at 10 of the 24 sites including seven seagrass beds and three saltmarsh creeks. Call rates ranged from 8 – 32.01 calls per two minutes. Of the 21-candidate metrics identified, toadfish call rates were positively correlated with richness of habitat types (r = 0.35) and total habitat cover (r = 0.47) at the patch scale, as well as oyster core area (r = 0.54), seagrass perimeter (r = 0.31), and total habitat area (r

= 0.35) at the landscape scale. Call rates were also correlated with carnivore CPUE (r = 0.32) and deployment number (r = -0.52; Fig. 8).

The model selection with AICc identified two models with similar support for the observed toadfish call rates. These included the model with patch-scale habitat, landscape-scale habitat, and abiotic variables as well as the model with only patch-scale habitat and abiotic variables. To fully capture variation explained by each metric category, the model with three categories was used in the variance partitioning analysis. This model captured 77.92% of the variance in toadfish call rates, with the most unique variance attributed to the abiotic metric, water temperature, at 32.31%, followed by patch-scale habitat metrics at 16.58%, and landscape-scale habitat metrics at 12.42% (Table 1).

Silver perch calls were observed at 14 sites across the first five deployments, including five seagrass beds, five saltmarsh creeks, and all four mudflats. Call rates ranged from 10.13 – 1083.04 and were correlated with ecological metrics from all four categories out of the 22 candidate ecological metrics identified. Specifically, at the habitat patch scale, silver perch call rates were negatively correlated with species richness (r = -0.52) and habitat type richness (r = -0.32). While at the landscape scale, call rates were correlated with seagrass core area (r = -0.36) and the distance to the nearest habitat patch (r = 0.52). The only community and abiotic metrics with correlations to silver perch call rates were soniferous species richness (r = -0.45) and water temperature (r = -0.51; Fig. 9).

Model selection via AICc identified the model with only landscape-scale habitat and abiotic variables as the best fit observed silver perch call rates. The most unique variance was explained by landscape scale habitat variables at 29.80%. Abiotic variables explained 16.07% of the variance and the model captured 55.68% of the total variance (Table 1).

<u>Transmission loss experiment</u>

The transmission loss experiment was conducted at both sites during an incoming high tide. Bathymetry at the seagrass site was more consistent, with the water depth ranging from 99.1 – 101.6 cm, with a mean of 101.6cm. At the unvegetated mudflat depth ranged from 71.1 – 114.3 cm, with a mean of 100.5 cm. Due to the length of the playback experiment, water depths during the trials decreased on average by 12.9 cm and 8.9 cm at the seagrass and mudflat site, respectively.

The effect of seagrass vegetation on signal transmission loss was dependent on frequency, with the largest differences between the sites observed at 1000 Hz, 2000, Hz, and 10,000 Hz (Fig. 10). Transmission loss of the 100 Hz and 200 Hz signals were very similar between the two sites. At 300 Hz, 400 Hz, and 500 Hz, transmission loss was slightly lower in the seagrass bed and the 300 Hz and 400 Hz signal were audible above background noise farther away from the sound source than at the mudflat. The opposite trend was observed at all frequencies above 1000 Hz, where signals propagated farther and with less transmission loss at the mudflat than at the seagrass bed.

Discussion

Sampling from diverse estuarine habitat mosaics captured soundscape differences between habitat types and across a continuum of habitat complexity. Pairing soundscape summaries with their respective habitat, community, and abiotic metrics revealed that differences between habitat types were correlated with patch- and landscape-scale habitat metrics, while landscape-scale habitat metrics tended to explain soundscape variation across the continuum of habitat complexity. Specifically, we observed four common soundscape types among all sites sampled and identified that landscape-scale habitat variables were important predictors across all

soundscape metrics summarized. In addition to landscape-scale habitat metrics, patch-scale habitat metrics tended to explain variation in SPL, whereas abiotic metrics were more important for explaining species-specific call rates. By reducing temporal variation and focusing on periods of peak acoustic activity, this study was able to explain spatial variation among estuarine soundscapes.

The role of landscape-scale habitat metrics in explaining soundscape spatial variation aligns with the current understanding that landscape context is an important driver of fish community composition in estuarine environments. For example, landscape-scale seagrass area and configuration were more important drivers of fish community richness and density than fine-scale seagrass biomass (Yeager et al. 2016). In oyster reef communities, landscape context influenced the strength of the effect reef restoration had on increasing fish density at multiple temporal scales (Grabowski et al. 2005; Ziegler et al. 2018). Fish communities in our study system also strongly relate to patch-scale habitat metrics, where species diversity and catch rates were higher at sites with both seagrass and saltmarsh, suggesting a positive relationship with habitat type richness (Baillie et al. 2015). Our results identified a similar effect of habitat on soundscape spectral composition for high frequency SPL and toadfish call rates, but the relationship between low frequency SPL and silver perch call rates with habitat metrics tended to be negative.

Comparison of soundscape spectral composition among all sites indicated four distinct soundscape types, two saltmarsh-like and two seagrass-like soundscapes. Because each species has a unique frequency signature, the power spectrum is a way to summarize the acoustic community of a site. Our results suggest that, like faunal communities, the acoustic community differs between habitat types and habitat metrics are important factors for discriminating between

habitat types. Patch-scale metrics were associated with variation between the habitat-associated soundscapes while landscape-scale metrics were correlated with both variation within and between the habitat-associated soundscapes. The relevance of landscape context for acoustic communities may explain the few sites that were not clustered with their same habitat type. For example, the soundscapes of saltmarsh creek B and mudflat 7 were in a seagrass-like cluster, but both sites include large seagrass areas at the landscape-scale and creek B was the one saltmarsh creek with seagrass included at the patch-scale. Similarly, seagrass 1, which is situated in within Middle Marsh -- a large, relic flood-tidal delta dominated by salt marsh -- was included in a saltmarsh-like cluster.

Whether the direction of the relationship between habitat and soundscape metrics agreed with previously published literature may be explained by mudflat-associated soundscapes. When mudflat-associated soundscapes had reduced acoustic activity, the effect of habitat was positive and agreed with the previously published literature. This was observed for high frequency SPL, which tended to be lower at mudflats than the other habitat types, and oyster toadfish, which were never detected at a mudflat. Conversely, when mudflat-associated soundscapes had increased acoustic activity compared to the other habitat types, as was observed for low frequency SPL and silver perch call rates, the relationship between habitat metrics and the soundscape tended to be negative. When present, silver perch chorusing, which extends from approximately 1 – 5 kHz, was the dominant feature of the low frequency soundscape, as such this trend with low frequency SPL is likely driven by silver perch chorusing as well.

The soundscapes of unvegetated mudflats in Pamlico Sound, NC are known to have lower SPLs in the 2 – 24 kHz range than nearby oyster reefs (Lillis et al. 2014). As a result, the high silver perch call rates at mudflats were unexpected. To investigate whether the silver perch

69

choruses originated on mudflats or propagated from adjacent habitat patches, we intentionally sampled a mudflat situated 2000 m from any structured habitat. At this site, mudflat A, we observed the highest number of silver perch calls among all sites. Silver perch calls were present in 45% of nighttime audio files, with an average call rate of 1083 calls per two minutes. This suggests that the fish calls recorded at the mudflats were occurring proximal to the hydrophone and not solely propagating from adjacent habitats. Call rates at mudflat A may have been elevated due to its position near Drum Inlet in Core Sound, as silver perch choruses have been documented to be more intense at inlet sites compared to inshore sites (Luczkovich et al. 2008). Our results suggest that unvegetated mudflats likely serve as spawning grounds for silver perch and may be undervalued as an essential fish habitat.

Cursory investigation of trends within each habitat type suggests that a negative relationship between seagrass metrics, at both patch and landscape scales, and low frequency SPL would still be apparent if mudflats were excluded from analyses. As such, it is possible that reduced SPL at seagrass beds could be the result of seagrass blades dampening sound propagation. The results of the transmission loss experiment suggest that seagrass does have a negative effect on sound propagation for frequencies above 1000 Hz. However, similar to previous reports, signals in the 300 – 400 Hz range propagated farther across the seagrass bed than unvegetated substrate, suggesting that seagrass blades may have a resonance effect at these frequencies (Wilson et al. 2013). Combined, the mixed effect of seagrass blades on frequencies within the low frequency band (100 – 2000 Hz) make it difficult to confidently interpret whether the negative relationship observed between seagrass and soundscape metrics are an ecological pattern or the results of the physics of sound propagation in shallow water.

While low frequency SPL was negatively correlated with patch-scale seagrass cover and canopy height as well as landscape-scale seagrass area, it was positively correlated with the seagrass perimeter to area ratio and oyster perimeter at the landscape scale. This trend suggests that low frequency SPL is higher in more fragmented seagrass landscapes than contiguous seagrass landscapes and in landscapes with a higher number of oyster reef patches. Correspondingly, high frequency SPL was positively correlated with landscape-scale oyster perimeter. These results pose a similar challenge to interpreting whether the observed trend is the result of ecological processes or the physics of sound propagation. It is possible that in patchy landscapes, increased areas of unvegetated substrate between structured habitat patches may facilitate sound propagation; however, it is interesting to consider whether this trend could be associated with edge effects on faunal communities.

A meta-analysis of seagrass community responses to edge and fragmentation effects identified that seagrass shoot densities tend to be lower in fragmented landscapes and in patch edges, but fish densities tend to be higher in patch edges (Yarnall et al. 2022). Similarly, increased faunal biomass has been documented in oyster reef edges compared to interiors (Davenport et al. 2022). While reduced shoot density in fragmented landscapes may facilitate sound propagation, seagrass shoot density at the patch scale was not correlated with SPL in either frequency band. Increased fish density in the patch edge and a positive effect of patchiness on sound propagation may interact to explain the positive effect of landscape patchiness observed. However, caution is warranted when interpreting possible effects of faunal density or biomass on the soundscape, as community metrics summarized in this study tended to be less important for explaining spatial variation in soundscape metrics.

Numerous studies in other ecosystems have identified positive correlations between acoustic indices, including SPL in multiple frequency bands, and faunal community metrics. (Nedelec et al. 2015; Butler et al. 2016; Freeman and Freeman 2016; Kaplan et al. 2018; Elise et al. 2019). As such, it was surprising that our results found community metrics were unimportant or explained a very small proportion of the variance in SPL and call rates. Perhaps the most unexpected result was that low frequency SPL was negatively correlated with silver perch CPUE. Despite the lack of importance of community metrics for explaining low frequency SPL, the multivariate results suggest that silver perch CPUE was correlated with variation within the seagrass-like soundscape clusters. Additionally, the average spectra of each cluster also revealed that presence of silver perch chorusing was relevant for discriminating between the two clusters within the habitat-associated soundscape types. Similar to the effect of habitat metrics at both scales, these conflicting results are likely due to the high silver perch call rates at mudflats and saltmarsh creeks, but low catch rates of silver perch at these habitats.

A possible explanation for the discrepancy between silver perch catch and call rates is that soundscape metrics were only summarized at night, but trawling was conducted during the day. Additionally, our ability to evaluate the relationship between the soundscape and faunal community may also have been limited by using a single community sampling method. Future studies in estuarine environments should consider the use of multiple sampling methodologies to more fully summarize the community present. Regardless of community sampling method, our results indicate that silver perch may primarily utilize saltmarsh creeks and mudflats nocturnally. This result highlights the value of soundscape monitoring as an effective method for identifying spawning habitats of soniferous fishes.

Seasonal patterns in fish call rates were evident for both oyster toadfish and silver perch, with call rates abruptly declining in mid-July and stopping completely in early August. Abiotic metrics captured this seasonal variation and were important predictors for both species. Periods of increased fish calling, or chorusing, are typically associated with spawning, and the observed seasonal patterns aligned with previously reported spawning phenology and chorusing behavior. Based on reports of gonad development and chorusing behavior the silver perch spawning season spans from March to August, with peak spawning occurring in June (Mok and Gilmore 1983; Luczkovich et al. 2008; Grammer et al. 2009; Ricci et al. 2016). As abiotic metrics explained 16% of the variation in silver perch call rates, our results suggest that the seasonal pattern in spawning-associated chorusing is correlated with water temperature. For oyster toadfish, reports of chorusing behavior suggest that the spawning season extends from March to August, with the timing of peak spawning varying among geographic regions (Fine 1978; Ricci et al. 2017a; Monczak et al. 2019). Our results align with early reports of toadfish chorusing behavior from Delaware to South Carolina, suggesting spawning peaks in early summer and decreases drastically in mid-July (Fine 1978). This seasonal pattern was accounted for by the correlation between toadfish call rates and sampling period, which explained 32% of the variation in toadfish call rates.

In coastal habitats, high frequency SPL and snapping shrimp snap rates are typically positively correlated with temperature and exhibit clear diel patterns, with peak acoustic activity at night during the summer (Bohnenstiehl et al. 2016; Lillis and Mooney 2018). While our results identified a positive correlation between temperature and high frequency SPLs during nighttime high tides, landscape- and patch-scale habitat metrics, not abiotic metrics, were identified as the most important predictors of high frequency SPL. We identified that spatial

variation in high frequency SPL was positively correlated with multiple measures of habitat complexity. The relationship between habitat complexity and snapping shrimp activity differs between habitat types, with a negative correlation in coral reef systems, (Nedelec et al. 2015; Freeman and Freeman 2016), a positive relationship in nearshore hardbottom habitats (Butler et al. 2017), and elevated SPLs at oyster reefs compared to unstructured mudflats (Lillis et al. 2014). Given the positive correlation with habitat richness, diversity, and cover of structured habitat, our results suggest that high frequency SPL may be indicative of habitat complexity in estuarine environments.

Of the 24 habitat patches summarized in this study, five of them were situated within or adjacent to Middle Marsh in Back Sound, NC. A previous study conducted in Middle Marsh by Ricci *et al.* (2017) found that silver perch call rates were positively correlated with seagrass cover at the patch-scale, but that oyster toadfish call rates and low frequency SPL did not have significant relationships with habitat metrics. Our results contrast with these findings as we found that patch-scale habitat metrics were unimportant for explaining silver perch call rates but did explain 16.6% and 25.3% of variation in oyster toadfish call rates and low frequency SPL, respectively. The conflicting results are possibly a result of the different spatial scale and range of habitat configurations sampled. For example, Ricci *et al.* sampled eight sites within Middle Marsh, seven of which would have been classified as saltmarsh creek in the present study. Additionally, the results may not be directly comparable as the present study quantified call rates while Ricci *et al.* (2017) qualitatively assessed the presence of fish chorusing. Taken together, our findings suggest that the relationship between habitat metrics and soundscape spatial variation varies across scales.

A limitation of using SPL to summarize low frequency soundscapes is that it includes the dynamics of multiple fish callers which each have unique responses to spatial heterogeneity in habitat, community, and abiotic metrics. As an aggregate metric, if two species are correlated with an underlying ecological pattern, but the directions of the correlations are opposite, then SPL would likely show no response. As a result, species-specific measures are more likely to identify trends across spatial heterogeneity. In the present study, we used previously developed detectors to quantify call rates for silver perch and oyster toadfish; however, at least four other fish call types were observed, including multiple spotted seatrout call types. All unidentified calls were between 200 – 1000 Hz and multiple call types occurred within the same two-minute audio files. The prevalence of these calls across all soundscapes can be seen in the 250 Hz peak and 600 – 1000 Hz peaks in the soundscape cluster power spectra. During initial analysis phases we attempted to classify these calls, but despite waveform, spectrogram, and aural inspection could not confidently and consistently differentiate between call types. To expand understanding of acoustic communities within estuarine soundscapes, more thorough documentation of fish call types and advancement of automated detection algorithms is needed.

In the present study we evaluated soundscapes across a wide variety of different estuarine habitat configurations and found that soundscape spatial variation was most explained by habitat metrics at multiple scales and abiotic metrics. Marine and estuarine soundscapes vary on diel and seasonal scales, by focusing on the diel periods of peak acoustic activity during the late-spring and summer, we successfully summarized soundscape spatial variation and identified associations with the underlying seascape. Meanwhile, the remaining seasonal variation was captured by abiotic metrics. Our findings that landscape-scale habitat metrics were important for explaining variation in all soundscape metrics summarized, aligns with current understanding of

how faunal communities relate to the seascape, and provides novel understanding of estuarine

soundscape variation. Lastly, unvegetated mudflat habitats consisted of active low frequency

soundscapes, contributing to unexpected negative relationships between habitat and soundscape

metrics. For soundscape monitoring of estuarine habitats to be successfully applied, further

research exploring how soundscapes vary within habitat types is needed.

REFERENCES

Baillie, C. J., J. M. Fear, and F. J. Fodrie. 2015. Ecotone Effects on Seagrass and Saltmarsh Habitat Use by Juvenile Nekton in a Temperate Estuary. Estuaries and Coasts 38:1414–1430.

Beck, M. W., R. D. Brumbaugh, L. Airoldi, A. Carranza, loRen D. Coen, C. Crawford, Om. Defeo, gRahaM J. Edgar, and B. Hancock. 2011. Oyster reefs at risk and recommendations for conservation, restoration, and management. BioScience 61(2).

Beck, M. W., K. L. Heck, K. W. Able, D. L. Childers, D. B. Eggleston, B. M. Gillanders, B. Halpern, C. G. Hays, K. Hoshino, T. J. Minello, R. J. Orth, P. F. Sheridan, and M. P. Weinstein. 2001. The Identification, Conservation, and Management of Estuarine and Marine Nurseries for Fish and Invertebrates. BioScience 51(8):633–641.

Bohnenstiehl, D. R. D., R. P. Lyon, O. N. Caretti, S. W. Ricci, and D. B. Eggleston. 2018. Investigating the utility of ecoacoustic metrics in marine soundscapes. Journal of Ecoacoustics 2(#R1156L).

Bohnenstiehl, D. R., A. Lillis, and D. B. Eggleston. 2016. The Curious Acoustic Behavior of Estuarine Snapping Shrimp: Temporal Patterns of Snapping Shrimp Sound in Sub-Tidal Oyster Reef Habitat. PloS one 11(1):e0143691.

Bolgan, M., M. C. P. Amorim, P. J. Fonseca, L. Di Iorio, and E. Parmentier. 2018. Acoustic complexity of vocal fish communities: A field and controlled validation. Scientific Reports.

Borker, A. L., R. T. Buxton, I. L. Jones, H. L. Major, J. C. Williams, B. R. Tershy, and D. A. Croll. 2020. Do soundscape indices predict landscape-scale restoration outcomes? A comparative study of restored seabird island soundscapes. Restoration Ecology 28(1):252–260.

Boström, C., S. J. Pittman, C. Simenstad, and R. T. Kneib. 2011. Seascape ecology of coastal biogenic habitats: Advances , gaps, and challenges. Marine Ecology Progress Series 427:191–217.

Butler, J., M. J. Butler Iv, and H. Gaff. 2017. Snap, crackle, and pop: Acoustic-based model estimation of snapping shrimp populations in healthy and degraded hard-bottom habitats. Ecological Indicators 77:377–385.

Butler, J., J. A. Stanley, and M. J. I. Butler. 2016. Underwater soundscapes in near-shore tropical habitats and the effects of environmental degradation and habitat restoration. Journal of Experimental Marine Biology and Ecology 479:89–96. Elsevier B.V.

Davenport, T. M., J. H. Grabowski, and A. R. Hughes. 2022. Edge effects influence the composition and density of reef residents on subtidal restored oyster reefs. Restoration Ecology:1–13.

Dimoff, S. A., W. D. Halliday, M. K. Pine, K. L. Tietjen, F. Juanes, and J. K. Baum. 2021. The

utility of different acoustic indicators to describe biological sounds of a coral reef soundscape. Ecological Indicators 124:107435. Elsevier Ltd.

Duarte, C. M., and D. Krause-Jensen. 2017. Export from Seagrass Meadows Contributes to Marine Carbon Sequestration. Frontiers in Marine Science 1(13).

Elise, S., I. Urbina-Barreto, R. Pinel, V. Mahamadaly, S. Bureau, L. Penin, M. Adjeroud, M. Kulbicki, and J. H. Bruggemann. 2019. Assessing key ecosystem functions through soundscapes: A new perspective from coral reefs. Ecological Indicators 107:105623.

Farina, A., G. Buscaino, M. Ceraulo, and N. Pieretti. 2014. The Soundscape approach for the assessment and conservation of Mediterranean landscapes: Principles and case studies. Journal of Landscape Ecology 7(1):10–22.

Fine, M. L. 1978. Seasonal and Geographical Variation of the Mating Call of the Oyster Toadfish Opsanus tau L. Oecologia 36(1):45–57.

Freeman, L. A., and S. E. Freeman. 2016. Rapidly obtained ecosystem indicators from coral reef soundscapes. Marine Ecology Progress Series 561:69–82.

Gasc, A., D. Francomano, J. B. Dunning, and B. C. Pijanowski. 2017. Future directions for soundscape ecology: The importance of ornithological contributions. Source: The Auk 1341(134):215–228.

Grabowski, J. H., A. R. Hughes, D. L. Kimbro, and M. A. Dolan. 2005. How habitat setting influences restored oyster reef communities. Ecology 86(7):1926–1935.

Grammer, G. L., N. J. Brown-Peterson, M. S. Peterson, and B. H. Comyns. 2009. Life history of silver perch bairdiella chrysoura (Lacepède, 1803) in North-Central Gulf of Mexico Estuaries. Gulf of Mexico Science 27(1):62–73.

Van Hoeck, R. V., A. B. Paxton, D. W. R. Bohnenstiehl, J. C. Taylor, F. J. Fodrie, D. P. Nowacek, C. M. Voss, and C. H. Peterson. 2020. Soundscapes of natural and artificial temperate reefs: similar temporal patterns but distinct spectral content. Marine Ecology Progress Series 649:35–51. Inter-Research Science Center.

Hovick, T. J., R. R. Elmore, S. D. Fuhlendorf, D. M. Engle, and R. G. Hamilton. 2015. Spatial heterogeneity increases diversity and stability in grassland bird communities. Ecological Applications 25(3):662–672.

Kaplan, M. B., M. O. Lammers, E. Zang, and T. A. Mooney. 2018. Acoustic and biological trends on coral reefs off Maui, Hawaii. Coral Reefs 37:121–133.

Kennedy, E. V., M. W. Holderied, J. M. Mair, H. M. Guzman, and S. D. Simpson. 2010. Spatial patterns in reef-generated noise relate to habitats and communities: Evidence from a Panamanian case study. Journal of Experimental Marine Biology and Ecology 395:85–92.

Kenworthy, W. J., J. C. Zieman, and G. W. Thayer. 1982. Evidence for the influence of

seagrasses on the benthic nitrogen cycle in a coastal plain estuary near Beaufort, North Carolina (USA). Oecologia 54:152–158.

Kline, L. R., A. I. DeAngelis, C. McBride, G. G. Rodgers, T. J. Rowell, J. Smith, J. A. Stanley, A. D. Read, and S. M. Van Parijs. 2020. Sleuthing with sound: Understanding vessel activity in marine protected areas using passive acoustic monitoring. Marine Policy 120(July):104138. Elsevier Ltd.

Lillis, A., D. Eggleston, and D. Bohnenstiehl. 2014. Estuarine soundscapes: distinct acoustic characteristics of oyster reefs compared to soft-bottom habitats. Marine Ecology Progress Series 505:1–17.

Lillis, A., and T. A. Mooney. 2018. Snapping shrimp sound production patterns on Caribbean coral reefs: relationships with celestial cycles and environmental variables. Coral Reefs 37:597–607.

Lindseth, A. V., and P. S. Lobel. 2018. Underwater soundscape monitoring and fish bioacoustics: A review. Fishes 3(3).

Luczkovich, J. J., R. C. Pullinger, S. E. Johnson, and M. W. Sprague. 2008. Identifying Sciaenid Critical Spawning Habitats by the Use of Passive Acoustics. Transactions of the American Fisheries Society 137(2):576–605.

Luczkovich, J. J., and M. W. Sprague. 2022. Soundscape Maps of Soniferous Fishes Observed From a Mobile Glider. Frontiers in Marine Science 9(March).

Lyon, R. P., D. B. Eggleston, D. R. Bohnenstiehl, C. A. Layman, S. W. Ricci, and J. B. Allgeier. 2019. Fish community structure, habitat complexity, and soundscape characteristics of patch reefs in a tropical, back-reef system. Marine Ecology Progress Series 609:33–48.

Maechler, M., P. Rousseeuw, A. Struyf, M. Hubert, and K. Hornik. 2019. cluster: Cluster Analysis Basics and Extensions.

Mok, H.-K., and R. G. Gilmore. 1983. ANALYSIS OF SOUND PRODUCTION IN ESTUARINE AGGREGATIONS OF POGONIAS CROMIS, BAIRD/ELLA CHRYSOURA, AND CYNOSCION NEBULOSUS (SCIAENIDAE). Bull. lnst. Zoo/. Academia Sinica 22(2):157–186.

Monczak, A., A. Berry, C. Kehrer, and E. W. Montie. 2017. Long-term acoustic monitoring of fish calling provides baseline estimates of reproductive timelines in the May River estuary, southeastern USA. Marine Ecology Progress Series.

Monczak, A., B. McKinney, C. Mueller, and E. W. Montie. 2020. What's all that racket! Soundscapes, phenology, and biodiversity in estuaries. PLoS ONE 15(9 September):1–18.

Monczak, A., C. Mueller, M. Miller, Y. Ji, S. Borgianini, and E. Montie. 2019. Sound patterns of snapping shrimp, fish, and dolphins in an estuarine soundscape of the southeastern USA. Marine Ecology Progress Series.

Mooney, T. A., L. Di Iorio, M. Lammers, T. Lin, S. L. Nedelec, M. Parsons, C. Radford, E. Urban, and J. Stanley. 2020. Listening forward: approaching marine biodiversity assessments using acoustic methods. Royal Society Open Science 7:201287.

Nedelec, S. L., S. D. Simpson, M. W. Holderied, A. N. Radford, G. Lecellier, C. Radford, and D. Lecchini. 2015. Soundscapes and living communities in coral reefs: temporal and spatial variation. Marine Ecology Progress Series 524:125–135.

Oksanen, J., F. G. Blanchet, M. Friendly, R. Kindt, P. Legendre, D. McGlinn, P. R. Minchin, R. B. O'Hara, G. L. Simpson, P. Solymos, M. H. H. Stevens, E. Szoecs, and H. Wagner. 2019. vegan: Community Ecology Package. R package version 2.5-5.

Orth, R. J., T. J. B. Carruthers, W. C. Dennison, C. M. Duarte, J. W. Fourqurean, K. L. Heck, A. R. Hughes, G. A. Kendrick, W. J. Kenworthy, S. Olyarnik, F. T. Short, M. Waycott, and S. L. Williams. 2006. A global crisis for seagrass ecosystems. BioScience 56(12):987–996.

Pijanowski, B. C., A. Farina, S. H. Gage, S. L. Dumyahn, and B. L. Krause. 2011. What is soundscape ecology? An introduction and overview of an emerging new science. Landscape Ecology 26(9):1213–1232.

Pittman, S. J., C. Caldow, S. D. Hile, and M. E. Monaco. 2007. Using seascape types to explain the spatial patterns of fish in the mangroves of SW Puerto Rico. Marine Ecology Progress Series 348:273–284.

R Core Team. 2020. R: A language and environment for statistical computing. R Foundation for Statistical Computing, Vienna, Austria.

Radford, C. A., J. A. Stanley, C. T. Tindle, J. C. Montgomery, and A. G. Jeffs. 2010. Localised coastal habitats have distinct underwater sound signatures. Marine Ecology Progress Series 401:21–29.

Ricci, S., D. Eggleston, D. Bohnenstiehl, and A. Lillis. 2016. Temporal soundscape patterns and processes in an estuarine reserve. Marine Ecology Progress Series 550:25–38.

Ricci, S. W., D. R. Bohnenstiehl, D. B. Eggleston, M. L. Kellogg, and R. P. Lyon. 2017a. Oyster toadfish (Opsanus tau) boatwhistle call detection and patterns within a large-scale oyster restoration site. PloS one 12(8):e0182757.

Ricci, S. W., D. B. Eggleston, and D. W. R. Bohnenstiehl. 2017b. Use of passive acoustic monitoring to characterize fish spawning behavior and habitat use within a complex mosaic of estuarine habitats.

Scyphers, S. B., S. P. Powers, K. L. Heck Jr, and D. Byron. 2011. Oyster Reefs as Natural Breakwaters Mitigate Shoreline Loss and Facilitate Fisheries. PLoS ONE 6(8):22396.

Staaterman, E., C. Paris, H. DeFerrari, D. Mann, an Rice, and E. D'Alessandro. 2014. Celestial patterns in marine soundscapes. Marine Ecology Progress Series 508:17–32.

Sueur, J., S. Pavoine, O. Hamerlynck, and S. Duvail. 2008. Rapid acoustic survey for biodiversity appraisal. PLoS ONE 3(12):e4065.

Tucker, D., S. H. Gage, I. Williamson, and S. Fuller. 2014. Linking ecological condition and the soundscape in fragmented Australian forests. Landscape Ecology 29:745–758.

Turner, M. G. 2005. Landscape ecology: What is the state of the science? Annual Review of Ecology, Evolution, and Systematics 36:319–344.

VanDerWal, J., L. Falconi, S. Januchowski, L. Shoo, and C. Storlie. 2014. SDMTools: Species Distribution Modelling Tools: Tools for processing data associated with species distribution modelling exercises.

Villanueva-Rivera, L. J., B. C. Pijanowski, J. Doucette, and B. Pekin. 2011. A primer of acoustic analysis for landscape ecologists. Landscape Ecology 26(9):1233–1246.

Wiens, J. A., R. L. Schooley, and R. D. Weeks. 1997. Patchy Landscapes and Animal Movements: Do Beetles Percolate? Page Oikos.

Wilson, C. J., P. S. Wilson, C. A. Greene, and K. H. Dunton. 2013. Seagrass meadows provide an acoustic refuge for estuarine fish. Marine Ecology Progress Series 472(1998):117–127.

Yarnall, A. H., J. E. Byers, L. A. Yeager, and F. J. Fodrie. 2022. Comparing edge and fragmentation effects within seagrass communities: A meta-analysis. Ecology 103(3):1–11.

Yeager, L. A., D. A. Keller, T. R. Burns, A. S. Pool, and F. J. Fodrie. 2016. Threshold effects of habitat fragmentation on fish diversity at landscapes scales. Ecology 97(8):2157–2166.

Ziegler, S. L., J. H. Grabowski, C. J. Baillie, and F. J. Fodrie. 2018. Effects of landscape setting on oyster reef structure and function largely persist more than a decade post-restoration. Restoration Ecology 26(5):933–942.

Table 3. 1 Proportion of variance in each sound metric explained by the ecological metric categories.

	Patch-scale habitat	Landscape-scale habitat	Community	Abiotic
Low frequency SPL	25.3 ↓	31.3 ↑↓	-	9.9 ↓
High frequency SPL	38.5 ↑	36.7 ↑	2.9 ↑	-
Toadfish call rate	16.6 ↑	12.4 ↑	-	32.3 ↓
Silver perch call rate	-	29.8 ↑↓	-	16.1 ↓
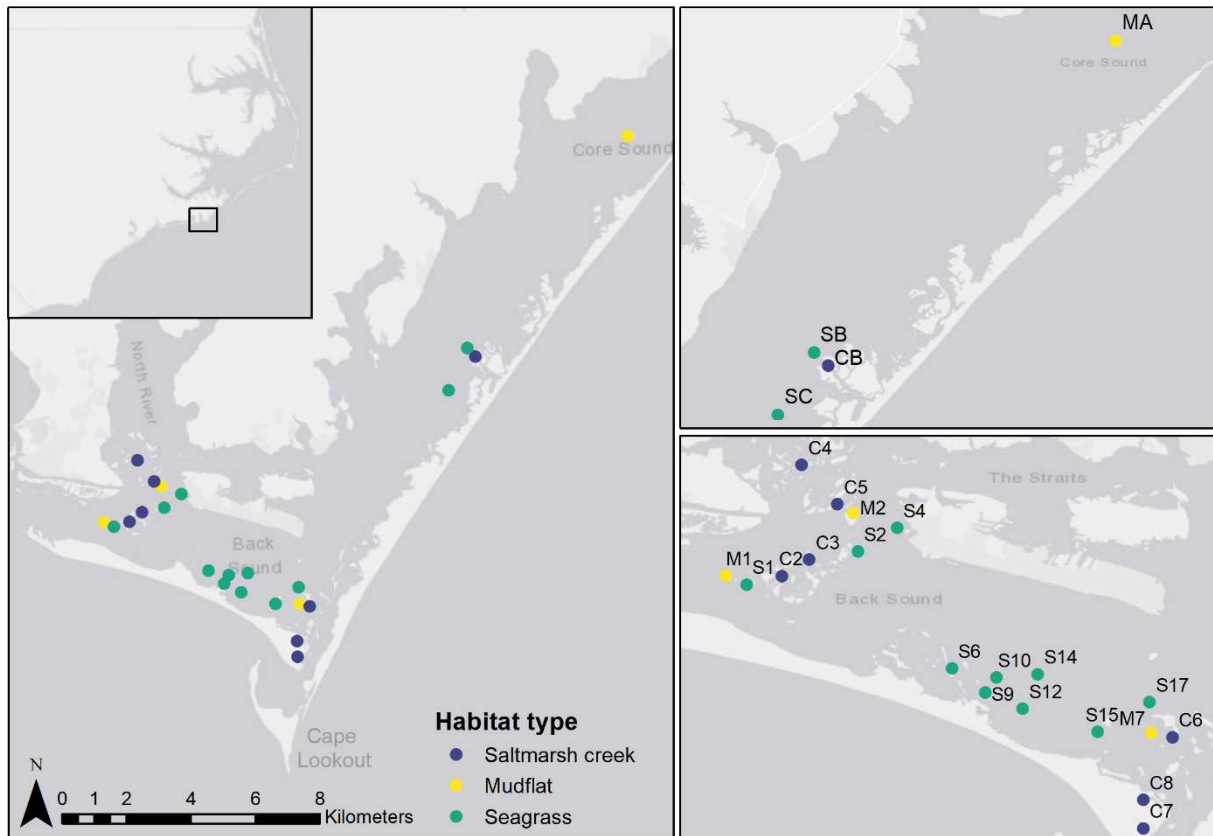
Figure 3. 1 Map of 24 habitat patches sampled and regional context for position of Back and Core sounds (Left). The geographic context near Cape Lookout, NC is shown in the inset map and local context is shown for labeled sites in Core (top right) Back (bottom right) sounds.
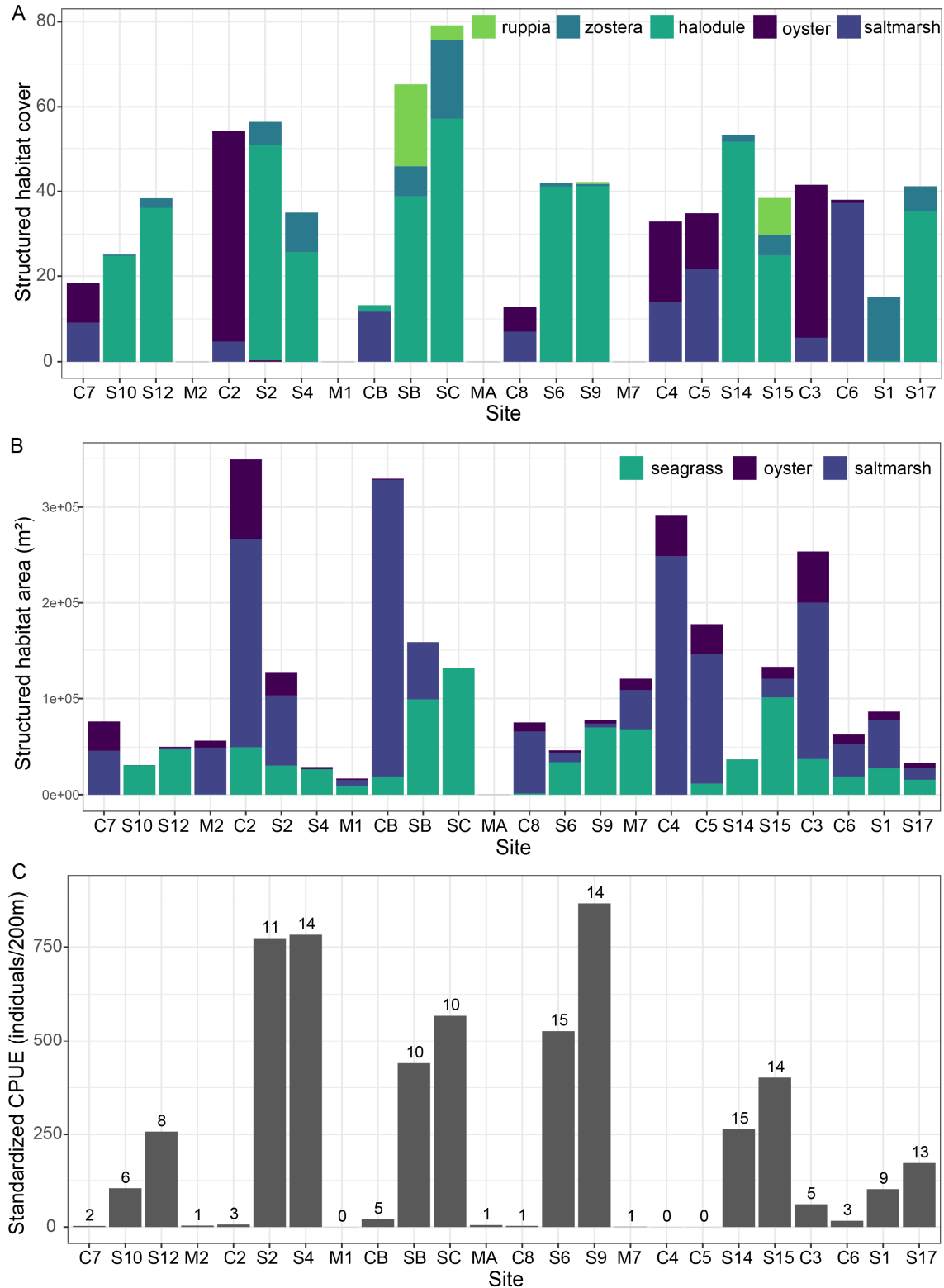
Figure 3. 2 Plots of observed habitat and community data. (A) Average percent cover observed in patch-scale quadrat sampling. (B) Total landscape-scale habitat area. (C) Total CPUE standardized to 200 m tows.
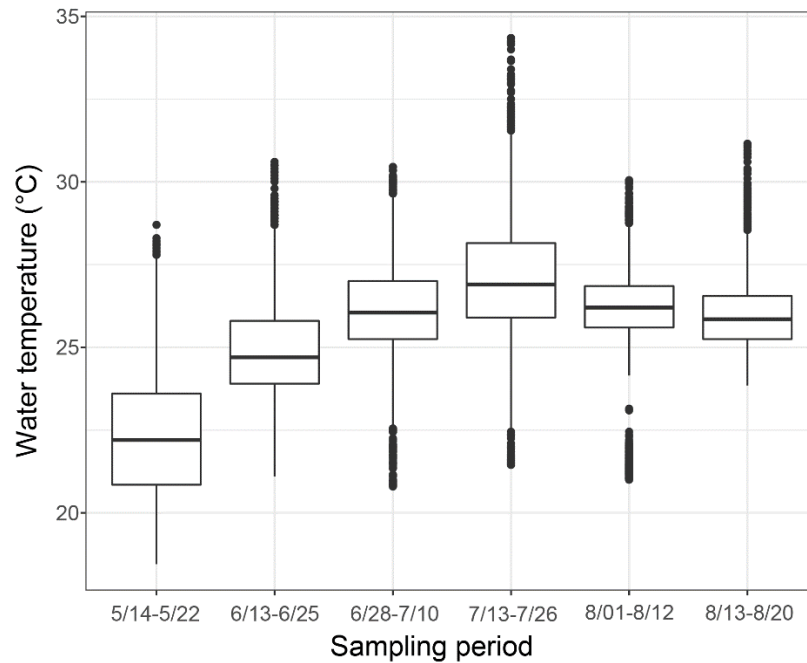
Figure 3. 3 Water temperatures recorded by the hydrophone during each two-minute recording cycle at night. The boxplots show the first and third quartiles, the center line is the mean, the whiskers extend to the most extreme values observed or to 1.5 times the inter-quartile range, and outliers are plotted individually.
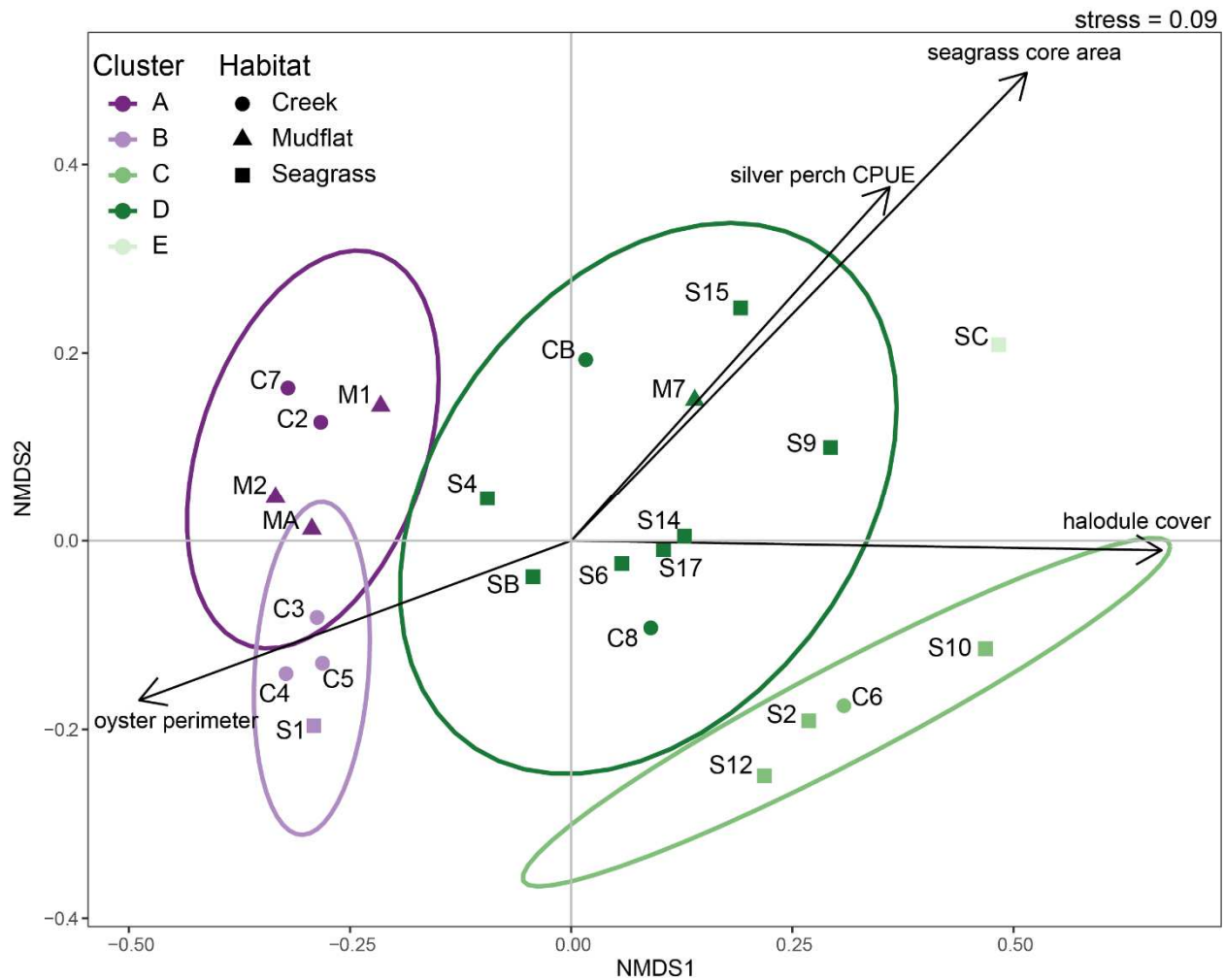
Figure 3. 4 Non-metric multidimensional scaling ordination plot where each point represents the average low frequency acoustic spectrum during nighttime high tides. The environmental vectors describe the magnitude and direction of significant correlations between ecological metrics and the ordination axis. The four soundscape clusters identified by cluster analysis are indicated by their 95% confidence ellipse. Cluster A and B consisted predominantly of saltmarsh creek and mudflat sites, while cluster C and D consisted predominantly of seagrass sites.
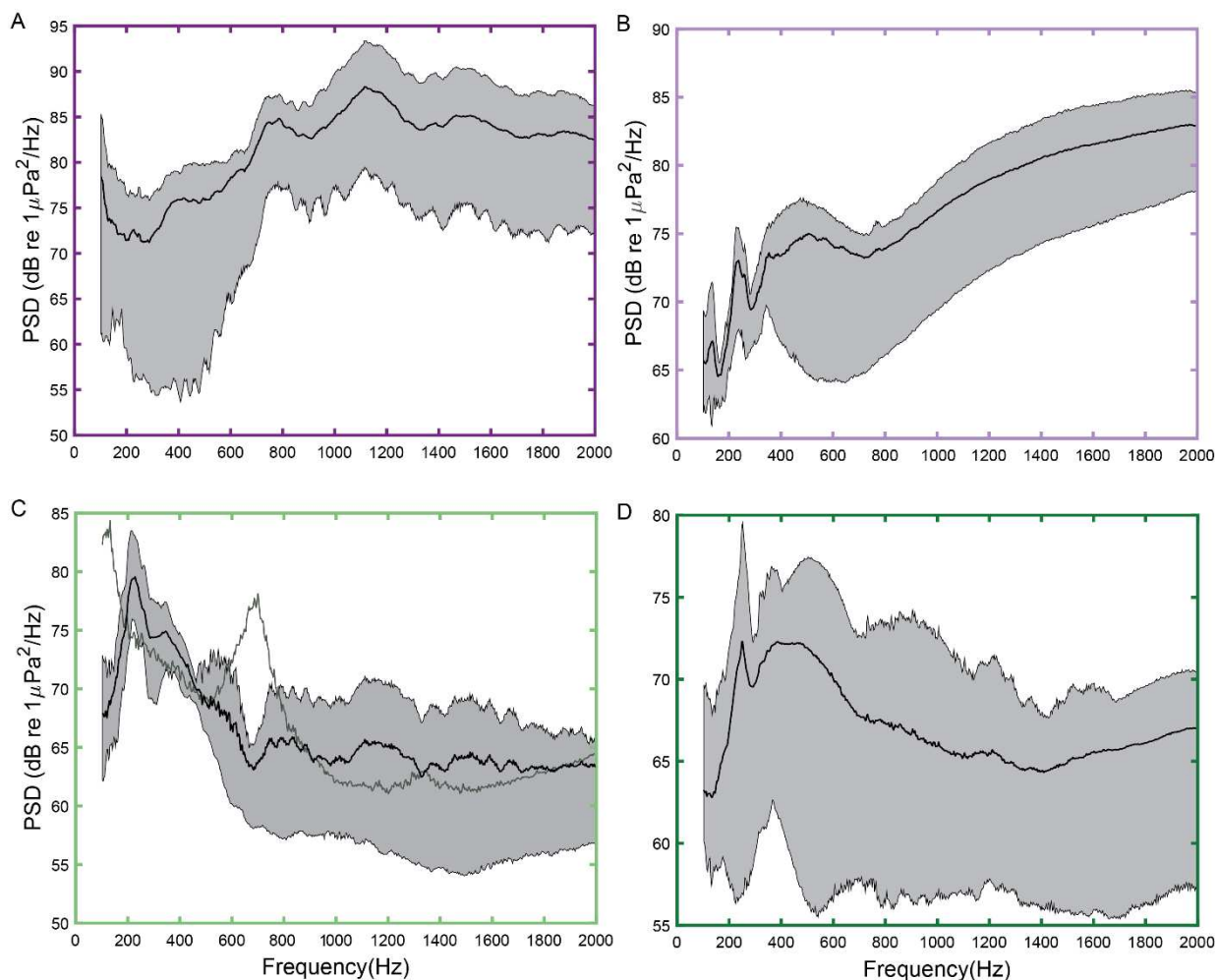
Figure 3. 5 Each plot describes the average low frequency acoustic spectrum of the sites within the corresponding cluster. The solid black line represents the average spectrum, and the shaded area shows the 5 – 95 quantile range. The single gray line in (C) shows the average spectrum of the outlier site with the cluster it was most similar to.
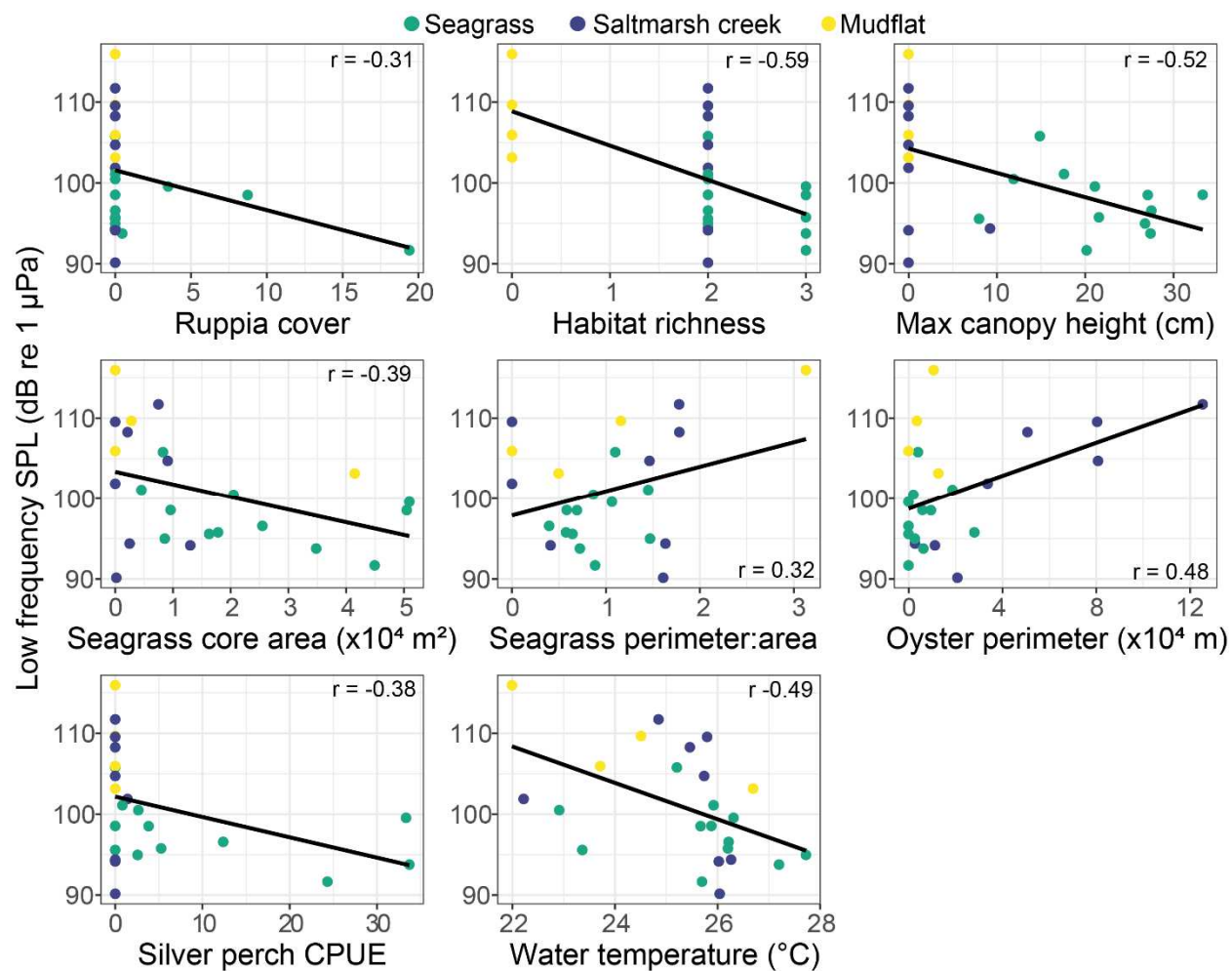
Figure 3. 6 Pairwise correlation plots between average low frequency SPL and ecological metrics. Only correlations with a magnitude greater than 0.3 are shown. SPLs are reported in units of dB re 1 uPa.
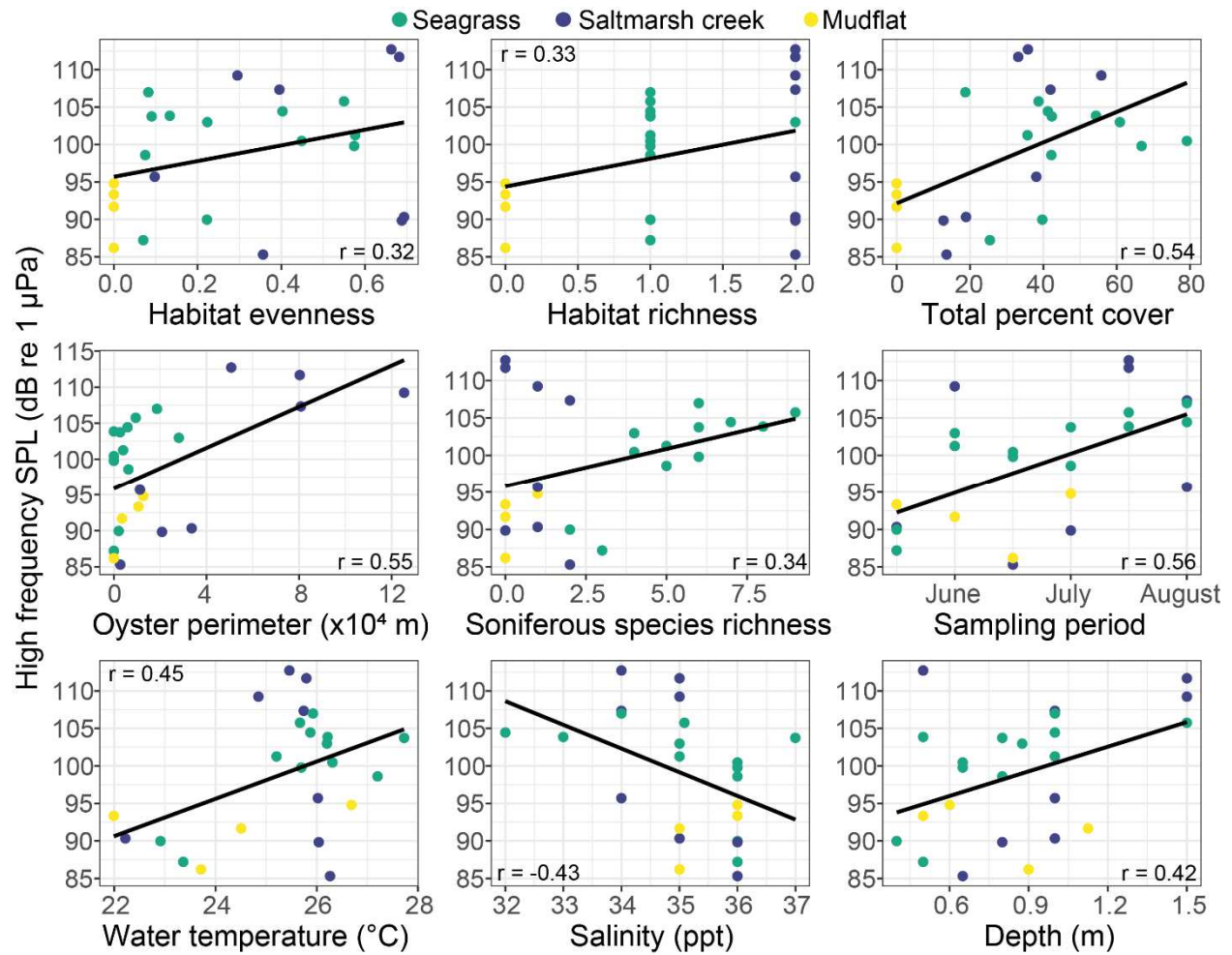
Figure 3. 7 Pairwise correlation plots between average high frequency SPL and ecological metrics. Only correlations with a magnitude greater than 0.3 are shown.
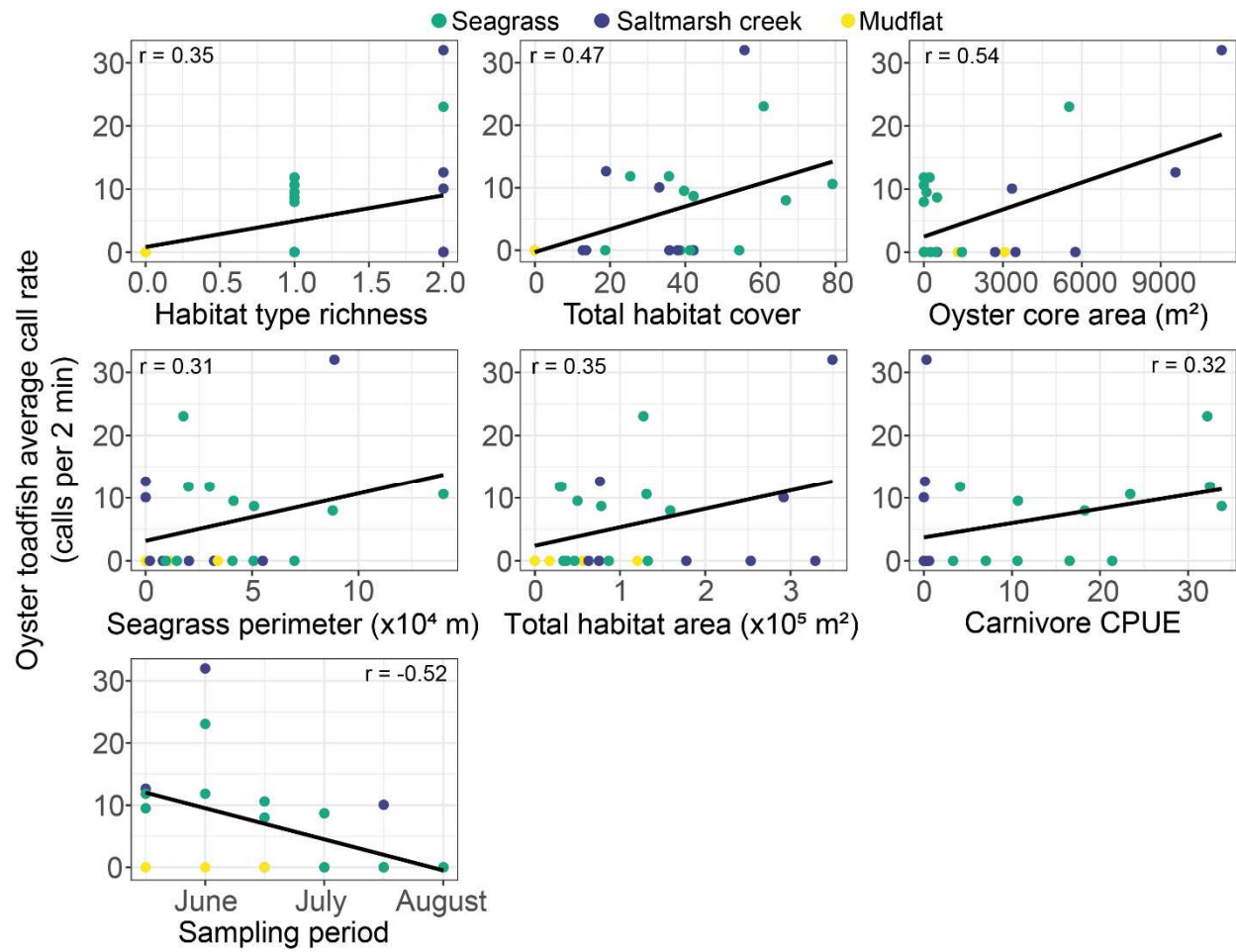
Figure 3. 8 Pairwise correlation plots between average toadfish call rates and ecological metrics. Only correlations with a magnitude greater than 0.3 are shown.
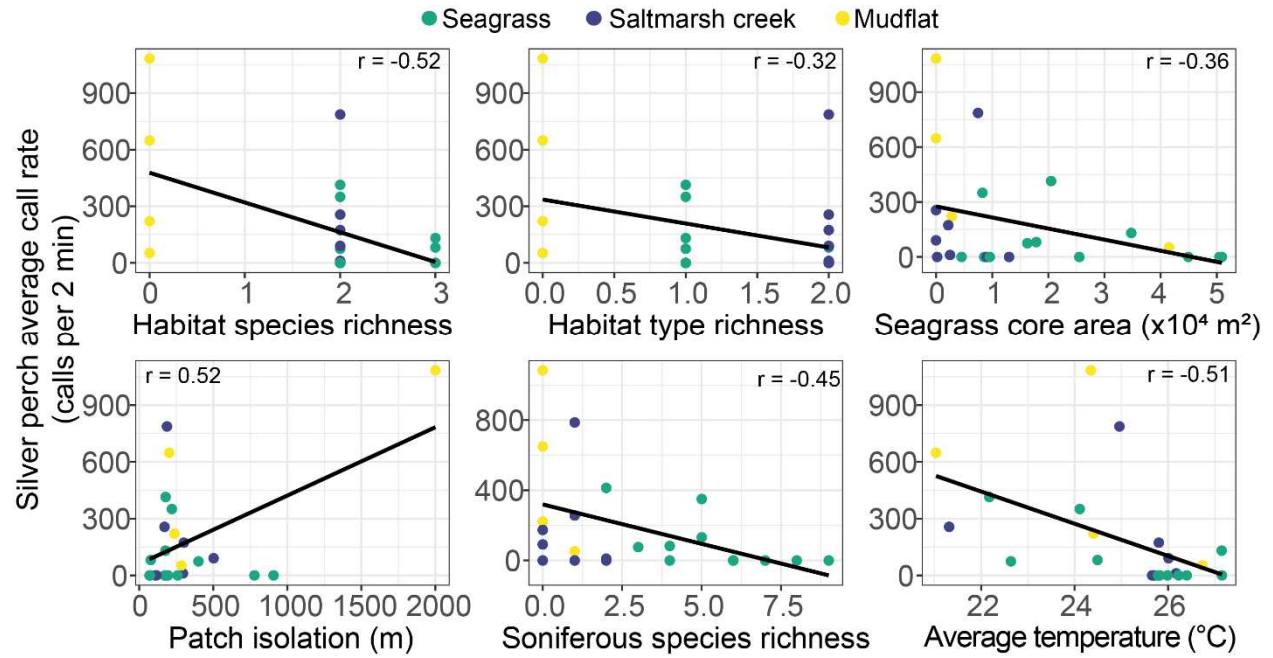
Figure 3. 9 Pairwise correlation plots between average silver perch call rates and ecological metrics. Only correlations with a magnitude greater than 0.3 are shown.
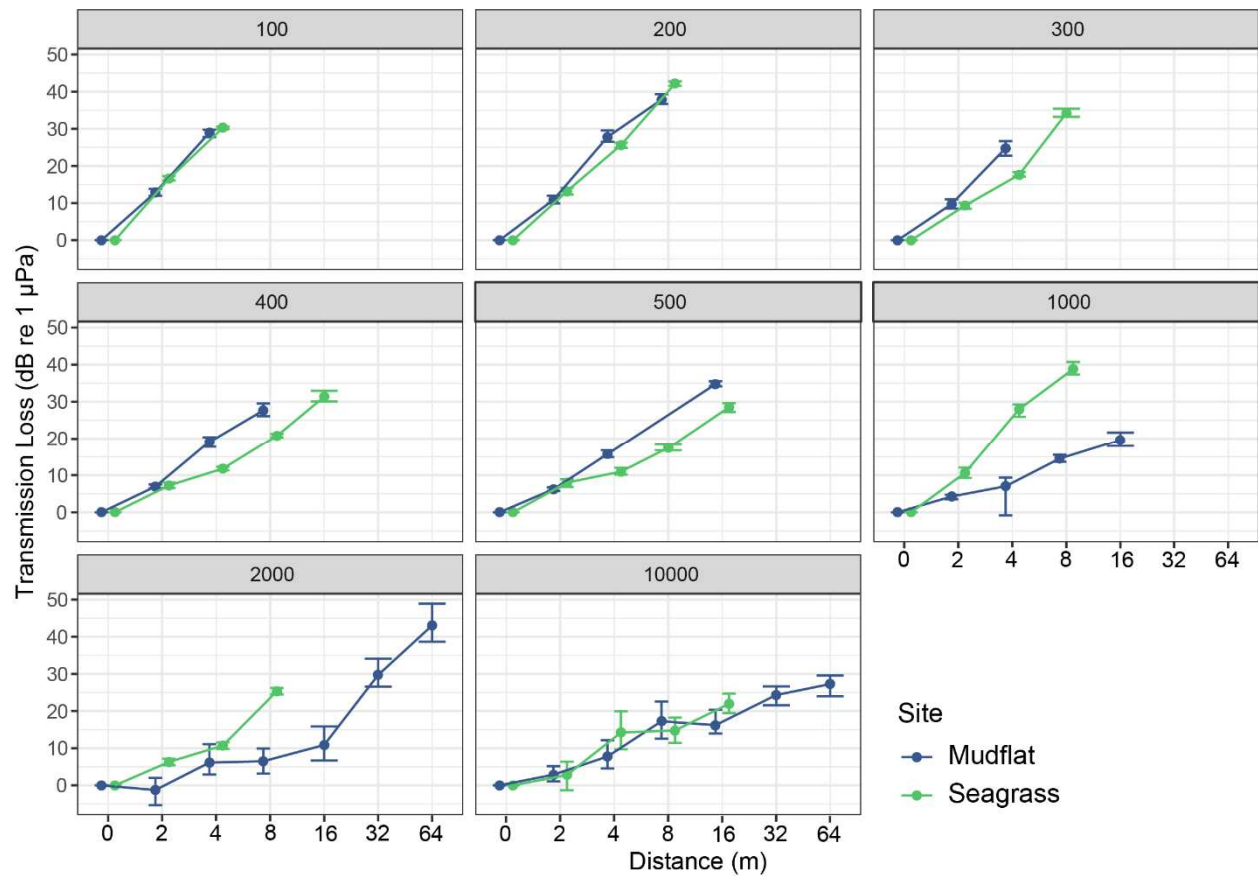
Figure 3. 10 Results of the transmission loss experiment. Each plot shows the average transmission loss calculated for a different frequency tone (Hz) at each distance radiating away from the sound source. Each point is the average among the 10 replicates and the error bars so the 5 – 95 quantile range.

CHAPTER 4: PASSIVE ACOUSTIC MONITORING COMPLEMENTS TRADITIONAL METHODS FOR ASSESSING MARINE HABITAT ENHANCEMENT OUTCOMES[2]

Introduction

Marine ecosystems are increasingly threatened by habitat degradation and overharvesting of fish populations (Halpern et al. 2019). In many regions, resource managers have attempted to combat the negative consequences of these threats through habitat enhancement, or the introduction of artificial, human-made structures (Baine 2001). These structures can help achieve an array of goals, including increasing habitat availability (Bortone 2011), enhancing fishery yield (Leitão et al. 2009), replacing the function of previously lost or degraded natural habitat (Pickering et al. 1998), supplementing existing habitat, and protecting sensitive habitats from destructive anthropogenic activity, such as benthic trawling (Relini & Relini 1989). Furthermore, habitat enhancement can help support coastal cultures and economies by creating new fishing and ecotourism opportunities, as well as reducing fishing pressure on natural habitats (Al-Horani and Khalaf 2013). While habitat enhancement offers many potential benefits to coastal ecosystems, ensuring a positive effect requires careful planning and assessment of habitat enhancement outcomes (Becker et al. 2018).

To assess whether the goals of habitat enhancement are achieved, enhancement projects require explicit statement of objectives paired with a consistent monitoring strategy following introduction of artificial structures (Pratt 1994). Depending on the intended goal of the habitat

---

enhancement, monitoring projects have focused on observing ecological or population dynamics (Rilov and Benayahu 2002), evaluating design effectiveness (Sherman et al. 2002), or assessing socioeconomic outcomes (Whitmarsh et al. 2008). A literature review on the trends in artificial reef research in the last 60 years, published by Lima et al. 2019 found that among habitat enhancement monitoring projects, ecology, and specifically community structure, was the most common research focus. Previous studies on artificial reef community development have found that colonization of introduced structures occurs rapidly (Cummings 1994), but often includes fluctuations in abundance and community structure over varied timescales (Scarcella et al. 2015). Understanding the patterns of community development, as well as the successional processes that underly them, can illuminate whether habitat enhancement efforts achieve the intended outcome and on what timescale.

A variety of monitoring methods are available to evaluate the effectiveness of habitat enhancement in achieving prescribed goals. Diver-based visual censuses and videography methods are most frequently used to assess community development following introduction of offshore artificial reefs (Lima et al. 2019). In coastal and intertidal ecosystems, by comparison, habitat enhancement monitoring is often accomplished using nets and traps. These traditional sampling methods face multiple challenges, including that they can be a time-consuming and expensive process that is dependent on appropriate environmental conditions and are further complicated by difficult to access locations. As a result, these methods involve a trade-off between the temporal resolution of sampling and duration of the monitoring effort (Bortone 2006). The resulting decisions made about monitoring study design can affect the ability to interpret the ecological implications of the results.

An alternative to traditional monitoring is passive acoustic monitoring (PAM), which records the soundscape, including biological, geological, and anthropogenic sounds. Because the detection of sound is independent of light availability and currents, PAM offers many advantages for sampling difficult to access habitats, especially where traditional monitoring is complicated by adverse weather conditions, changing tides, turbidity, complex benthic structures, and nocturnal animal activity. Furthermore, PAM is a non-invasive method with reduced observer bias or artefacts compared to visual census (Van Parijs et al. 2009). Recently, there has been rapidly rising interest in developing PAM methodologies that can be used in management or conservation contexts, such as biodiversity assessment (Mooney et al. 2020), evaluation of habitat restoration (Butler et al. 2016), and tracking population distribution shifts associated with climate change (Davis et al. 2020).

The use of artificial habitats for the management, restoration, and enhancement of marine ecosystems has expanded to a global practice with active artificial reef programs across temperate and tropical regions (Seaman 2007). In the presented case study, we evaluated the trajectory of soundscape development on a newly deployed artificial reef offshore of North Carolina (NC), USA. Specifically, we tested whether and on what timescale the soundscape of a new artificial reef converged with that of a nearby established artificial reef and evaluated the trajectory of soundscape development through temporal patterns in species-specific sound production. This passive acoustic monitoring was conducted simultaneously with underwater time-lapse videography, the results of which were previously published in Paxton et al. 2018. In addition to the soundscape analyses, we compared the qualitative conclusions drawn from each monitoring methodology.

Methods

To enhance understanding of the trajectory of community development following artificial reef deployment, our team opportunistically monitored the fish community and soundscape using time-lapse underwater videography and passive acoustic methods at a newly deployed artificial reef and a nearby established artificial reef in Onslow Bay, NC, USA. The seafloor of Onslow Bay is heterogenous, consisting of intermixed regions of rocky-reef ledges, exposed hardbottom pavements, sand flats, and numerous artificial reefs (Gregg and Murphey 1994, Riggs et al. 1996). This complexity, in combination with its position near a biogeographic boundary between temperate and topical systems, makes it a useful system to explore community development dynamics. The two reefs sampled consisted of an existing 89-m long landing craft repair ship named USS *Indra*, scuttled in 1992 (34.5623°N, 76.8515°W; henceforth called "established reef"), and a newly deployed 33-m long US Army tugboat, renamed *James J. Francesconi,* (34.5634°N, 76.8552°W; henceforth called "new reef"), that was scuttled by the NC Division of Marine Fisheries' (DMF) Artificial Reef program on May 7, 2016. The two reefs lie 438m apart, at a depth of 20m, within the state-designated artificial reef site AR-330 (Comer & Love-Adrick 2016; Fig. 1). Given their proximity, we assumed that the environmental conditions at each site were the same.

Within AR-330 there are numerous additional artificial reef structures that were not sampled (Fig. 1). Approximately 50 m west of the new reef, a second vessel (20m tugboat) was sunk on the same day in 2016. All other artificial reefs were deployed between 1990 – 2012 and would be considered established communities. Most of these structures are of low-vertical relief, created out of miscellaneous materials including concrete pipes, reef balls, or fiberglass domes. There are also six high vertical relief reefs made of other vessel types including sailboats, barges,

and an aircraft (Comer and Love-Adrick 2016). The reef types are distinguished by vertical relief because they often support different fish communities (Paxton et al. 2017). Adjacent to the sampled established reef lies two sailboats, ~33 and 50m away, as well as multiple regions of concrete pipes ~200 – 300m away. Nearest to the sampled new reef is a small group of fiberglass domes ~50m away, and multiple regions of concrete pipes that range from ~100 – 400m away.

We monitored both reefs during six sampling periods between two-weeks and 11-months following deployment of the new reef. The sampling dates were: 18 – 24 May 2016; 22 – 27 Jul. 2016; 14 – 17 Sep. 2016; 27 – 31 Oct. 2016; 3 – 7 Dec. 2016; and 21 – 26 Apr. 2017. The soundscape was recorded concurrently and continuously on the new and established artificial reefs. Recordings were made using a calibrated omni-directional hydrophone at a 96kHz sampling rate (SoundTrap 202 STD, Ocean Instruments, New Zealand). The hydrophones were mounted to a 0.5m tall weighted, metal frame and placed on top of the artificial reef structure at the stern of the ship. The positions were fixed across all sampling periods. All acoustic analyses were conducted in MATLAB (MATLAB 2018) using purpose-written code.

The continuous recordings were subsampled to two-minute samples every 15 minutes to match the duty cycle commonly used in marine passive acoustic research. This subsampling reduced computational challenges associated with acoustic analysis while retaining the natural variability of the underwater soundscape (Bohnenstiehl et al. 2018). The data were response corrected to micropascals (μPa) using a hydrophone specific calibration value. Initial analyses in the time and frequency domain revealed a substantial amount of anthropogenic noise intrusion and several anomalously high amplitude impulsive signals, likely produced when a swimming animal collided with the hydrophone or instrument frame (i.e., "fish bumps", Buskirk et al. 1981, Bowman & Wilcock 2014). Even a single fish-bump within a two-minute audio file distorted the

97

average power spectrum and sound pressure level (SPL), complicating the interpretation of biological acoustic activity. To reduce the impact of these anomalies, each two-minute file was subdivided into consecutive nonoverlapping 5-second windows, and the data were further subsampled by selecting the four quietest windows within the file (sensu Van Hoeck et al 2020). All subsequent analyses were conducted using the average power spectrum and root-mean-square (RMS) amplitude calculated from these subsamples. Comparisons of power spectral density (PSD) and the SPL timeseries between the full two-minute files and subsamples confirmed that the anomalies were removed, but the natural biological variability was preserved (see Fig. S1 in Van Hoeck et al 2020).

The frequency content of each file was described by its average acoustic spectra calculated by Fourier transform (NFFT = 2^{15} points, 0% overlap, Hanning window). To analyze the sounds associated with fish and invertebrates separately, the data were divided into low and high frequency bands of 0.15 – 2 kHz, dominated by fish sounds, and 7 – 15 kHz, dominated by snapping shrimp (*Alpheus* sp.), respectively. The selected frequency bands intentionally exclude intermediate frequencies that contain overlaps between fish and invertebrate sounds (e.g., Ricci et al. 2016). The RMS sound pressure level (SPL) within each frequency band was calculated by summing the power within the limits of the frequency band.

To evaluate how the soundscape developed on the newly deployed reef in relation to the established reef, we investigated the SPL timeseries of the low and high frequency bands and calculated the correlation coefficient between the two sites within each sampling period. The timeseries were visualized using a 3-point moving average to smooth out stochastic variability in SPL and improve interpretation of diel patterns. In addition to the correlation coefficient, we qualitatively compared the distribution of observed SPLs for each site within sampling period to

evaluate whether the soundscapes had converged. Due to observed diel patterns in SPL with increased biological acoustic activity at dusk, we isolated the files between sunset and astronomical twilight (~1.25-1.75 hr duration) for further inspection. This method also excluded a series of harmonic sounds observed at midnight on both sites whose source could not be determined as biological or anthropogenic.

We conducted a two-way repeated measures ANOVA to investigate whether there was an interactive effect between site and sampling period on the observed dusk SPLs in both frequency bands. We summarized each site by calculating the average SPL at dusk for each day within a sampling period; as such, each day was considered a replicate. We confirmed the assumptions of the ANOVA were met by checking for outliers and inspecting QQ plots for normality. While there was one outlier in the low frequency band and two in the high frequency band, removing the outliers did not change the results of the ANOVA, so we proceeded with all data points. Because the interaction between site and sampling period was significant, we evaluated the effect of site during each sampling period using a one-way ANOVA. Lastly, to understand which comparisons were driving observed differences between the sites, we conducted pairwise t-tests between the sites at each sampling period. All statistical analyses were conducted in R version 4.0.2 using the "rstatix" package (R Core Team 2020, Alboukadel 2021).

Next, we evaluated the trajectory of community development in the soundscape by comparing the average low frequency dusk power spectrum on each reef within sampling period using the $0.05 - 0.95$ quantiles as a measure of variance. As animal vocalizations have distinct time and frequency characteristics, seasonal changes in power spectral density facilitated identification of species-specific colonization patterns for soniferous species. To evaluate whether the identities of fishes producing sounds were the same between the new and established

reef, we visually screened the spectrogram of each two-minute file and aurally confirmed species identity when applicable. During multiple sampling periods, frequent vocalizations by a toadfish species (*Opsanus* sp.; first two harmonics 0.15 – 0.4 kHz) (e.g., Fine, 1978; Ricci et al. 2017) and an unidentified species (0.4 – 0.8 kHz) were recorded. Due to the strength of these vocalizations in the acoustic spectra, we focused on the temporal patterns of these vocalizations to understand the dynamics of low frequency soundscape development.

We acknowledge that identifying the source of recorded sounds and interpreting the ecological significance of our results are complicated by aspects of our study design as well as the presence of other structured habitats adjacent to both the new and established reefs (Fig. 1.) Because this was an opportunistic study, the new reef site was not monitored before the tugboat was scuttled. Additionally, single element hydrophones, like the SoundTraps used in this study, are not able to determine source locations. Consequently, the relative amplitudes of the signals recorded at both reefs must be used to make inferences about the source location. Assuming a simple cylindrical spreading model, the minimum transmission loss from the surrounding habitats to the new reef would be ~17 dB. If calls recorded on the established reef were sourced on-reef, but those recorded on the new reef originated from the surrounding habitats, we would expect calls recorded at the new reef to have systematically lower amplitudes. However, if the received call amplitudes are similar between the two reefs, it would imply that either sound production is local to both reefs or that both recordings are sampling the ambient soundscape sourced from more distant habitats. We evaluate these scenarios specifically for oyster toadfish boat whistles by haphazardly selecting calls at both reef sites and comparing the SPL within their lowest harmonic band.

Lastly, to evaluate whether results from passive acoustic monitoring and video monitoring were analogous, complementary, or conflicting, we compared the qualitative conclusions drawn from each method. The comparison consisted of community dynamics including the rate of colonization and whether convergence was observed, as well as colonization dynamics of specific taxonomic groups, including demersal fishes, piscivorous fishes, and invertebrates.

Results

Diel patterns in the low frequency soundscape (0.15 – 2kHz) varied between the reefs and across sampling periods, often associated with changes in dominant vocalizers. During the first two sampling periods, mean SPLs on the two reefs were within 5.3 and 6.5 dB of one another, respectively. At two-weeks post deployment of the new reef the correlation coefficient was 0.48 and at two-months post-deployment the correlation coefficient was 0.54. During the third sampling period, four months following artificial reef deployment, the SPL timeseries of the reefs were highly correlated (cc = 0.93), night SPLs on the new reef were occasionally higher than those of the established reef, and the distributions of observed SPLs on each site were closely aligned with a mean SPL difference of less than 1 dB (Fig 2). The third sampling period contained multiple sound sources that dominated the low frequency soundscape on both reefs, including one feature below 0.5 kHz at dusk and a second at 0.5 – 1.5 kHz in the hours around midnight. The identity of these sounds could not be determined.

During all subsequent sampling periods, SPLs on the new reef tended to be lower than those of the established reef, but their timeseries remained similar. The correlation coefficient between the timeseries on each reef was 0.67 with a mean SPL difference of 9.9 dB at five-

101

months, and 0.64 with a mean SPL difference of 5.9 dB at seven-months post-deployment of the new reef. During the final sampling period, eleven-months following reef deployment, the timeseries were highly correlated (cc = 0.84) and low frequency SPL again closely aligned between the sites with a mean SPL difference of 3.9 dB (Fig. 2).

Comparisons of dusk SPLs revealed that the low frequency soundscape (0.15 – 2kHz) varied by an interaction between site and sampling period (repeated measures ANOVA, $F_{5,15} =$ 24.831, p < 0.001). One-way ANOVAs of the effect of site within sampling period identified statistically significant differences in dusk SPL between the established reef and the new reef during May ($F_{1,6}$ = 521.0, p < 0.001), July ($F_{1,5}$ = 336.0, p < 0.001), September ($F_{1,3}$ =11.2, p = 0.04), October ($F_{1,4}$ = 137.0, p < 0.001), and December ($F_{1,6}$ = 68.1, p = 0.001). Pairwise comparisons between the sites within each sampling period revealed that SPLs were lower on the new reef during all deployments except September, when they were higher on the new reef, and April, when they did not differ between the reefs (Fig. 3a).

Diel patterns in the high frequency soundscape (7 – 15kHz), predominately snapping shrimp snaps, were consistent across both reefs and all sampling periods (Fig. 4). While SPLs on the new reef were always lower than those on the established reef, similar temporal patterns resulted in strong correlations between the timeseries in each sampling period, with correlation coefficients ranging between 0.81 and 0.94. The strength of this correlation varied across all sampling periods, with no apparent trend relating to time since artificial reef sinking. Inspection of the observed SPL distributions showed that they did not overlap during the first four sampling periods but did become more similar during the final two sampling periods, with the greatest overlap observed during the final sampling period. Moreover, the mean difference in SPL

between the reefs decreased from 17.4 dB during the first sampling period, to 10.3 dB during the final sampling period.

Dusk SPLs in the high frequency soundscape (7 – 20kHz) varied by an interaction between site and sampling period (repeated measures ANOVA, $F_{5,15} = 47.6$, $p < 0.001$). One-way ANOVAs on the effect of site within sampling period and pairwise comparisons between the sites revealed that SPLs were significantly lower on the new reef during all sampling periods (May: $F_{1,5} = 11891.0$, $p < 0.001$; Jul: $F_{1,5} = 4215.0$, $p < 0.001$; Sep: $F_{1,3} = 1254.0$, $p < 0.001$; Oct: $F_{1,4} = 10487.0$, $p < 0.001$; Dec: $F_{1,5} = 394.0$, $p < 0.001$; Apr: $F_{1,5} = 394.0$, $p < 0.001$). Inspection of the seasonal variation within each site revealed that average high frequency SPLs on the established reef increased by 0.7 dB between the first two sampling periods but increased by 5.2 dB on the new reef (Fig. 3b).

Analysis of the average low frequency power spectrum at dusk revealed that soundscape activity on both reefs varied seasonally. Comparisons between the reefs, and specifically the 0.05 – 0.95 quantile range, suggest that dusk acoustic activity on the new reef exhibited greater variability. Across all sampling periods, acoustic activity in some frequency bands did overlap, such as 0.15 – 0.4 kHz in May, and 0.4 – 0.8 kHz in July and October; additionally, the power spectrum on both reefs closely aligned during September and April (Fig. 5). The PSD consistently increased from 1 – 2 kHz on the established reef due to snapping shrimp activity overlap in the low frequency band.

Spectrogram inspection of audio files at dusk revealed that during the first and last sampling periods, in May 2016 and April 2017, the same vocalizations were observed. On the established reef, the May and April soundscape both consisted of choruses of an unidentified knock in the 0.4 – 0.8 kHz range (Fig.5; Fig. 6). Similarly, on the established reef, the May

soundscape included frequent toadfish vocalizations while the April soundscape contained toadfish choruses. Conversely, on the newly deployed reef, the May soundscape consisted of frequent toadfish vocalizations, but the unidentified knock chorus was absent. In April, eleven-months following artificial reef deployment, toadfish and knock choruses were present on both reefs (Fig. 6). During the first sampling period, the average SPL of the first toadfish harmonic on the established reef was 99.8 dB, and the maximum observed was 110 dB. On the new reef, the average SPL was 97.4 dB, and the maximum was 104 dB.

Previously published results of the underwater video analyses revealed that fishes rapidly colonized the new reef structure and that the community composition on the two reefs converged within five months (Paxton et al. 2018). While the results of video monitoring and PAM both suggest rapid fish colonization and soniferous fish community alignment, the video analysis suggested that the trajectory of community development consisted of conspicuous, water-column species appearing first (e.g., jacks (*Carangidae)* and scad (*Decapterus* sp.)) and demersal species (e.g., black sea bass (*Centropristis* striata)) exhibiting relatively slower colonization. In contrast, frequent toadfish vocalizations on the new reef during the first sampling period, observed at a similar sound level to those on the established reef, suggests that some cryptic, demersal species may have rapidly colonized the new reef (Table 1).

Discussion

We investigated the trajectory of soundscape development on a newly deployed artificial reef and a nearby established reef using passive acoustic monitoring and compared the results to that of traditional monitoring via underwater videos. Though video monitoring provided detailed analysis of colonization trajectory, PAM provided additional insights into community

development not captured by visual monitoring. Specifically, the video data suggested that demersal species did not colonize the new reef until five-months after its deployment whereas PAM revealed that at least one cryptic, demersal species (i.e., toadfish) may have been present at the new reef within two-weeks. Moreover, the high frequency soundscape revealed details of invertebrate colonization not available from video monitoring. Our findings demonstrate that passive acoustic monitoring is a promising complement to traditional visual surveys to assess the effectiveness of habitat enhancement, by elucidating a more holistic view of community development dynamics.

Passive acoustic monitoring

The results of PAM identified seasonally variable low frequency soundscapes with periods of temporary alignment between the reefs. Due to the opportunistic nature of this study, we were unable to monitor the soundscape at the new reef prior to artificial reef deployment. This lack of a soundscape baseline, complicated interpretation the variability as soundscape development or seasonal variability.

The alignment of the soundscapes (SPL timeseries correlation, similarity in dusk SPL and dusk power spectra) during September and April occurred when they were dominated by fish chorusing and other persistent low frequency sounds. Because fish chorusing is a periodic phenomenon, and the timing of the toadfish and unidentified knock chorusing match previous soundscape descriptions of offshore reefs in our study region, we expect this alignment would persist annually (Rice et al. 2016, Van Hoeck et al. 2020). Despite the temporal variation in soundscape alignment, the SPL correlation between the sites was never lower than during the

first two sampling periods, indicating that the diel soundscape patterns were becoming more similar over time.

Investigation of the power spectrum of each soundscape was the most informative measure of community development and alignment between the reefs. Because animal vocalizations are species-specific, with a unique time and frequency signature, we were able to track the presence and behavior of multiple soniferous species. By focusing on the first and last sampling period, when the established reef soundscape consisted of the same dominant vocalizers, comparisons between the power spectra of the reefs facilitated interpretation of colonization dynamics of chorusing species. Specifically, the power spectra revealed rapid colonization by toadfish, and slower colonization by the species producing the unidentified knock.

Without visual confirmation, we are unable to say for certain whether toadfish were present on-reef within two weeks; however, comparison between the received call amplitudes provides evidence that toadfish were vocalizing proximal to the hydrophone on both reefs. For example, the sound level of the first toadfish harmonic observed on each reef during the first sampling period differed by only 2 dB, with amplitudes approaching the documented source levels for toadfish boatwhistles (Luczkovich et al. 2017). Additionally, during the first sampling period, choruses of the unidentified knock (0.4 – 1.2 kHz) were recorded on the established reef, but not the new reef, suggesting that not all low frequency sounds were transmitted between the reefs.

Current limitations of PAM include the challenges of identifying vocalizations to species and interpreting soundscape dynamics. While our findings reveal exciting ecological implications for colonization of novel habitat by cryptic species and soundscape development

generally, we are unable to interpret the ecological implications of the slower colonization by the unidentified knock species compared to the toadfish species or of the unidentified sound sources observed in September. Additionally, without a control site at unstructured habitat within our study region, we are unable to interpret ecological significance of ambient soundscape variability during non-chorusing periods. Due to the battery-life constraints of the underwater video cameras, we sampled the reefs during multiple short sampling periods. If the hydrophones had been deployed separately from the cameras and recorded on a duty cycle for the duration of the study period, we may have captured additional colonization dynamics. With increased global coverage of marine soundscape studies and advancements in automated detection and classification, the number of documented vocalizations and acoustic catalogues are increasing. These technologies and open-access sharing will be crucial for expanding the practical application of PAM to monitoring and conservation contexts.

PAM and traditional method comparisons

Throughout the literature on passive acoustic monitoring of marine soundscapes and its application to management questions, a common theme has been the benefit of PAM for understanding the presence of cryptic fishes and invertebrates (Staaterman et al. 2017, Putland et al. 2018, Mooney et al. 2020). For example, despite decades of monthly diver-based visual census in a marine protected area in the Adriatic Sea, it was unknown that a cryptic cusk eel, *Ophidion rochei*, was present until it was identified by PAM (Picciulin et al. 2019). Within the context of this study, PAM identified colonization of novel habitat by toadfish, a cryptic demersal fish species, approximately four months earlier than detected for conspicuous demersal fish species by video monitoring. Previous diver-based visual censuses of fish communities in

Onslow Bay suggest that toadfish have a very low density of 1 individual per hectare (Whitfield et al. 2014) and are usually found on top of artificial reef structure as opposed to adjacent sand flats (Rosemond et al. 2018). As fish choruses are associated with spawning behaviors, it is likely that toadfish populations have higher densities, at least seasonally, and that these visual surveys may have underestimated the density of cryptic fishes.

Although invertebrates were not the focus of the underwater video monitoring, our snapping shrimp results align with the findings of other studies on invertebrate colonization dynamics. The strong correlation between the high frequency SPL timeseries, but ~17 dB difference in SPL suggests that the snaps recorded on the new reef during early sampling periods originated on adjacent habitats. The sustained lower SPLs on the new reef suggest that snapping shrimp density had not converged with that of the established reef by 11-months post artificial reef deployment. Despite this, the substantial increase in dusk SPL on the new reef but not the established reef between the first two and the last two sampling periods suggests that snapping shrimp may have begun to colonize the new reef within two-months after artificial reef deployment and that their density continued to increase. Similar to our findings, benthic assemblages on artificial reefs offshore of Southeastern Florida, USA were variable for the first four years following artificial reef deployment (Thanner et al. 2006), and on artificial reefs in the Red Sea, the benthic community still hadn't stabilized after 10 years (Perkol-Finkel and Benayahu 2005).

Ecological context of colonization trajectory

Hypotheses explaining the trajectory of novel habitat colonization often center around priority effects and their resulting trophic interactions (Fukami 2015). For example, the rapid

colonization by planktivorous fish species documented by video monitoring was hypothesized to be driven by high zooplankton abundance above the novel structure. Manipulative experiments in coral reef communities suggest that high abundances of these fishes in the water-column could facilitate colonization by piscivorous species, which through predation pressure, could inhibit demersal species colonization (Almany 2003, Stier et al. 2017). It was also hypothesized that demersal species may have been slower to colonize because they often rely on benthic biota as a food source, which is slower to appear on novel structures (Paxton et al. 2018).

Interestingly, the rapid colonization by toadfish identified by PAM suggests that not all demersal species were excluded by early arrival of piscivores, nor were they deterred by the lack of benthic biota present in the early stages. This finding may provide support for the hypothesis that the role of physical structure as refuge is an important driver of colonization dynamics and community structure (Hixon and Beets 1993, Caley and John 1996, Schroeter et al. 2015). For example, a species that relies primarily on the physical structure for refuge could be expected to quickly colonize novel habitat (Keller et al. 2017). Toadfish, which predominately hide in crevices in the habitat structure, may rely more heavily on the presence of structure than prey availability for colonization (Fine 1978). In oyster reef systems, Oyster toadfish (*Opsanus tau*) are known to facilitate oyster survival by eliciting predator avoidance behavior by mud crabs, thereby reducing mud crab predation on juvenile oysters (Grabowski 2004). If similar trophic dynamics occur on offshore reefs, then it could be hypothesized that the rapid colonization by toadfish may facilitate the colonization of the reef structure by benthic biota, as well as the subsequent colonization of conspicuous demersal species that rely on this biota as a food source.

In the context of evaluating habitat enhancement outcomes, the comparison with an adjacent established reef was essential to interpreting the time-lags of community development

on the newly deployed reef. While PAM revealed additional insights compared to video monitoring within the first two-weeks following artificial reef deployment, it is important to note that the PAM time-series consisted of six sampling periods, up to 11-months following deployment of the new reef, whereas the video time series consisted of only the first three sampling periods, up to four-months post reef deployment. This extended soundscape sampling revealed nuanced information on colonization patterns, specifically the unidentified knock species and snapping shrimp, not available in the video data.

Though our research is a case study on offshore artificial reefs, the use of artificial structures as supplemental habitat or replacement for degraded natural habitat is common across marine systems (Becker et al. 2018). Our findings demonstrate that passive acoustics, especially when used in combination with traditional methods, offer a compelling approach to elucidate patterns and time-lags in community development and improve assessment of habitat enhancement outcomes.

REFERENCES

Al-Horani, F. A., and M. A. Khalaf. 2013. Developing artificial reefs for the mitigation of man-made coral reef damages in the Gulf of Aqaba, Red Sea: Coral recruitment after 3.5 years of deployment. Marine Biology Research 9:749–757.

Alboukadel, K. 2021. rstatix: Pipe-Friendly Framework for Basic Statistical Tests.

Almany, G. R. 2003. Priority effects in coral reef fish communities. Ecology 84:1920–1935.

Baine, M. 2001. Artificial reefs: a review of their design, application, management and performance. Ocean & Coastal Management 44:241–259.

Becker, A., M. D. Taylor, H. Folpp, and M. B. Lowry. 2018. Managing the development of artificial reef systems: The need for quantitative goals. Fish and Fisheries 19:740–752.

Bortone, S. A. 2006. A perspective of artificial reef research: The past, present, and future. Bulletin of Marine Science 78:1–8.

Bortone, S. A. 2011. Introduction to the role of artificial reefs play in fisheries management. Pages 1–5 in S. A. Borton, F. P. Brandini, G. Fabi, and S. Otake, editors. Artificial reefs in fisheries management. CRC Press, Boca Raton, FL.

Butler, J., J. A. Stanley, and M. J. I. Butler. 2016. Underwater soundscapes in near-shore tropical habitats and the effects of environmental degradation and habitat restoration. Journal of Experimental Marine Biology and Ecology 479:89–96.

Caley, M. J., and J. S. John. 1996. Refuge Availability Structures Assemblages of Tropical Reef Fishes. The Journal of Animal Ecology 65:414.

Comer, A. M., and R. Love-Adrick. 2016. North Carolina Division of Marine Fisheries Artificial Reef Guide. NC Division of Marine Fisheries, Morehead City, North Carolina, USA.

Cummings, S. L. 1994. Colonization of a nearshore artificial reef at Boca Raton (Palm Beach County), Florida. Bulletin of Marine Science 55:1193–1215.

Davis, G. E., M. F. Baumgartner, P. J. Corkeron, J. Bell, C. Berchok, J. M. Bonnell, J. Bort Thornton, S. Brault, G. A. Buchanan, D. M. Cholewiak, C. W. Clark, J. Delarue, L. T. Hatch, H. Klinck, S. D. Kraus, B. Martin, D. K. Mellinger, H. Moors-Murphy, S. Nieukirk, D. P. Nowacek, S. E. Parks, D. Parry, N. Pegg, A. J. Read, A. N. Rice, D. Risch, A. Scott, M. S. Soldevilla, K. M. Stafford, J. E. Stanistreet, E. Summers, S. Todd, and S. M. Van Parijs. 2020. Exploring movement patterns and changing distributions of baleen whales in the western North Atlantic using a decade of passive acoustic data. Global Change Biology 26:4812–4840.

Fine, M. L. 1978. Seasonal and Geographical Variation of the Mating Call of the Oyster Toadfish Opsanus tau L. Oecologia 36:45–57.

Fukami, T. 2015. Historical Contingency in Community Assembly: Integrating Niches, Species Pools, and Priority Effects. Annual Review of Ecology, Evolution, and Systematics 46:1–23.

Grabowski, J. H. 2004. Habitat complexity disrupts predator-prey interactions but not the trophic cascade on oyster reefs. Ecology 85:995–1004.

Gregg, K., and S. Murphey. 1994. The role of vessels as artificial reef material on the Atlantic and Gulf of Mexico coasts of the United States. Special Report Number 38 of the Atlantic States Marine Fisheries Commission. Morehead City, North Carolina, USA.

Halpern, B. S., M. Frazier, J. Afflerbach, J. S. Lowndes, F. Micheli, C. Scarborough, and K. A. Selkoe. 2019. Recent pace of change in human impact on the world's ocean. Scientific Reports 9:11609.

Hixon, M. A., and J. P. Beets. 1993. Predation, prey refuges, and the structure of coral-reef fish assemblages. Ecological Monographs 63:77–101.

Van Hoeck, R. V., A. B. Paxton, D. W. R. Bohnenstiehl, J. C. Taylor, F. J. Fodrie, D. P. Nowacek, C. M. Voss, and C. H. Peterson. 2020. Soundscapes of natural and artificial temperate reefs: similar temporal patterns but distinct spectral content. Marine Ecology Progress Series 649:35–51.

Keller, D. A., R. K. Gittman, R. K. Bouchillon, and F. J. Fodrie. 2017. Life stage and species identity affect whether habitat subsidies enhance or simply redistribute consumer biomass. Journal of Animal Ecology 86:1394–1403.

Leitão, F., M. N. Santos, K. Erzini, and C. C. Monteiro. 2009. Diplodus spp. assemblages on artificial reefs: Importance for near shore fisheries. Fisheries Management and Ecology 16:88–99.

Lima, J. S., I. R. Zalmon, and M. Love. 2019. Overview and trends of ecological and socioeconomic research on artificial reefs. Marine Environmental Research 145:81–96.

Luczkovich, J. J., C. S. Krahforst, K. E. Kelly, and M. W. Sprague. 2017. The Lombard effect in fishes: How boat noise impacts oyster toadfish vocalization amplitudes in natural experiments. Page 10035 Proceedings of Meetings on Acoustics. Acoustical Society of America.

MATLAB. 2018. 9.1.0.441655 (R2019a). The MathWorks Inc., Natick, Massachusetts.

Mooney, T. A., L. Di Iorio, M. Lammers, T. Lin, S. L. Nedelec, M. Parsons, C. Radford, E. Urban, and J. Stanley. 2020. Listening forward: approaching marine biodiversity assessments using acoustic methods. Royal Society Open Science 7:201287.

Van Parijs, S. M., C. W. Clark, R. S. Sousa-Lima, S. E. Parks, S. Rankin, D. Risch, and I. C. Van Opzeeland. 2009. Management and research applications of real-time and archival passive acoustic sensors over varying temporal and spatial scales. Marine Ecology Progress Series

395:21–36.

Paxton, A. B., E. A. Pickering, A. M. Adler, J. C. Taylor, and C. H. Peterson. 2017. Flat and complex temperate reefs provide similar support for fish: Evidence for a unimodal species-habitat relationship. PLoS ONE 12:e0183906.

Paxton, A. B., L. W. Revels, R. C. Rosemond, R. V. Van Hoeck, H. R. Lemoine, J. C. Taylor, and C. H. Peterson. 2018. Convergence of fish community structure between a newly deployed and an established artificial reef along a five-month trajectory. Ecological Engineering 123:185–192.

Perkol-Finkel, S., and Y. Benayahu. 2005. Recruitment of benthic organisms onto a planned artificial reef: shifts in community structure one decade post-deployment. Marine Environmental Research 59:77–99.

Picciulin, M., L. Kéver, E. Parmentier, and M. Bolgan. 2019. Listening to the unseen: Passive acoustic monitoring reveals the presence of a cryptic fish species. Aquatic Conservation: Marine and Freshwater Ecosystems 29:202–210.

Pickering, H., D. Whitmarsh, and A. Jensen. 1998. Articial Reefs as a Tool to Aid Rehabilitation of Coastal Ecosystems: Investigating the Potential. Marine Pollution Bulletin 37:505–514.

Pratt, J. R. 1994. Artificial habitats and ecosystem restoration: Managing for the future. BULLETIN OF MARINE SCIENCE 55:268–275.

Putland, R. L., A. G. Mackiewicz, and A. F. Mensinger. 2018. Localizing individual soniferous fish using passive acoustic monitoring. Ecological Informatics 48:60–68.

R Core Team. 2020. R: A language and environment for statistical computing. R Foundation for Statistical Computing, Vienna, Austria.

Relini, G., and L. Orsi Relini. 1989. Artificial reefs in the Ligurian Sea (Northwestern Mediterranean): Aims and Results. Bulletin of Marine Science 44:743–751.

Ricci, S., D. Eggleston, D. Bohnenstiehl, and A. Lillis. 2016. Temporal soundscape patterns and processes in an estuarine reserve. Marine Ecology Progress Series 550:25–38.

Rice, A. N., J. L. Morano, K. B. Hodge, and C. A. Muirhead. 2016. Spatial and temporal patterns of toadfish and black drum chorusing activity in the South Atlantic Bight. Environmental Biology of Fishes 99:705–716.

Riggs, S. R., S. W. Snyder, A. C. Hine, and D. L. Mearns. 1996. Hardbottom morphology and relationship to the geological framework: Mid-Atlantic continental shelf. Journal of Sedimentary Research 66:830–846.

Rilov, G., and Y. Benayahu. 2002. Rehabilitation of coral reef-fish communities: The importance of artificial-reef relief to recruitment rates. Bulletin of Marine Science 70:185–197.

Rosemond, R. C., A. B. Paxton, H. R. Lemoine, S. R. Fegley, and C. H. Peterson. 2018. Fish use of reef structures and adjacent sand flats: implications for selection minimum buffer zones between new artificial reefs and exisiting reefs. Marine Ecology Progress Series 587:187–199.

Scarcella, G., F. Grati, L. Bolognini, F. Domenichetti, S. Malaspina, S. Manoukian, P. Polidori, A. Spagnolo, and G. Fabi. 2015. Time-series analyses of fish abundance from an artificial reef and a reference area in the central-Adriatic Sea. Journal of Applied Ichthyology 31:74–85.

Schroeter, S. C., D. C. Reed, and P. T. Raimondi. 2015. Effects of reef physical structure on development of benthic reef community: A large-scale artificial reef experiment. Marine Ecology Progress Series 540:43–55.

Seaman, W. 2007. Artificial habitats and the restoration of degraded marine ecosystems and fisheries. Hydrobiologia 580:143–155.

Sherman, R. L., D. S. Gilliam, and R. E. Spieler. 2002. Artificial reef design: Void space, complexity, and attractants. ICES Journal of Marine Science 59:196–200.

Staaterman, E., M. B. Ogburn, A. H. Altieri, S. J. Brandl, R. Whippo, J. Seemann, M. Goodison, and J. E. Duffy. 2017. Bioacoustic measurements complement visual biodiversity surveys: preliminary evidence from four shallow marine habitats. Marine Ecology Progress Series 575:207–215.

Stier, A. C., S. W. Geange, K. M. Hanson, and B. M. Bolker. 2017. Predator density and timing of arrival affect reef fish community assembly. Ecology 94:1057–1068.

Thanner, S. E., T. L. McIntosh, and S. M. Blair. 2006. Development of benthic and fish assemblages on artificial reef materials compared to adjacent natural reef assemblages in Miami-Dade County, Florida. Bulletin of Marine Science 78:57–70.

Whitfield, P. E., R. C. Muñoz, C. A. Buckel, B. P. Degan, D. W. Freshwater, and J. A. Hare. 2014. Native fish community structure and Indo-Pacific lionfish Pterois volitans densities along a depth-temperature gradient in Onslow Bay, North Carolina, USA. Marine Ecology Progress Series 509:241–254.

Whitmarsh, D., M. N. Santos, J. Ramos, and C. C. Monteiro. 2008. Marine habitat modification through artificial reefs off the Algarve (southern Portugal): An economic analysis of the fisheries and the prospects for management. Ocean and Coastal Management 51:463–468.

Table 4. 1 Comparison of qualitative conclusions drawn from video and passive acoustic monitoring.

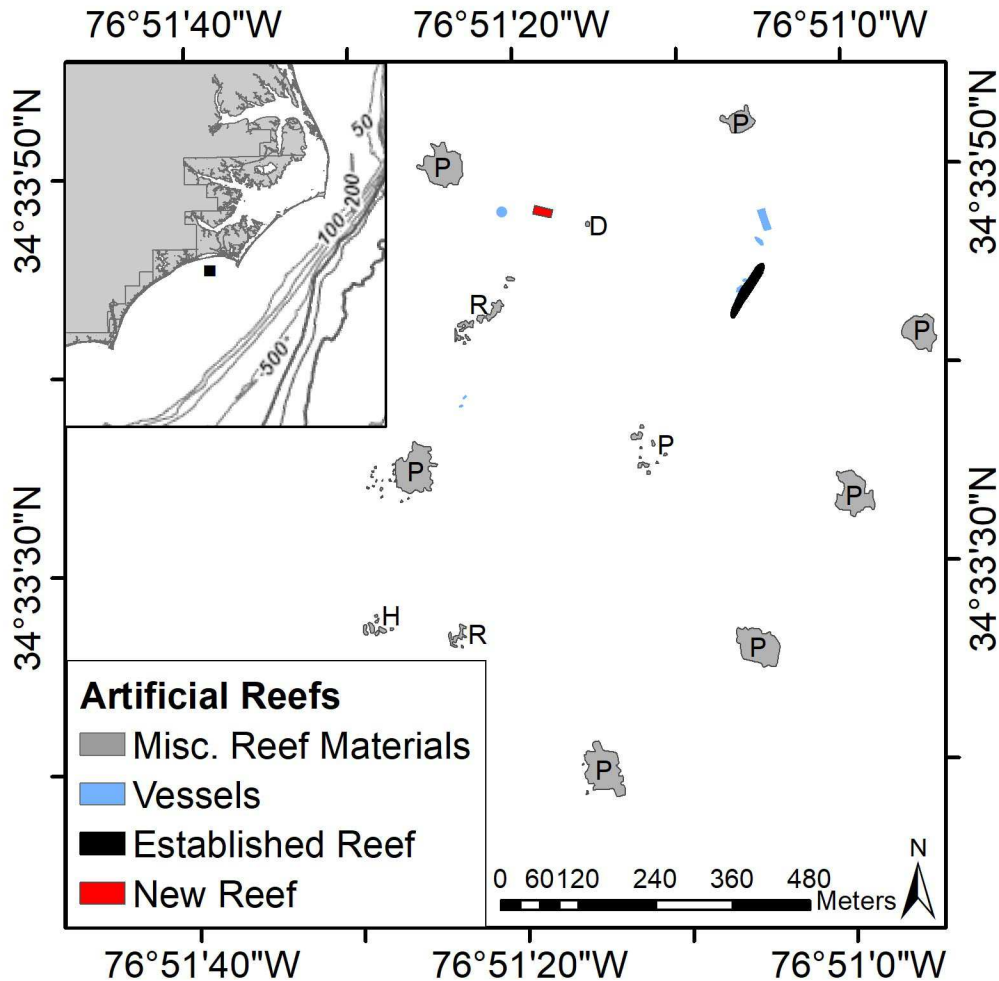| Conclusions drawn	Video Monitoring	PAM
Rapid fish colonization	Yes	Yes
Fish community convergence	Yes	Mixed (fish chorusing alignment)
Demersal species colonization	5 months	Toadfish within two weeks
Piscivorous species colonization	Within two-weeks	Not available
Invertebrate colonization	Not available	Increasing, but not converged

Figure 4. 1 Position of AR-330 within Onslow Bay, NC, USA (inset map) and of the sampled reefs in relation to each other and surrounding artificial reefs. The reefs sampled in this study are labelled as "Established reef" and "New reef" as referred to in the text. The "Miscellaneous Reef Materials" consist of artificial structures with low vertical relief (P: concrete pipes, R: reef balls, H: "H" units, D: fiberglass domes) that were deployed between 1990 and 2005. The "Vessels" consist of high relief structures (e.g., sailboats and aircraft) deployed between 1994 and 2012, except for the vessel point adjacent to the new reef, which is a tugboat deployed on the same day as the new reef (7 May 2016). (Inset basemap: General Bathymetric Chart of the Oceans; NOAA NCEI).

Figure 4. 2 Correlation between the low frequency (0.15 – 2 kHz) SPL timeseries. SPL timeseries (left), SPL distribution (center), and timeseries correlation with 1:1 line and correlation coefficient (cc; right). Comparisons between the SPL timeseries show that the established reef (black) had a stable temporal pattern, with dusk (gray bands) peaks in acoustic activity, while the new reef (red) exhibited more diurnal variability.
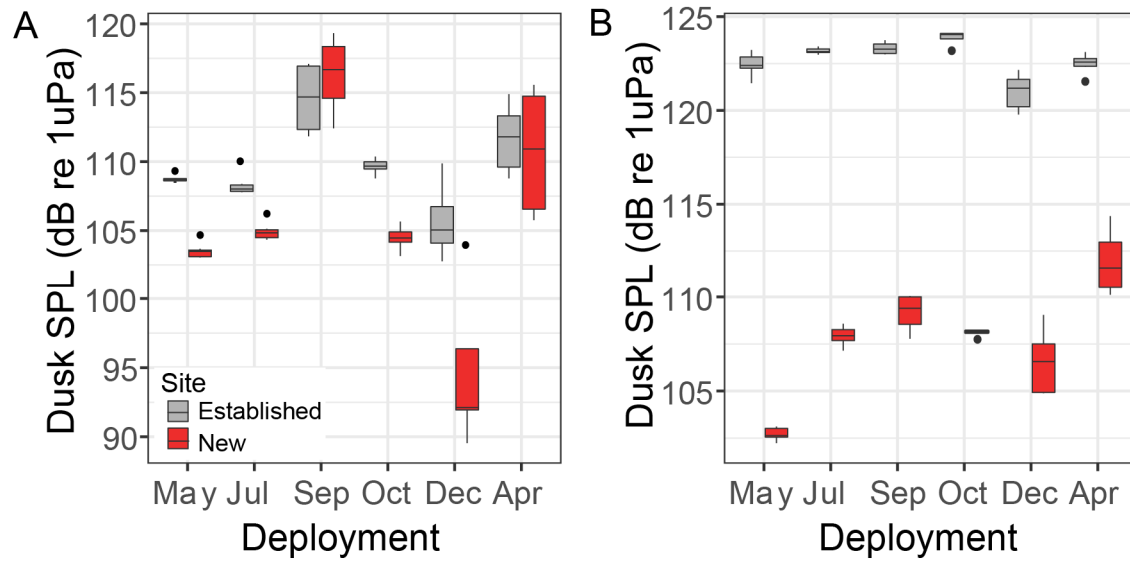
Figure 4. 3 Dusk SPL in the (a) low frequency and (b) high frequency bands. Note that the time scale of the x-axis is not linear. The black bar is the median while the lower and upper edges of the box are the first and third quartiles. The whiskers extend to either the most extreme value or to 1.5 times the interquartile range and any outliers are plotted individually.
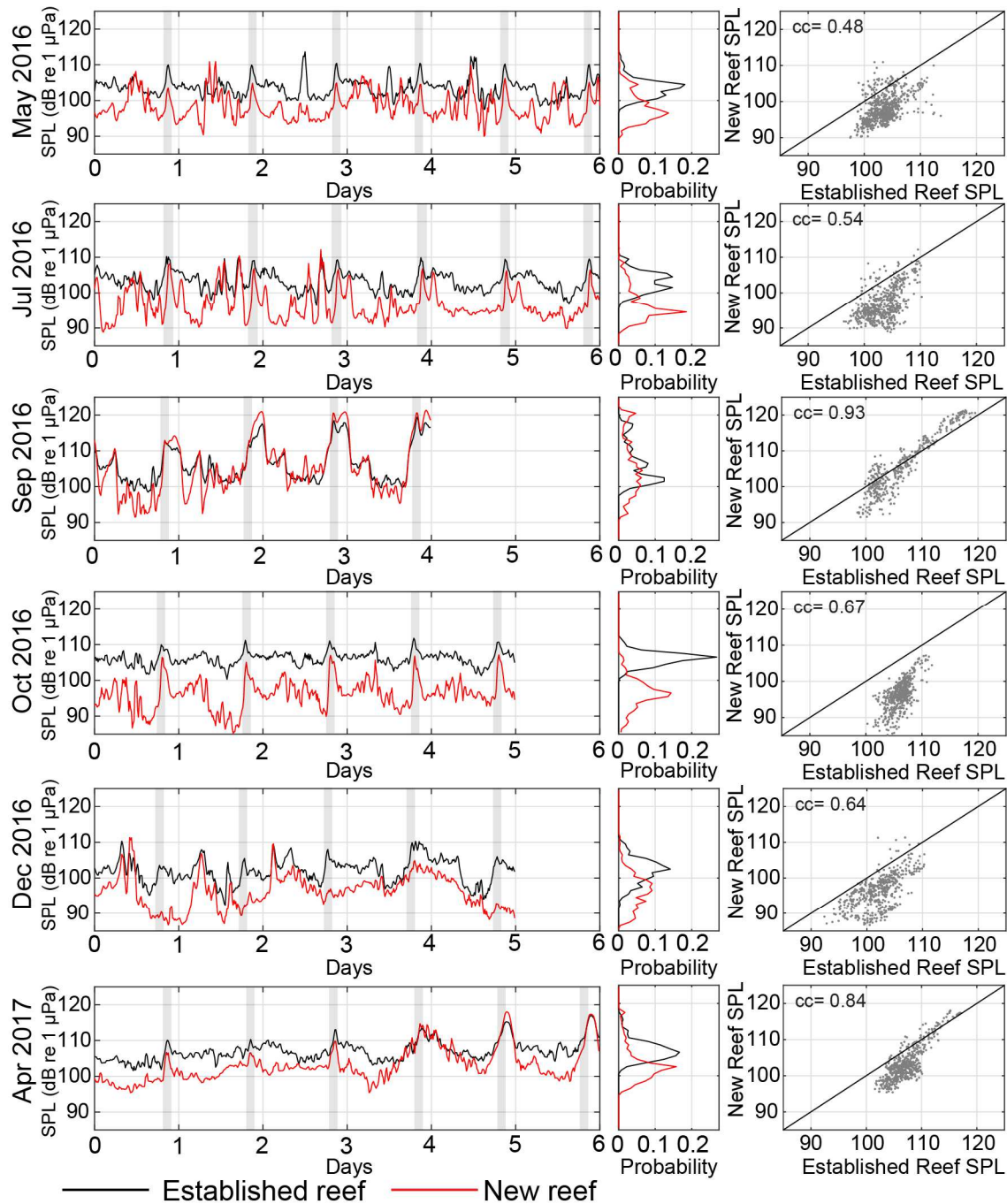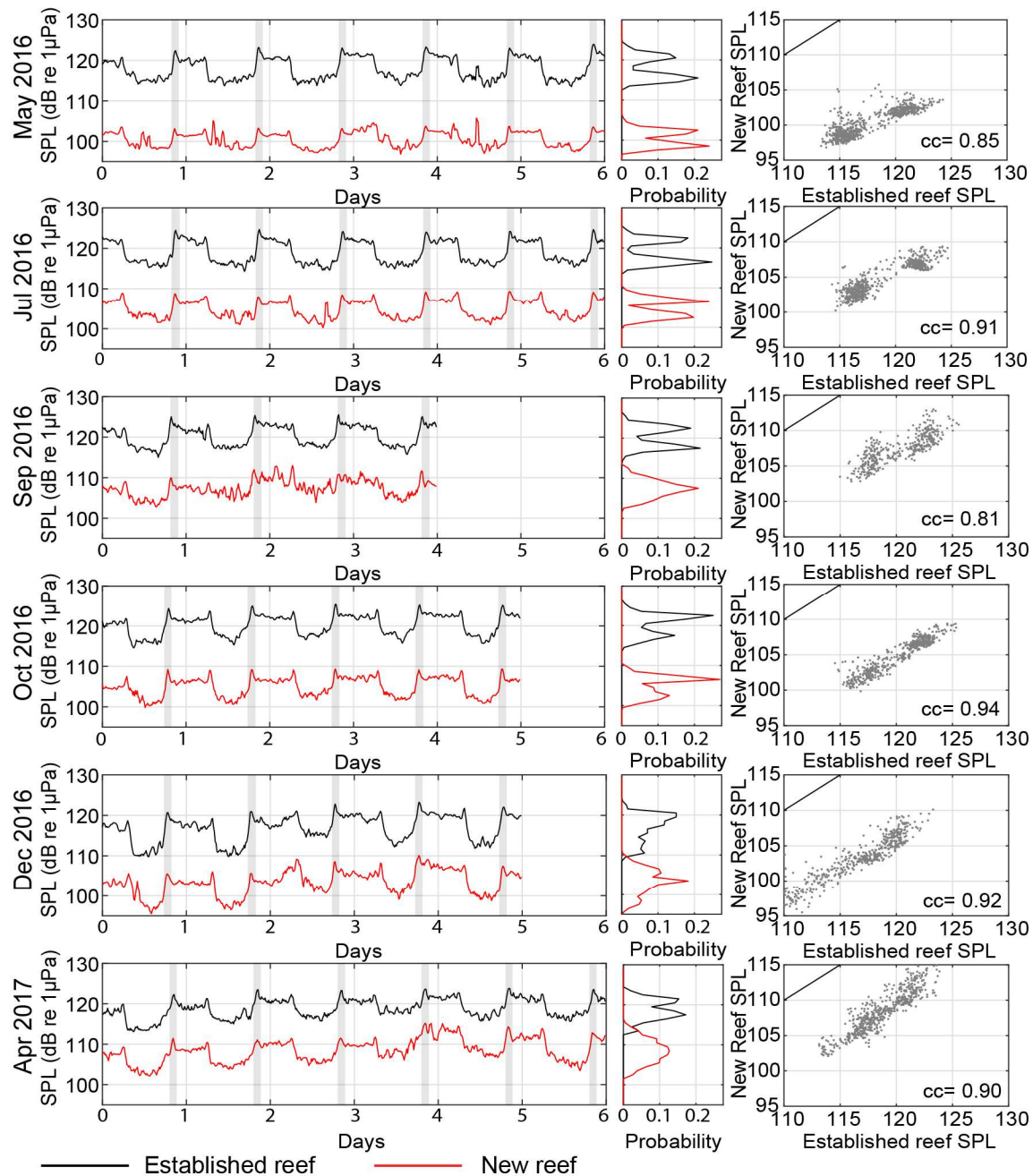
Figure 4. 4 Correlation between the high frequency (7 – 15 kHz) SPL timeseries. SPL timeseries (left), SPL distribution (center), and timeseries correlation with 1:1 line and correlation coefficient (cc; right). Despite consistently lower SPLs on the new reef (red) than the established reef (black), their timeseries were highly correlated during all sampling periods.
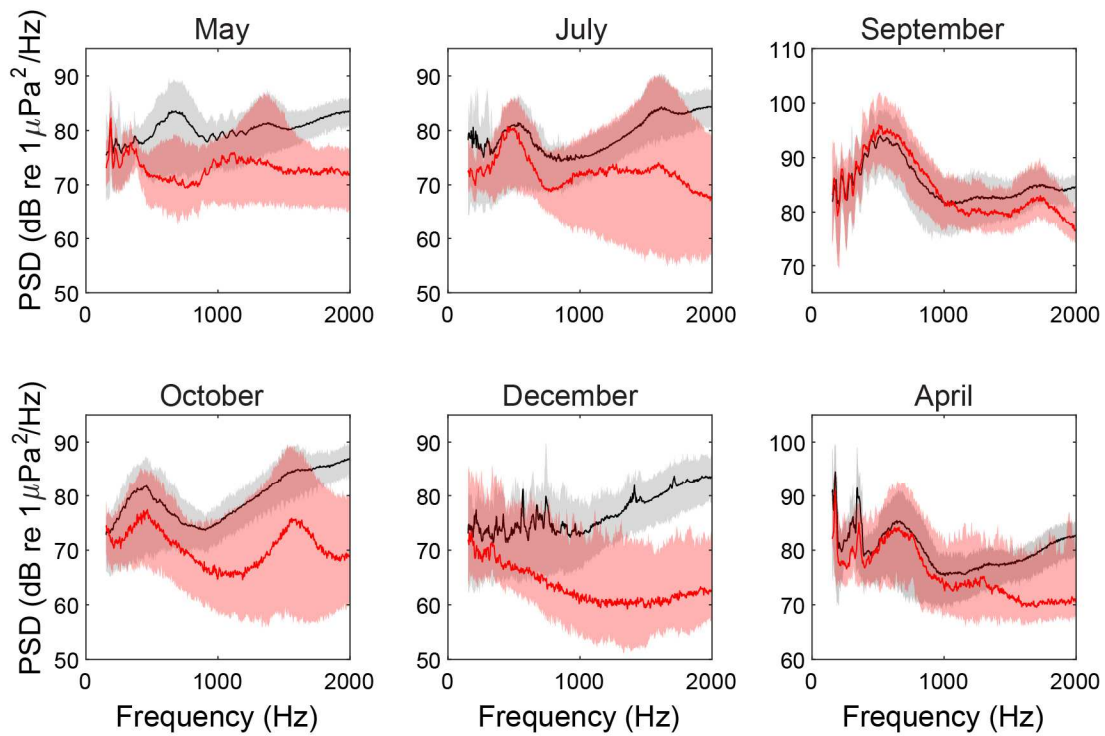
Figure 4. 5 Average low frequency power spectrum at dusk. The shaded regions show the 0.05 – 0.95 inter-quantile range (IQR) for each reef. The 190 Hz peak on both reefs during May indicates the rapid colonization of toadfish, while the absence of the 500 – 1000 Hz peak on the new reef during May and its presence in April, indicates the slower colonization by the unidentified knock species.
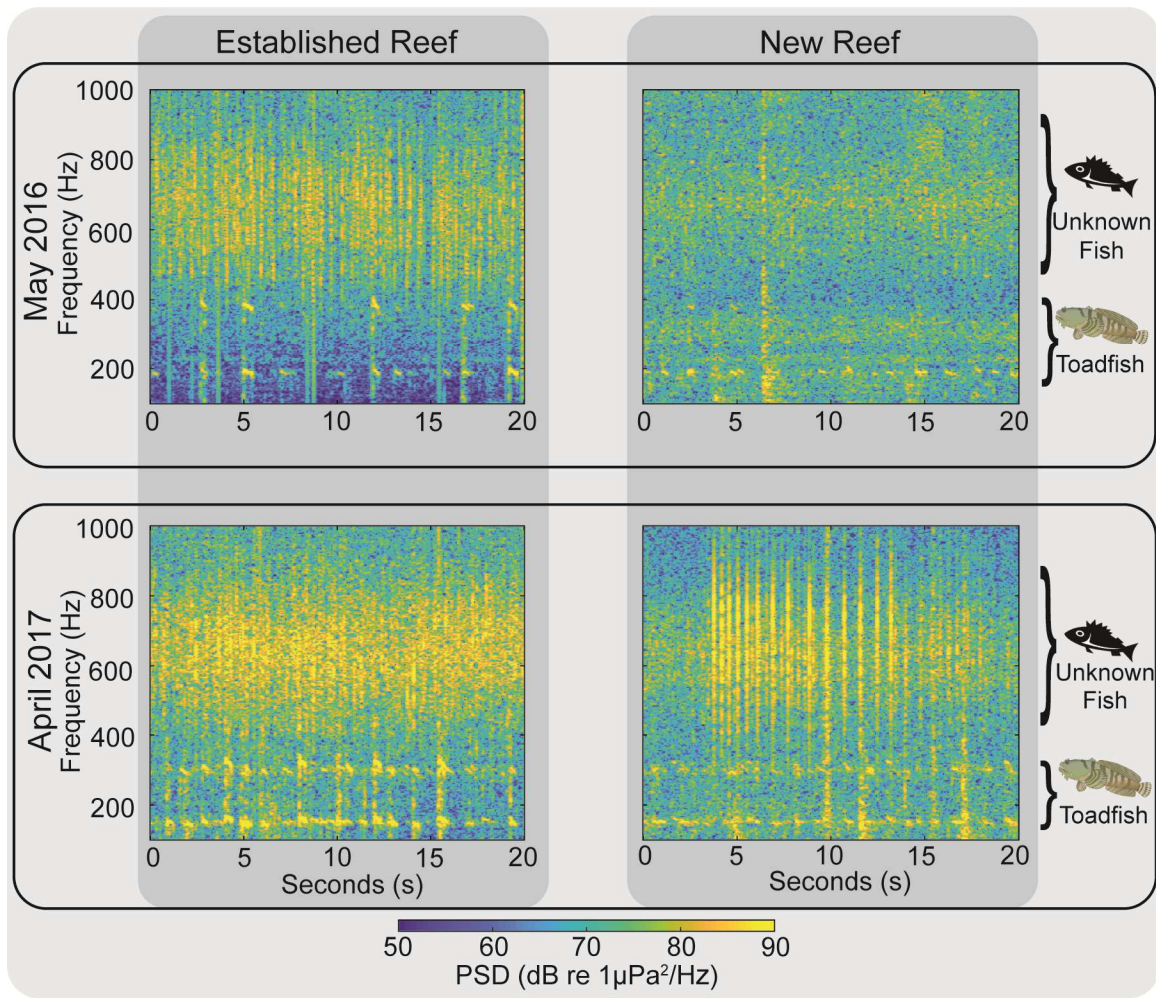
Figure 4. 6 Representative spectrograms of the dusk soundscape on both reefs during the May 2016 and April 2017 sampling periods. The spectrograms are 20 second samples from a representative file, recorded at the same time on both reefs. Comparisons among the four soundscapes suggest that toadfish rapidly colonized the new reef, shown by vocalizations present on both reef during May 2016, while the unknown knock species exhibited a slower colonization, demonstrated by the presence of chorusing on established reef and lack of chorusing on the new reef during May.

CHAPTER 5: COMPARING ATLANTIC COD SPAWNING DYNAMICS ACROSS A BIOGEOGRAPHIC BOUNDARY: INSIGHTS FROM PASSIVE ACOUSTIC MONITORING[3]

Introduction

To meet demand for a transition to renewable energy, offshore wind energy development is rapidly expanding in the United States. As a result, there has been increasing effort to understand the potential interactions between marine ecosystems and offshore wind farms throughout all phases of development. Evidence suggests that interactions can include positive effects for some species such as increased epibiont abundance (Hutchison et al. 2020) and fish densities (Bergström et al. 2013; Stenberg et al. 2015) around the turbine structure as well as negative effects to existing complex habitat (Guarinello and Carey 2020). For marine animals, acoustic disturbance can result in masking auditory communication, displacement, hearing loss (Popper and Hawkins 2019), and increased stress (Wysocki et al. 2006). Each phase of offshore wind energy development includes different sources of potential interactions with unique spatiotemporal risk zones. During project siting, operation, and decommissioning, most disturbance stems from vessel activity and associated noise at the wind energy area. This noise pollution generally has a small spatial effect but persists over multiple decades. Conversely, the construction phase involves numerous sources of potential disturbance that can occur at both small and large spatial scales and persist over multiple years. These disturbances include habitat

---

effects from construction of turbine foundations and cable laying as well as acoustic effects from vessel activity and pile-driving (Mooney et al. 2020).

Due to the risk of broad spatial and temporal overlap, interactions between the construction phase of offshore wind energy development and marine ecosystems have received the most attention. A priority concern is pile driving which results in loud, impulsive noise pollution that is sustained during all times of day for multiple weeks and can propagate at elevated sound levels for tens of kilometers away from the source (Bailey et al. 2010; Andersson et al. 2017). Impulsive sounds have complex effects on the behavior, movement, and physiology of marine animals, the magnitude of which depends on distance from the sound source as well as the role of acoustic communication in the behavior and life history characteristics of the species (Madsen et al. 2006). For example, comparison of sound exposure criteria for bottlenose dolphins to measured sound levels from pile driving revealed that auditory damage was possible within 100m of the sound source, but behavioral effects could extend to 50km (Bailey et al. 2010). In fishes, exposure to pile driving sounds has been shown to affect the behavior of certain species, such as European seabass and Atlantic cod, by negatively affecting group cohesion (Herbert-Read et al. 2017) as well as eliciting changes in depth and movement away from the sound source (Neo et al. 2016; van der Knaap et al. 2022). Moreover, experimental exposure to noise reduced spawning success in two goby species due to reduced acoustic courtship by males and lack of spawning by females (de Jong et al. 2018). The combined effects of ground-disturbing activities on habitats and acoustic disturbance from construction on fish spawning is of particular concern for species that use acoustic communication during courtship and are unlikely to successfully shift reproduction to locations that are not disturbed, such as those that exhibit high fidelity to a spawning site (de Jong et al. 2020).

Of the US offshore wind energy projects currently in development, many are located off Southern New England and the Mid-Atlantic Bight in the Western North Atlantic Ocean. As a result, understanding potential interactions between offshore wind energy and fisheries resources, specifically Atlantic cod *Gadus morhua*, has become a management priority in the region. Atlantic cod have a complex metapopulation structure consisting of multiple subpopulations each with multiple spawning components (Zemeckis et al. 2014a). Within these components individuals exhibit high spawning site fidelity that is generally consistent in space and time each year (Robichaud and Rose 2001; Zemeckis et al. 2014b). During the spawning season, cod migrate to the spawning site and form dense aggregations within which reproductive males defend small territories (Nordeide and Folstad 2000; Fudge and Rose 2009). This aggregation behavior includes a courtship ritual where males produce repetitive grunt-like sounds to attract a mate (Brawn 1961a; Finstad and Nordeide 2004). Sound production is thought to play a role in mate choice, as sound intensity and sound-producing muscle mass are correlated with male body size and mating success, respectively (Brawn 1961b; Hutchings et al. 1999; Rowe and Hutchings 2008). This combination of spawning site fidelity and use of acoustic communication during spawning could make Atlantic cod vulnerable to acoustic and physical disturbance from offshore wind energy development.

Successful spawning is critical to sustain and rebuild populations and experiments have shown that repeated exposure of Atlantic cod to anthropogenic noise can reduce the number of viable embryos produced by more than 50%, due to decreased egg production and fertilization rates (Sierra-Flores et al. 2015). Furthermore, spawning disturbance associated with offshore wind energy development may have interactive effects with other anthropogenic and natural stressors. In the US, Atlantic cod spawning components have experienced consistent declines

due to interacting pressures from overexploitation (Ames 2004; Zemeckis et al. 2014c), loss of stock stability (Reich and DeAlteris 2009), a mismatch between biological stock structure and management (Kerr et al. 2014), environmental variability (Brander 2005; Friedland et al. 2013), and range contraction due to climate change induced thermal habitat loss (Nye et al. 2009; Friedland et al. 2020). In theory, a metapopulation structure should buffer against fluctuations in spawning success of discrete components while maintaining the overall stock complex (Stephenson 1999; Rose et al. 2011); however, attempts to rebuild the Atlantic cod stock have been unsuccessful (Lilly et al. 2008; Lindegren et al. 2013; Zemeckis et al. 2014a) and much of the population structure has been lost (Ames 2004). In an attempt to improve the management and recovery of the Atlantic cod stock, recent research has focused on expanding the understanding of connectivity between sub-populations and their relative roles in maintaining the stock. Atlantic cod have historically been managed as two US stocks, the Gulf of Maine stock and Georges Bank stock which includes the Southern New England subpopulation, but a recent synthesis has identified five genetically distinct subpopulations (McBride et al. 2021). Current understanding suggests that most of the spawning stock biomass remains in the Gulf of Maine which consists of distinct winter and spring spawning subpopulations. Southern New England supports its own distinct spawning group but also receives imports of eggs and larvae from Gulf of Maine winter spawners (McBride et al. 2021).

Studies of spatiotemporal spawning dynamics within the Gulf of Maine, Georges Bank, and other global Atlantic cod stocks have identified that spawning generally occurs over a multiple month period, with peaks in grunt activity at night near the new and full moons (Grabowski et al. 2015; Zemeckis et al. 2019). Studies of winter spawning aggregations throughout Massachusetts Bay, in the western Gulf of Maine, have identified that within the

125

October to January spawning period the seasonal timing of peak grunt activity varies among individual aggregations with deeper sites exhibiting a peak later in the spawning season (Zemeckis et al. 2019; Caiger et al. 2020). Compared to the Gulf of Maine and Georges Bank, relatively little data exist regarding the dynamics and structure of cod in Southern New England waters. To better understand interactions with offshore wind energy development and support stock rebuilding, a broader understanding of the spatiotemporal spawning dynamics of Atlantic cod in Southern New England is needed.

To fill the knowledge gap regarding potential interactions between Atlantic cod and offshore wind energy development in Southern New England, we employed multiple passive acoustic monitoring technologies to infer the spatiotemporal spawning dynamics of Atlantic cod in and around planned offshore wind energy lease areas. Due to the role of sound production in cod spawning, passive acoustic monitoring offers multiple advantages including access to long-term data from a non-invasive approach. The temporal dynamics of spawning-associated grunt activity identified near Cox Ledge in Southern New England waters were also compared to those identified in an analogous study of the geographically separated winter-spawning subpopulation in Massachusetts Bay within the western Gulf of Maine. Given the lack of data on Atlantic cod in Southern New England, the goal of this comparison was to assess whether the observed dynamics were similar to those of other spawning groups. Our comparison may strengthen managers ability to draw inferences about potential interactions between Atlantic cod spawning and offshore wind energy from sparse data and facilitate interpretation of our results in context of the broader stock complex.

Study Area

Passive acoustic monitoring of Atlantic cod spawning-associated grunts was conducted in Southern New England waters, with survey effort concentrated between Block Island and Martha's Vineyard and at depths between 30 – 50 m (Figure 1). The main bathymetric feature in the study area is Cox Ledge, an area of complex, rocky substrate southeast of Block Island. Cox Ledge is used by commercial and recreational fishing fleets and is included as essential fish habitat for all life stages of Atlantic cod (Lough 2004; DeCelles et al. 2017).

To assess potential interactions between Atlantic cod spawning and offshore wind energy, the study intentionally sampled multiple lease areas planned for development within the Rhode Island and Massachusetts Wind Energy Area including the South Fork, and portions of Revolution, and Sunrise Wind Farms (Figure 2). The South Fork Wind Farm spans 55.4 km^2 on Cox Ledge with cable connections extending along the seafloor to New York. To date, the South Fork Wind is the only project in the sampling area that has received full approval to begin construction, planned for late 2022, and will consist of up to 12 turbines and one substation (BOEM and NMFS 2021). The Revolution Wind Farm spans 334.8 km^2 on Cox Ledge and the surrounding region with cables extending to Rhode Island. Construction of less than 100 turbines is anticipated to begin in 2023 (Revolution Wind 2021). The Sunrise Wind Farm spans 351.4 km^2 south of Cox Ledge with cables extending to New York. Construction of 59 – 122 turbines is proposed to begin in 2024 (Sunrise Wind 2021).

Methods

Data collection

Passive acoustic monitoring data were collected from fixed-station recording instruments (2013-2015 and 2020-2022) and mobile autonomous underwater gliders (2019-2022) (Table 1;

Figure 2). Fixed-station data facilitated the interpretation of temporal patterns, while glider-based surveys offered broad spatial coverage. The sampling locations were selected to ensure sampling within and around the wind lease areas as well as at putative spawning sites identified from historical data in the region and fishery-dependent data.

From 2013-2015, fixed-station data in Southern New England were collected by the Northeast Large Pelagic Survey Collaborative (consisting of the New England Aquarium, Cornell University Bioacoustics Research Program, the University of Rhode Island, and the Center for Coastal Studies) to document ambient noise conditions and the occurrence of marine mammals in the context of eventual offshore wind energy development (Kraus et al. 2016). However, the recording equipment used was also capable of recording the presence of cod grunts. During the sampling period, five marine autonomous recording units (MARUs) were successfully deployed throughout the Rhode Island and Massachusetts Wind Energy Areas (Figure 1b). The MARUs recorded continuously at a 2 kHz sampling rate with a 10-800 Hz band pass filter to reduce electrical interference and prevent aliasing. The gain and sensitivity, respectively, were 23.5 dB re 1 μPa and -168 dB re 1V/μPa (± 3dB between 10-1000 Hz). Identical MARU units have previously been used in other regions to characterize the spawning-associated grunt activity of cod (Hernandez et al. 2013; Zemeckis et al. 2019; Caiger et al. 2020).

From 2020 – 2022, fixed-station sound data were recorded continuously during the presumed spawning season at two sites using SoundTrap ST500s (Ocean Instruments, New Zealand) at a sampling rate of 48kHz. These sites were selected as putative cod spawning sites based on analysis of the 2013 – 2015 fixed-station data as well as telemetry and glider data recorded during 2019 – 2020. Specifically, telemetry data from the 2019 – 2020 glider deployment identified presence of multiple tagged cod at both sites and analysis of the 2013 –

128

2015 data provided evidence of a local spawning aggregation at site A (Figure 1B). The hydrophone at site A had a gain of 1.8 dB and sensitivity of -177 dB re 1 µPa/V. The hydrophone at site B had a gain of 1.9 dB and a sensitivity of -177.4 dB re 1 µPa/V.

The glider-based recorder was a digital acoustic monitoring instrument (DMON) (Baumgartner et al. 2013) mounted to a Mobile Slocum autonomous glider (Teledyne Webb Research)(Rudnick et al. 2004). The DMON recorded at a 2 kHz sampling rate. The glider was programmed to follow a grid consisting of 12 North-South transects that were separated by 5km. However, due to currents and oceanographic conditions, the glider deviated somewhat from this path. The programmed glider track was updated between deployments to improve spatial-temporal replication of the survey area. In 2019, the glider swam the grid from east to west, then reversed and traveled west to east covering a 2400 km^2 area from December 21, 2019 – March 22, 2020 (Figure 1c). In 2020 and 2021, the glider swam the same 12 transects except that southern extent was limited to the 50-m isobath (Figure 1d). Additionally, the glider swam east to west then flew back to start, passing directly over fixed station sites A and B on the way, and repeated the east-west circuit shifted 3-minutes east, covering an 1800 km^2 area in total. In each year the glider surveyed from November 11, 2020 – February 25, 2021 and from November 5, 2021 – February 7, 2022.

Cod grunt detection

All passive acoustic data were analyzed with a cod grunt detector (Urazghildiiev and Van Parijs 2016) executed in MATLAB then manually validated in Raven 1.5 (KLY-CCB 2014). The detector performance was evaluated during development using data from a 24-hour period at 19 MARUs. The probability of cod grunt detection ranged from 0.42 – 1.00 and the probability of

false detection ranged from 0.0083 – 0.16 (Urazghildiiev and Van Parijs 2016). For the 2013 –
2015 data, sites A, C, and D were analyzed from October 1, 2013 – January 31, 2014, during the
presumed spawning season based on fishery-dependent observations and maturity data from
previous field studies (McBride et al. 2021). Because sites E and F were outside the focal region
of the current study, they were analyzed during a shorter period of the presumed spawning
season, from November 15, 2013 – December 10, 2013. During the 2013 – 2014 season, multiple
cod grunts on consecutive days were only observed at site A; therefore, only site A was analyzed
the following year from October 1, 2014 – January 1, 2015. Site A was also analyzed every
Monday from February 18, 2013 – February 12, 2014 to confirm the bounds of the spawning
season. All 2019 – 2022 fixed-station and glider data were analyzed for the full deployment.

After evaluation by the cod detector, all possible grunt detections were validated in
Raven. For thorough review, all detections were visualized from 10-400 Hz in a 5x5 spectrogram
grid and context spectrogram. The grid spectrogram was generated with a 256-point FFT, 75%
overlap, and a 1 s time-pad. The context spectrogram was generated with a 1024-point FFT, 75%
overlap, and a 10 s time-pad. Positive cod detections were identified through auditory and visual
confirmation only when at least two harmonics were visible with the characteristic frequency
down sweep and the fundamental frequency was between 40-80 Hz. The presence of grunts and
the total number of grunts detected (ie., grunt rate) were summarized by hour.

Statistical analysis

Generalized linear mixed modeling (GLMM) was used to evaluate the temporal
correlations between spawning-associated grunt activity of Atlantic cod and multiple natural,
environmental cycles. Grunt activity was summarized as the presence of cod grunts each hour

and the number of grunts per hour (henceforth "grunt rate"). Grunt rate is inferred to indicate increased spawning activity as experimental results indicate higher grunt rates occur during the peak spawning period and are associated with increased egg production (Rowe and Hutchings, 2006). Statistical methods were analogous to those used in Caiger et al. (2020) to characterize spawning activity of winter-spawning cod in Massachusetts Bay, facilitating a comparison between the two regions. To prevent spurious correlations and facilitate comparisons, the threshold for data inclusion was grunt observations on at least 10 days and during at least two percent of hours during the spawning season as used in previous passive acoustic monitoring of Atlantic cod grunt activity (Zemeckis et al 2019; Caiger et al. 2020). Grunt presence and grunt rate were summarized by hour, and their temporal correlations were evaluated separately. Grunt presence was modeled with a binomial distribution while grunt rate was modeled with a zero-inflated negative binomial distribution.

The global models for grunt presence and rate included the effect of multiple natural cycles (annual, seasonal, diel, and lunar) that have been identified as associated with timing of cod-grunt activity in other spawning stock components (Zemeckis et al. 2019). The spawning season year spanned October to January and was treated as a factor variable. Day-of-year as well as the diel, lunar, and semi-lunar cycles were treated as circular variables to facilitate modeling both the timing and magnitude of their effect (Zar 1999; Caiger et al. 2020). As such, each variable was converted to radians and their effect consisted of a sin and cosine term in the model. To reduce the effect of serial autocorrelation among the residuals, the effect of week was included as a random effect in the model.

The remaining candidate models for grunt presence and rate consisted of the top models (ΔAIC $\leq$ 5) identified for each process in the Massachusetts Bay study (Caiger et al. 2020).

Because the Southern New England dataset consists of only one site, the candidate models for Southern New England could not include the effect of site, depth, or interaction between site and day of the year. In addition, the random effect of week was dropped from the zero-inflated component of the grunt rate model but retained in the conditional component. All models were evaluated using an information criteria-based model selection procedure using AIC. The effect of each natural cycle was calculated using estimated marginal means. To facilitate comparison of the temporal correlations between regions, the confidence interval ($\alpha = 0.05$) was estimated for the marginal mean of each variable for both Massachusetts Bay and Southern New England. All statistical analyses were conducted in R version 4.0.3 (R Core Team 2020), the models were built using the glmmTMB package (Brooks et al. 2017), and estimated marginal means were calculated using the emMeans package (Lenth 2021).

Results

For the 2013 – 2015 fixed-station data, three out of five sites had at least one cod grunt detection. Only site A had repetitive detections inferred as an active spawning aggregation (Figure 1). A total of 1035 grunts were observed at site A across the 2013 - 2014 and 2014 - 2015 spawning seasons, one grunt was observed at site C on December 13, 2013, and one grunt was observed at site D on December 25, 2013. No grunts were observed at sites E or F. Sites C, D, E and F were not evaluated during the 2014 – 2015 spawning season due to the lack of repetitive grunts during the 2013 – 2014 spawning season.

For the 2020 – 2022 data, six grunts were observed at the two fixed-station sites sampled. At site A, one grunt was observed on November 19, 2020 and December 22, 2021. At site B, one grunt was observed each day on November 29, December 1, and December 15, 2020 as well as

132

January 4, 2021. The 2020 – 2022 deployments at site A were intended to resample the aggregation observed in the 2013 – 2015 data; however, due to oceanographic conditions at the time of deployment the recorder locations at site A unintentionally differed by approximately 228 m with the 2020 – 2022 site located 113º to the southeast. The low number of grunts observed from 2020 – 2022 did not meet the threshold for data inclusion, so all further temporal analysis only includes the 2013 – 2015 data.

The glider-based survey observed a total of 31 cod grunts across three deployments, with one grunt observed during the 2019 – 2020 deployment on January 19, 2020, 12 grunts observed during the 2020 – 2021 deployment from November 15, 2020 – January 8, 2021, and 18 grunts observed during the 2021 – 2022 deployment between November 6, 2021 – January 4, 2022. Grunts were observed at all times of day, but 9 out of the 12 grunts during the 2020 – 2021 spawning season were observed at night. During the 2021 – 2022 spawning season, 16 grunts were observed within a 45-minute period on December 9. Across all deployments, three grunts were observed within or adjacent to the wind lease areas while the remaining grunts were concentrated in the western half of the study area in water between 25 – 50 m deep (Figure 2).

The analysis of one day per week at site A from February 2013 – February 2014 did not identify any cod grunts outside of October – January, suggesting that analysis during this period was sufficient to capture spawning-associated grunt activity. For the 2013 – 2015 spawning season data at site A, grunt activity was concentrated in November and December with only 36 grunts (3.5% of the total observed) in October and January. More grunts were observed during 2013 – 2014 compared to 2014 – 2015. In 2013, the maximum number of grunts per day was 125 on November 26, 2013, while in 2014 the maximum was 60 grunts on December 24, 2014 (Figure 3). During months when the maximum grunt activity was observed, grunts were detected

at all times of day, otherwise the observed grunt rate per hour was highest during the day (Figure 4A, B). During 2013, observed grunt activity appeared to be associated with the lunar cycle, with most grunts occurring between the full and waning moon (Figure 4C, D). In 2014, grunt activity was more variable with greatest number of grunts observed between the new and full moon.

Generalized linear mixed modeling of the 2013 – 2015 data when an inferred spawning aggregation was observed elucidated clear temporal patterns in grunt activity. Modeling grunt presence identified the global model as the best fit for the Southern New England data (Table 2). The candidate model without the semi-lunar cycle as a predictor was the second best fit and was nearly indistinguishable from the global model. Grunt presence was estimated to be most likely during mid-day, between the full and waning moon (Figure 5). The asymmetrical lunar pattern suggests an effect of the semi-lunar cycle with a second, smaller increase in grunt probability between the new and waxing moon. Seasonally, the highest probability of grunt occurrence was on December 5th (Figure 6A).

Overall, the temporal correlations of grunt presence with multiple natural cycles were similar to those in Massachusetts Bay, though the magnitude of the correlations tended to be stronger at the Southern New England site. Specifically, data from both regions identified similar support for multiple models with varying lunar terms included, but the Massachusetts Bay data suggested a much weaker effect of the diel and lunar cycles on grunt presence (Figure 5). Both regions followed a similar seasonal pattern with grunt activity concentrated in November and December, though the peak in grunt presence in Massachusetts Bay had a significant interaction with site and was estimated to occur on November 20th overall, approximately two weeks earlier than at the Southern New England site (Figure 6A).

The temporal correlations with grunt rate in Southern New England were also best explained by the global model, where both the grunt rate terms, and zero-inflated terms included all candidate predictor variables (Table 2; Figure 3). Due to the high proportion of zeroes in the grunt rate dataset, inclusion of the zero-inflated substantially improved model fit over a negative binomial distribution alone. The highest grunt rate was estimated to occur at noon near the full moon (Figure 7B, 7D). Similar to grunt presence, the asymmetrical lunar pattern indicated an effect of both the lunar and semi-lunar cycle with the highest grunt rates estimated to occur just after the full and new moons and lower grunt rates near the waxing waning moons. Seasonally, the maximum grunt rate was estimated to occur on November 26th, about one week before the peak in grunt presence (Figure 6B).

The grunt rate model best supported by the Massachusetts Bay data included the same temporal correlations for the grunt rate as the Southern New England model but did not include the semi-lunar cycle as a zero-inflated term. While the overall grunt rate was higher in Massachusetts Bay and they exhibited different diel correlations (Figure 7A, B), the correlations with lunar cycle were very similar between the two regions (Figure 7C, D). Similarly, the seasonal trend followed the same pattern, but the peak grunt rate was estimated to occur on December 5th, approximately two-weeks later than in Southern New England (Figure 6B). However, there was significant spatial heterogeneity in the seasonal profile of cod spawning activity in Massachusetts Bay and the results of the present study of Southern New England cod are well within this range.

Discussion

The use of multiple passive acoustic monitoring strategies to assess the spatiotemporal spawning dynamics of Atlantic cod in Southern New England recorded the presence of

occasional cod grunts throughout the study area and successfully captured the dynamics of a spawning aggregation during two consecutive years. Analysis of spawning associated grunt dynamics identified that peak grunt activity occurred during the day, near the full moon in late November to early December. While there were fine-scale differences between the temporal patterns of grunt activity observed in Southern New England versus Massachusetts Bay, the broad-scale seasonality was very similar. Over the sampling period, the number of grunts detected at the inferred spawning aggregation at Site A decreased and the aggregation was not detected during the 2020 or 2021 sampling period; however, the glider results suggest that spawning cod were still present throughout the region. Overall, evidence from the fixed-station and glider data in Southern New England suggests that Atlantic cod spawning overlaps with wind lease areas in the region.

Some temporal dynamics of inferred spawning identified in the Southern New England study aligned with those in Massachusetts Bay. For example, the peak spawning season for winter cod in Massachusetts Bay consistently occurred between November and December, with intermittent grunts extending into October and January at certain sites. Studies have reported correlations between grunt activity and lunar cycles, with grunt presence associated with the lunar cycle and grunt rate associated with both the lunar and semi-lunar cycles (Zemeckis et al. 2014a; Grabowski et al. 2015). While the Southern New England data revealed an association between grunt presence and both the lunar and semi-lunar cycles, the probability of grunt presence was much higher between the full and waning moon than between the new and waxing moon, suggesting that the semi-lunar cycle has a relatively smaller effect on grunt presence than the lunar cycle. Conversely, grunt rate in the Massachusetts Bay and Southern New England data revealed a stronger effect of the semi-lunar cycle with peaks near the full and new moons. The

timing of spawning is thought to occur when oceanographic and ecological conditions are best

suited to the success of the released eggs and subsequent larvae (Cushing 1990). These

consistent correlations with the semi-lunar cycle may be indicative of larval transport to

favorable habitats or retention and settlement of larvae during times of unique oceanographic

conditions (Lough et al. 2006).

In the scope of identifying the peak spawning period, both regions were consistent, with

peak grunt presence and rate estimated to occur within a three-week period from late November

to early December. Within the spawning season, however, the peak grunt rate occurred before

peak grunt presence in Southern New England while the opposite was true in Massachusetts Bay.

This slight difference in grunt trend throughout the spawning season may be indicative of

aggregation level differences between spawning components or interannual variation of lunar

cycle timing within the month, rather than a regional difference. For example, the magnitude of

grunt activity at the Southern New England aggregation in 2013 was much higher than that of the

subsequent spawning season. Additionally, the peak in grunt activity was observed in November

in 2013 and in December in 2014 This variation between the two years sampled likely explains

the different relationship between maximum predicted presence and rate. In contrast to the single

aggregation sampled in Southern New England, the Massachusetts Bay data set captured

spawning dynamics over a much broader area and period by sampling 16 sites across 10 years.

Both the comparison study and additional studies of Atlantic cod temporal grunt dynamics in

Massachusetts Bay have identified a significant interaction between site and seasonal peak grunt

rate, where the peak in grunt activity occurs later at deeper sites (Zemeckis et al. 2019; Caiger et

al. 2020). This significant interaction suggests that individual spawning aggregations within a

subpopulation may exhibit their own unique temporal correlations that maximize the success of

spawning in their specific oceanographic conditions. Lastly, grunt activity in Massachusetts Bay was not summarized in January and a few sites had increasing observed grunts throughout the month of December, suggesting that there may have been grunts missed during January. This difference in sampling period may also contribute to the difference in grunt patterns within the spawning season.

One difference between the two regions was that grunt presence had a stronger association with the diel and lunar cycles in Southern New England than in Massachusetts Bay. Due to the large difference in the number of aggregations sampled between the two studies it is difficult to discern whether this pattern is a regional difference or indicative of aggregation level differences. Because the Massachusetts Bay results summarize the average temporal dynamics across all sites, it could be expected that the estimated marginal means for Massachusetts Bay would report a weaker association with a specific natural cycle. As previously mentioned, it is known that the timing of peak grunt activity varies among aggregations within a subpopulation, so it is plausible that discrete aggregations have unique correlations with other natural cycles as well. It is also useful to note that while the strength of temporal associations with grunt rate were similar between the regions, the magnitude of grunt rate was higher for Massachusetts Bay likely due to greater abundances.

Of the natural cycles explored, the diel cycle was the most inconsistent between the two regions, where peak grunt activity occurred at night in Massachusetts Bay and during the day in Southern New England. Many field (Zemeckis et al. 2019; Caiger et al. 2020) and laboratory studies (Brawn 1961a; Kjesbu 1989; Hutchings et al. 1999) report cod spawning and grunt activity increasing at night, especially for winter-spawning cod stocks. Despite this, passive acoustic monitoring of the spring-spawning subpopulation in Massachusetts Bay also identified

an increase in grunt activity during the day (Hernandez et al. 2013). Similar to the present study in Southern New England, this study consisted of a single MARU. Because cod grunts are relatively quiet compared to other marine sound sources, successful detection of a cod grunt requires that fish are very close to the receiver. The only documented source level for Atlantic cod grunts is 127 dB re 1μPa at 1m and estimates of their communication radii in a variety of background and anthropogenic noise conditions ranged from 1.3 – 21.6 m (Nordeide and Kjellsby 1999; Stanley et al. 2017). Moreover, Atlantic cod are known to exhibit diel movements where individuals aggregate in one location during the day and travel to surrounding areas or shift their position within the aggregation to defend a territory at night (Dean et al. 2014). Hernandez et al. (2013) suggested that one explanation for the discrepancy in grunt activity is that the receiver could have been located near the daytime aggregation site and diel movements caused individual cod to move outside of the detection radius of the receiver at night leading to an apparent lack of grunt activity. Similar behavioral migrations and receiver locations could explain the uncommon diel association observed in Southern New England.

Following identification of a spawning aggregation at site A in 2013 – 2015, the goal of resampling this site in 2020 and 2021 was to evaluate whether temporal grunt dynamics were stable over time. However, only one grunt was detected at site A in 2020 and 2021. Given the five-year gap in sampling, it is possible that the populations may have declined below detectable levels of abundance or may no longer have been detectable by passive acoustic monitoring due to a shift in aggregation location, accidental changes in sampling location, or the use of different recorder types. The US Atlantic cod stocks have been classified as overfished since 2010 (Zemeckis et al. 2014c). Additionally, because the Southern New England spawning components are situated at the southern extreme of the population, they are the most vulnerable to climate

139

impacts, including thermal habitat loss, loss of prey biomass, and increased species interactions (Fogarty et al. 2008; Nye et al. 2009; Friedland et al. 2013). As such, the spawning aggregation observed in 2013 – 2015 reflects the dynamics of a smaller baseline population. Successful formation of a spawning aggregation in some species is density dependent, where the aggregation does not form at low abundances (Domeier 2012). The small number of observed grunts in 2019 – 2022 may be indicative of a highly disorganized spawning population in which the aggregation behavior has been further disrupted. The high site fidelity of Atlantic cod poses challenges for aggregation recovery following disruption. For example, the onset of a gill-net fishery in Massachusetts Bay fully disrupted an aggregation of spawning cod, causing most individuals to leave the aggregation site and not return (Dean et al. 2012). Despite this, results from a recent review of extirpated fish spawning aggregations suggest that recovery of the aggregation is possible if given enough time following strict enforcement of spatial protection or temporal moratoria on fishing (Chollett et al. 2020). In the absence of management protections for spawning cod, the combination of historically low population sizes, high spawning site fidelity, and increasing climate impacts make recolonization of an extirpated spawning aggregation unlikely for Atlantic cod in the region.

Beyond the possibility that the aggregation was no longer present, the lack of observed grunts may be due to limitations of passive acoustic monitoring for Atlantic cod. Atlantic cod spawning aggregations are typically spatially consistent between years, with variation generally less than 1 km. Despite this, because cod grunts are relatively quiet, even shifts on the order of 100 m could cause grunts to occur outside the detection radius of the hydrophone. Similarly, due to the gap in sampling from 2015 to 2020, the aggregation was monitored with two different recorder types whose geographic position varied by 228 m. The realized recording radius of

passive acoustic monitoring can be difficult to assess and whether an acoustic signal is detected depends on multiple factors including the source level of the signal, the distance from the receiver, and the ambient background noise. As such, it is quite possible that the shift in sampling location or changes in cod detector performance on different acoustic data sources was the cause of the lack of detections in 2020 - 2022. To that end, the lack of detection is not necessarily indicative of true absence of spawning cod in the vicinity of the historical spawning site.

This study intentionally leveraged multiple passive monitoring technologies to provide a broad spatiotemporal sample of Atlantic cod grunt activity in Southern New England. Each methodology used includes a tradeoff between spatial and temporal coverage and the multi-method approach and adaptive sampling between years was intended to balance these tradeoffs and improve sampling coverage. For example, during the 2020 – 2022 glider deployments, the glider was programmed to travel directly over the two fixed-station sites. During these deployments, a grunt was observed on November 16, 2020 and November 6, 2021 in the vicinity of the historical aggregation at site A. Given the detection date near the onset of increased grunt activity in 2013, if the aggregation was still present in large numbers and actively spawning, we would likely expect to have observed more grunts in this area. Overall, the sparse data observed by the glider and fixed station sites in 2019 – 2021 as well as deviations of the glider from the planned path make it difficult to conclude whether the lack of grunts are a result of insufficient sampling locations and timing or are true absences. Future research with a denser array of fixed-station receivers, or a finer-scale glider survey could reduce uncertainty regarding whether the patterns observed in the present study (i.e., diminished activity at historical spawning sites in

2020, lack of grunts in the eastern portion of the study area, and the unique diel trend) are a result of gaps in the sampling coverage or true ecological patterns.

Between previous studies of Atlantic cod spawning dynamics and population structure in the Western North Atlantic Ocean (Zemeckis et al. 2014a; McBride et al. 2021), annual trawl surveys for groundfish by the Northeast Fisheries Science Center (Lough 2004), and local ecological knowledge of fishers (DeCelles et al. 2017) it is known that Southern New England waters, and specifically Cox Ledge, host critical habitats for Atlantic cod eggs, larvae, and spawning adults. However, little has been known of the specific location and timing of spawning in the region. In the present study, passive acoustic monitoring in 2013 – 2015 revealed the dynamics of a spawning aggregation near Cox Ledge and within wind lease areas. Moreover, comparison with Massachusetts Bay winter-spawning cod confirmed that the dynamics observed in Southern New England are largely the same as those in other regions, with the peak spawning period in November and December. As a result, spatial and temporal interactions between offshore wind energy construction and Atlantic cod are likely in Southern New England. Despite the limited number of cod grunts observed during the 2019 – 2022 sampling periods, the results of the regional comparison reduce uncertainty regarding the likelihood of temporal overlap between current construction timelines and cod spawning.

Among the many possible interactions between offshore wind energy development and fisheries, fine-scale habitat effects and broad-scale acoustic effects are the greatest concerns for Atlantic cod spawning aggregations. Due to the high site fidelity of Atlantic cod spawning aggregations, status of the stock as overfished, and southern range contraction due to climate change, if a turbine foundation or underground cable was located at the aggregation site, the spawning aggregation would be disrupted and may fail to relocate to an undisturbed area (de

Jong et al. 2020). On a broader scale, the acoustic disturbance from pile driving overlaps in frequency with cod grunt activity (Popper and Hawkins 2019), increasing the risk of auditory masking and disruption of cod behavior over the scale of tens of kilometers (Hammar et al. 2014; Mooney et al. 2020). There have been recent advances in technologies to minimize the acoustic impacts from pile driving (i.e., bubble curtains); however, temporal restrictions on disruptive activities are one of the most successful measures for mitigating disturbance to and facilitating recovery of aggregation-spawning fishes during vulnerable periods (Erisman et al. 2017; Chollett et al. 2020; Mooney et al. 2020). Though these measures have had limited success for rebuilding Atlantic cod stocks following overfishing (Clarke et al. 2015), temporal restrictions on fishing have had numerous successes for other fish populations (Burton et al. 2005; Nemeth 2005; Hamilton et al. 2011). Under the Marine Mammal Protection Act, current construction plans for offshore wind in the region only restrict pile driving from January to April to mitigate disturbance for North Atlantic Right Whales (BOEM and NMFS 2021). While some Atlantic cod spawning does occur in January, the results presented here show that the vast majority of inferred spawning activity occurs in November and December, leaving cod vulnerable to disturbance from pile driving and other construction activity.

At large population sizes, Atlantic cod spawning aggregations have been recorded producing a loud, persistent rumbling, frequently referred to as a fish chorus (Brawn 1961a; Nordeide and Kjellsby 1999). The lack of persistent cod grunts throughout the region and the relatively small number of grunts at an inferred aggregation are likely a result of low abundances in the region and limitations of passive acoustic monitoring for Atlantic cod. The quiet nature of a cod grunt requires a recorder to be in very close proximity to the individual, while the aggregating behavior among small populations makes it challenging to sample the right place at

the right time. Despite these limitations, the use of multiple passive acoustic monitoring

technologies offers spatial and temporal data from a non-invasive method that is specific to

spawning individuals and doesn't require physical capture and dissection (Van Parijs et al. 2009;

Rowell et al. 2015; Zemeckis et al. 2019). Moreover, while many vessel-based surveys are not

able to operate during the construction and operation of a wind farm, passive acoustic monitoring

remains a viable survey option. This advantage results in baseline data that can be compared to

data collected both during and after construction, facilitating long-term assessment of

interactions between offshore wind energy and fishery resources.

REFERENCES

K. Lisa Yang Center for Conservation Bioacoustics (KLY-CCB). 2014. Raven Pro: Interactive Sound Analysis Software. The Cornell Lab of Ornithology, Ithaca, NY.

Ames, E. P. 2004. Atlantic cod stock structure in the Gulf of Maine. Fisheries 29(1):10–28.

Andersson, M. H., S. Andersson, J. Ahlsén, L. Andersson, J. Hammar, L. K. Persson, J. Pihl, P. Sigray, and A. Wikström. 2017. A framework for regulating underwater noise during pile driving: A technical Vindval report. Page Report 6775. Stockholm, Swedem.

Bailey, H., B. Senior, D. Simmons, J. Rusin, G. Picken, and P. M. Thompson. 2010. Assessing underwater noise levels during pile-driving at an offshore windfarm and its potential effects on marine mammals. Marine Pollution Bulletin 60(6):888–897.

Baumgartner, M. F., D. M. Fratantoni, T. P. Hurst, M. W. Brown, T. V. N. Cole, S. M. Van Parijs, and M. Johnson. 2013. Real-time reporting of baleen whale passive acoustic detections from ocean gliders. Journal of the Acoustical Society of America 134(3):1814–1823.

Bergström, L., F. Sundqvist, and U. Bergström. 2013. Effects of an offshore wind farm on temporal and spatial patterns in the demersal fish community. Marine Ecology Progress Series 485:199–210.

Brander, K. M. 2005. Cod recruitment is strongly affected by climate when stock biomass is low. ICES Journal of Marine Science 62(3):339–343.

Brawn, V. M. 1961a. Sound Production By the Cod (*Gadus callarias L.*). Behavior 18(4):239–255.

Brawn, V. M. 1961b. Aggessive behaviour in the cod (*Gadus callarias L.*). Behavior 18:107–147.

Brooks, M. E., K. Kristensen, K. J. Van Benthem, A. Magnusson, C. W. Berg, A. Nielsen, H. J. Skaug, M. Maechler, and B. M. Bolker. 2017. glmmTMB Balances Speed and Flexibility Among Packages for Zero-inflated Generalized Linear Mixed Modeling. The R Journal 9(2):378–400.

Burton, M. L., K. J. Brennan, R. C. Muñoz, and R. O. Parker. 2005. Preliminary evidence of increased spawning aggregations of mutton snapper (Lutjanus analis) at Riley's Hump two years after establishment of the Tortugas South Ecological Reserve. Fishery Bulletin 103(2):404–410.

Caiger, P. E., M. J. Dean, A. I. DeAngelis, L. T. Hatch, A. N. Rice, J. A. Stanley, C. Tholke, D. R. Zemeckis, and S. M. Van Parijs. 2020. A decade of monitoring Atlantic cod Gadus morhua spawning aggregations in Massachusetts Bay using passive acoustics. Marine Ecology Progress Series 635:89–103.

Chollett, I., M. Priest, S. Fulton, and W. D. Heyman. 2020. Should we protect extirpated fish spawning aggregation sites? Biological Conservation 241:108395.

Clarke, J., D. M. Bailey, and P. J. Wright. 2015. Evaluating the effectiveness of a seasonal spawning area closure. ICES Journal of Marine Science 72(9):2627–2637.

Cushing, D. H. 1990. Plankton production and year-class strength in fish populations: an update of the match/mismatch hypothesis. Advances in Marine Biology 26(C):249–293.

Dean, M. J., W. S. Hoffman, and M. P. Armstrong. 2012. Disruption of an atlantic cod spawning aggregation resulting from the opening of a directed gill-net fishery. North American Journal of Fisheries Management 32(1):124–134.

Dean, M. J., W. S. Hoffman, D. R. Zemeckis, and M. P. Armstrong. 2014. Fine-scale diel and gender-based patterns in behaviour of Atlantic cod (*Gadus morhua*) on a spawning ground in the Western Gulf of Maine. ICES Journal of Marine Science 71(6):1474–1489.

DeCelles, G. R., D. Martins, D. R. Zemeckis, and S. X. Cadrin. 2017. Using Fishermen's Ecological Knowledge to map Atlantic cod spawning grounds on Georges Bank. ICES Journal of Marine Science 74(6):1587–1601.

de Jong, K., M. C. P. Amorim, P. J. Fonseca, C. J. Fox, and K. U. Heubel. 2018. Noise can affect acoustic communication and subsequent spawning success in fish. Environmental Pollution 237:814–823.

de Jong, K., T. N. Forland, M. C. P. Amorim, G. Rieucau, H. Slabbekoorn, and L. D. Sivle. 2020. Predicting the effects of anthropogenic noise on fish reproduction. Reviews in Fish Biology and Fisheries 30:245–268.

Domeier, M. L. 2012. Revisiting Spawning Aggregations: Definitions and Challenges. Pages 1–20 *in* Y. Sadovy de Mitcheson and P. L. Colin, editors. Reef Fish Spawning Aggregations: Biology, Research and Management. Springer, Dordrecht, Netherlands.

Erisman, B., W. Heyman, S. Kobara, T. Ezer, S. Pittman, O. Aburto-Oropeza, and R. S. Nemeth. 2017. Fish spawning aggregations: where well-placed management actions can yield big benefits for fisheries and conservation. Fish and Fisheries 18:128–144.

Finstad, J. L., and J. T. Nordeide. 2004. Acoustic behaviour of spawning cod (*Gadus morhua L.*). Environmental Biology of Fishes 70(1978):427–433.

Fogarty, M., L. Incze, K. Hayhoe, D. Mountain, and J. Manning. 2008. Potential climate change impacts on Atlantic cod (*Gadus morhua*) off the northeastern USA. Mitigation and Adaptation Strategies for Global Change 13(5–6):453–466.

Friedland, K. D., J. Kane, J. A. Hare, R. G. Lough, P. S. Fratantoni, M. J. Fogarty, and J. A. Nye. 2013. Thermal habitat constraints on zooplankton species associated with Atlantic cod (*Gadus morhua*) on the US Northeast Continental Shelf. Progress in Oceanography 116:1–13.

Friedland, K. D., J. A. Langan, S. I. Large, R. L. Selden, J. S. Link, R. A. Watson, and J. S. Collie. 2020. Changes in higher trophic level productivity, diversity and niche space in a rapidly warming continental shelf ecosystem. Science of the Total Environment 704:135270. Elsevier LTD.

Fudge, S. B., and G. A. Rose. 2009. Passive-and active-acoustic properties of a spawning Atlantic cod (*Gadus morhua*) aggregation. Page ICES Journal of Marine Science.

Grabowski, T. B., B. J. McAdam, V. Thorsteinsson, and G. Marteinsdóttir. 2015. Evidence from data storage tags for the presence of lunar and semi-lunar behavioral cycles in spawning Atlantic cod. Environmental Biology of Fishes 98(7):1767–1776.

Guarinello, M. L., and D. A. Carey. 2020. Multi-modal approach for benthic impact assessments in moraine habitats: a case study at the Block Island Wind Farm. Estuaries and Coasts.

Hamilton, R. J., T. Potuku, and J. R. Montambault. 2011. Community-based conservation results in the recovery of reef fish spawning aggregations in the Coral Triangle. Biological Conservation 144(6):1850–1858.

Hammar, L., A. Wikström, and S. Molander. 2014. Assessing ecological risks of offshore wind power on Kattegat cod. Renewable Energy 66:414–424.

Herbert-Read, J. E., C. C. Ioannou, L. Kremer, R. Bruintjes, A. N. Radford, and C. C. Ioannou. 2017. Anthropogenic noise pollution from pile-driving disrupts the structure and dynamics of fish shoals. Proceedings of the Royal Society B 284:20171627.

Hernandez, K. M., D. Risch, D. M. Cholewiak, M. J. Dean, L. T. Hatch, W. S. Hoffman, A. N. Rice, D. Zemeckis, and S. M. Van Parijs. 2013. Acoustic monitoring of Atlantic cod (*Gadus morhua*) in Massachusetts Bay: implications for management and conservation. ICES Journal of Marine Science 70(3):628–635.

Hutchings, J. A., T. D. Bishop, and C. R. McGregor-Shaw. 1999. Spawning behaviour of Atlantic cod, *Gadus morhua*: evidence of mate competition and mate choice in a broadcast spawner. Canadian Journal of Fisheries and Aquatic Sciences 56:97–104.

Hutchison, Z. L., M. L. Bartley, S. Degraer, P. English, A. Khan, J. Livermore, B. Rumes, and J. W. King. 2020. Offshore wind energy and benthic habitat changes lessons from block island wind farm. Oceanography 33(4):58–69.

Kerr, L. A., S. X. Cadrin, and A. I. Kovach. 2014. Consequences of a mismatch between biological and management units on our perception of Atlantic cod off New England. ICES Journal of Marine ScienceS 71(6):1366–1381.

Kjesbu, S. 1989. The spawning activity of cod, *Gadus morhua L*. Journal of Fish Biology 34:195–206.

Kraus, S. D., S. Leiter, K. Stone, B. Wikgren, C. Mayo, P. Hughes, R. Kenney, C. W. Clark, A. N. Rice, B. J. Estabrook, and J. Tielens. 2016. Northeast Large Pelagic Survey

Collaborative Aerial and acoustic surveys for large whales and sea turtles. Herndon, Virgina.

Lenth, R. V. 2021. emmeans: Estimated Marginal Means, aka Least-Squares Means. R package version 1.7.0.

Lilly, G. R., K. Wieland, B. J. Rothschild, S. Sundby, K. F. Drinkwater, K. Brander, G. Otterson, J. E. Carscadden, G. B. Stenson, G. A. Chouinard, D. P. Swain, N. Daan, K. Enberg, M. O. Hammill, A. Rosing-Asvid, H. Svedang, and A. Vazquez. 2008. Decline and Recovery of Atlantic Cod (*Gadus morhua*) Stocks throughout the North Atlantic. Pages 39–66 Resiliency of Gadid Stocks to Fishing and Climate Change. Fairbanks, Alaska.

Lindegren, M., S. Waldo, P. A. Nilsson, H. Sveda, and A. Persson. 2013. Towards sustainable fisheries of the Oresund cod (*Gadus morhua*) though sub-stock specific assessment and management recommednations. ICES Journal of Marine Science 70(6):1140–1150.

Lough, R. G. 2004. Essential Fish Habitat Source Document: Atlantic Cod, *Gadus morhua*, Life History and Habitat Characteristics. Woods Hole, MA.

Lough, R. G., C. G. Hannah, P. Berrien, D. Brickman, J. W. Loder, and J. A. Quinlan. 2006. Spawning pattern variability and its effect on retention, larval growth and recruitment in Georges Bank cod and haddock. Marine Ecology Progress Series 310(1998):193–212.

Madsen, P. T., M. Wahlberg, J. Tougaard, K. Lucke, and P. Tyack. 2006. Wind turbine underwater noise and marine mammals: Implications of current knowledge and data needs. Marine Ecology Progress Series 309:279–295.

Management, B. of O. E., and N. M. F. Service. 2021. Record of Decision South Fork Wind Farm and South Fork Export Cable Project Construction and Operations Plan.

McBride, R. S., T. Ames, I. Andrushchenko, S. X. Cadrin, J. M. Cournane, M. Dean, G. R. Decelles, L. A. Kerr, A. I. Kovach, N. Overgaard, G. Puncher, R. K. Smedbol, Y. Wang, and D. R. Zemeckis. 2021. Atlantic cod stock structure working group draft proposed biological stocks.

Mooney, T. A., M. H. Andersson, and J. Stanley. 2020. Acoustic impacts of offshore wind energy on fishery resources an evolving source and varied effects across a wind farm's lifetime. Oceanography 33(4):82–95.

Nemeth, R. S. 2005. Population characteristics of a recovering US Virgin Islands red hind spawning aggregation following protection. Marine Ecology Progress Series 286:81–97.

Neo, Y. Y., J. Hubert, L. Bolle, H. V. Winter, C. Ten Cate, and H. Slabbekoorn. 2016. Sound exposure changes European seabass behaviour in a large outdoor floating pen: Effects of temporal structure and a ramp-up procedure. Environmental Pollution 214:26–34.

Nordeide, J. T., and I. Folstad. 2000. Is cod lekking or a promiscuous group spawner? Fish and Fisheries 1:90–93.

Nordeide, J. T., and E. Kjellsby. 1999. Sound from spawning cod at their spawning grounds. ICES Journal of Marine Science 56(3):326–332.

Nye, J. A., J. S. Link, J. A. Hare, and W. J. Overholtz. 2009. Changing spatial distribution of fish stocks in relation to climate and population size on the Northeast United States continental shelf. Marine Ecology Progress Series 393:11–129.

Popper, A. N., and A. D. Hawkins. 2019. An overview of fish bioacoustics and the impacts of anthropogenic sounds on fishes. Journal of Fish Biology 94:692–713.

R Core Team. 2020. R: A language and environment for statistical computing. R Foundation for Statistical Computing, Vienna, Austria.

Reich, D. A., and J. T. DeAlteris. 2009. A simulation study of the effects of spatially complex population structure for Gulf of Maine Atlantic Cod. North American Journal of Fisheries Management 29:116–126.

Revolution Wind, L. 2021. Construction & Operations Plan Revolution Wind Farm.

Robichaud, D., and G. A. Rose. 2001. Multiyear homing of Atlantic cod to a spawning ground. Canadian Journal of Fisheries and Aquatic Sciences 58(12):2325–2329.

Rose, G. A., R. J. Nelson, and L. G. S. Mello. 2011. Isolation or metapopulation: Whence and whither the Smith Sound cod? Canadian Journal of Fisheries and Aquatic Sciences 68(1):152–169.

Rowe, S., and J.A. Hutchings. 2006. Sound production by Atlantic cod during Spawning. Transactions of the American Fisheries Society. 135:529-538.

Rowe, S., and J. A. Hutchings. 2008. A link between sound producing musculature and mating success in Atlantic cod. Journal of Fish Biology 72(3):500–511.

Rowell, T. J., R. S. Nemeth, M. T. Scharer, and R. S. Appeldoorn. 2015. Fish sound production and acoustic telemetry reveal behaviors and spatial patterns associated with spawning aggregations of two Caribbean groupers. Marine Ecology Progress Series 518:239–254.

Rudnick, D. L., R. E. Davis, C. C. Eriksen, D. M. Fratantoni, and M. J. Perry. 2004. Underwater gliders for ocean research. Marine Technology Society Journal 38(2):73–84.

Sierra-Flores, R., T. Atack, H. Migaud, and A. Davie. 2015. Stress response to anthropogenic noise in Atlantic cod *Gadus morhua L*. Aquacultural Engineering 67:67–76.

Stanley, J. A., S. M. Van Parijs, and L. T. Hatch. 2017. Underwater sound from vessel traffic reduces the effective communication range in Atlantic cod and haddock. Scientific Reports 7:14633.

Stenberg, C., J. G. Støttrup, M. Van Deurs, C. W. Berg, G. E. Dinesen, H. Mosegaard, T. M. Grome, and S. B. Leonhard. 2015. Long-term effects of an offshore wind farm in the North

Sea on fish communities. Marine Ecology Progress Series 528:257–265.

Stephenson, R. L. 1999. Stock complexity in fisheries management: A perspective of emerging issues related to population sub-units. Fisheries Research 43(1–3):247–249.

Sunrise Wind, L. 2021. Construction & Operations Plan Sunrise Wind Farm Project. New York, NY.

Urazghildiiev, I. R., and S. M. Van Parijs. 2016. Automatic grunt detector and recognizer for Atlantic cod (*Gadus morhua*). Journal of the Acoustical Society of America 139:2532.

van der Knaap, I., H. Slabbekoorn, T. Moens, D. Van den Eynde, and J. Reubens. 2022. Effects of pile driving sound on local movement of free-ranging Atlantic cod in the Belgian North Sea. Environmental Pollution 300(January):118913. Elsevier Ltd.

Van Parijs, S. M., C. W. Clark, R. S. Sousa-Lima, S. E. Parks, S. Rankin, D. Risch, and I. C. Van Opzeeland. 2009. Management and research applications of real-time and archival passive acoustic sensors over varying temporal and spatial scales. Marine Ecology Progress Series 395:21–36.

Wysocki, L. E., J. P. Dittami, and F. Ladich. 2006. Ship noise and cortisol secretion in European freshwater fishes. Biological Conservation 128:501–508.

Zar, J. 1999. Biostatistical Analysis, 4th edition. Prentice Hall, Upper Saddle River, NJ.

Zemeckis, D. R., M. J. Dean, and S. X. Cadrin. 2014a. Spawning dynamics and associated management implications for Atlantic cod. North American Journal of Fisheries Management 34:424–442.

Zemeckis, D. R., M. J. Dean, A. I. Deangelis, S. M. Van Parijs, W. S. Hoffman, M. F. Baumgartner, L. T. Hatch, S. X. Cadrin, C. H. McGuire, and R. O'Driscoll. 2019. Identifying the distribution of Atlantic cod spawning using multiple fixed and glider-mounted acoustic technologies. ICES Journal of Marine Science 76(6):1610–1625. Oxford University Press (OUP).

Zemeckis, D. R., W. S. Hoffman, M. J. Dean, M. P. Armstrong, and S. X. Cadrin. 2014b. Spawning site fidelity by Atlantic cod (*Gadus morhua*) in the Gulf of Maine: implications for population structure and rebuilding. ICES Journal of Marine Science 71(6):1356–1365.

Zemeckis, D. R., D. Martins, L. A. Kerr, and S. X. Cadrin. 2014c. Stock identification of Atlantic cod (*Gadus morhua*) in US waters: an interdisciplinary approach. ICES Journal of Marine Science 71(6):1490–1506.

Table 5. 1 Passive acoustic monitoring sites and deployment details for fixed-station receivers in Southern New England.

Site	Latitude (ºN)	Longitude (ºW)	Effort (days)	Years Sampled	Depth (m)
A	41.1421	71.1038	156	2013 – 2015	33
	41.1413	71.1013	202	2020 – 2022	32
B	41.0406	71.2195	202	2020 – 2022	41
C	40.9978	71.1683	73	2013 – 2014	51
D	40.9955	70.8642	73	2013 – 2014	50
E	40.7436	70.4607	26	2013	52
F	40.5993	70.5617	26	2013	59

Table 5. 2 Candidate models for temporal correlations of Atlantic cod grunt activity in Southern New England. The model with the best fit was used for all comparisons with Massachusetts Bay. Included predictor variables are year (Y), hour of the day (H), lunar cycle (L1), semi-lunar cycle (L2), day of the year (J), and week of the year (rW).

Grunt presence model terms		df	AICc	ΔAIC
Y + H + L1 + L2 + J + rW		**11**	**1398.8**	**0.00**
Y + H + L1 + J + rW		9	1402.8	4.00
Y + H + L2 + J + rW		9	1445.6	46.75
Y + H + J + rW		7	1452.3	53.51
Grunt rate model terms	**Zero-inflated terms**			
Y + H + L1 + L2 + J + rW	**Y + H + L1 + L2 + J**	**22**	**2271.9**	**0.00**
Y + H + L1 + L2 + J + rW	Y + H + L1 + J	20	2351.8	79.92
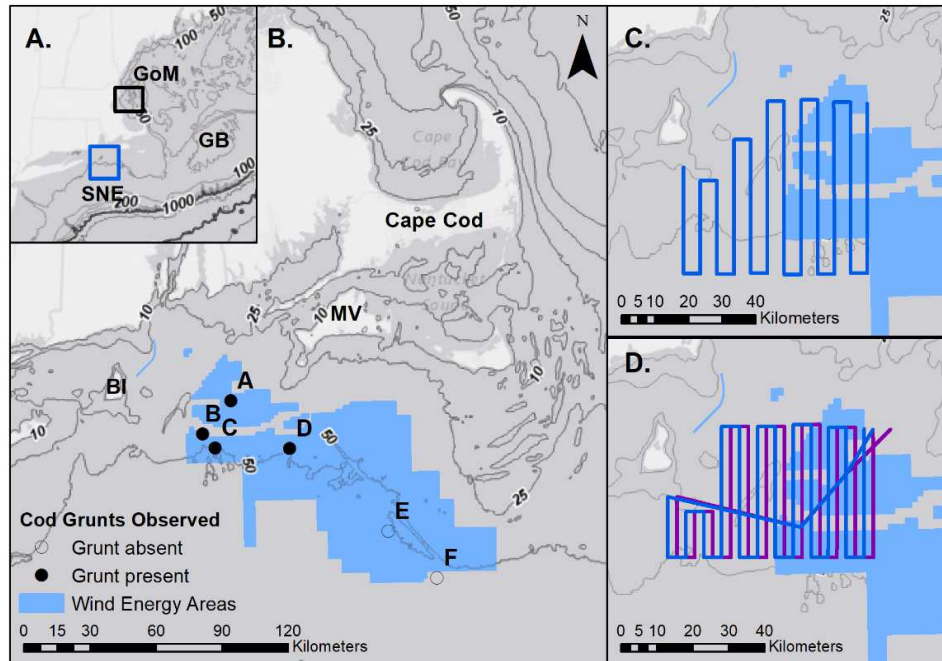
Figure 5. 1 Maps of the study area and sampling effort. (A) Regional context for comparison between Massachusetts Bay (black box) and Southern New England (blue box). The text labels indicate the location of general cod spawning regions in the Gulf of Maine (GoM), Georges Bank (GB), and Southern New England (SNE). (B) SNE study area including the full Massachusetts-Rhode Island Wind Energy Area and the location of fixed-station receivers. (C) Programmed glider track during the 2019 – 2020 sampling effort. (D) Programmed glider track during the 2020 – 2021 sampling effort. To improve spatiotemporal coverage, the glider alternated between the blue and purple tracks throughout the deployment.
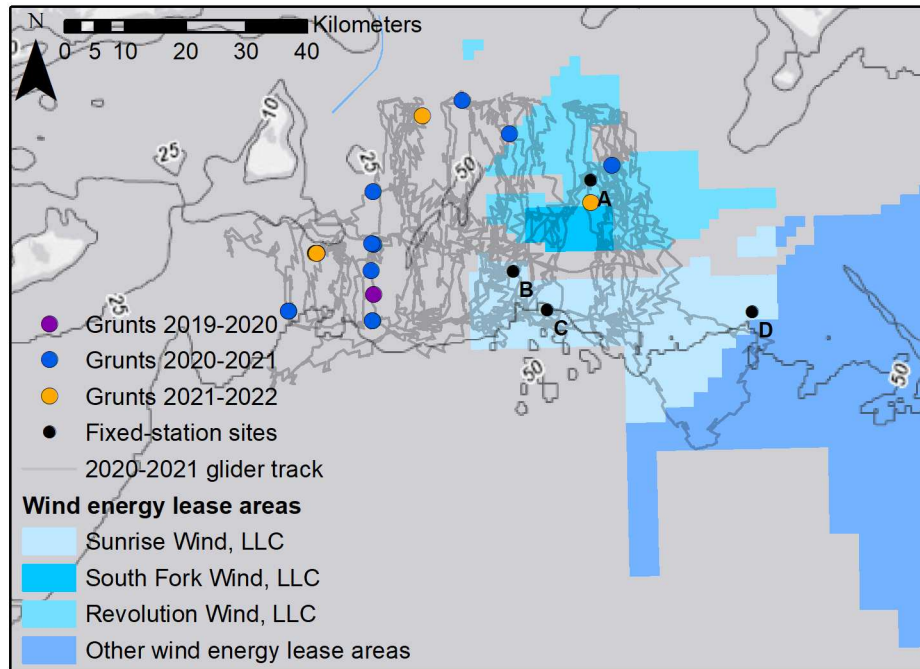
Figure 5. 2 Location of observed grunts during the glider survey in all years. The realized glider track during the 2020 – 2021 deployment, fixed-station recorders, and relevant lease areas within the Rhode Island/Massachusetts Wind Energy Area are also plotted for spatial reference.
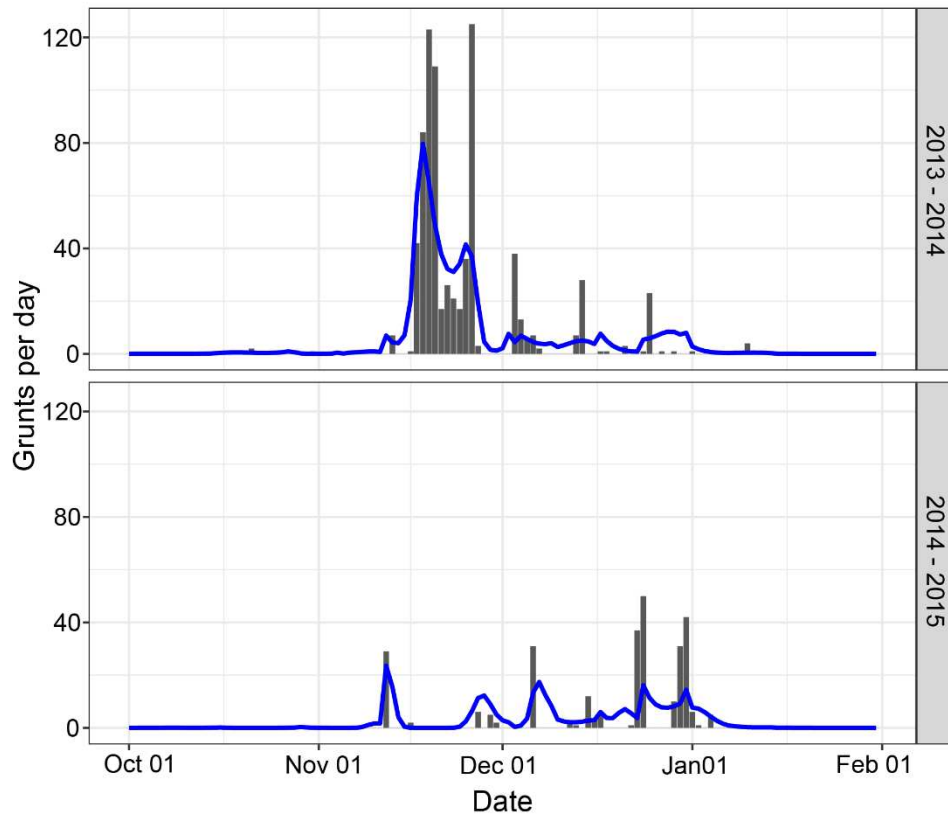
Figure 5. 3 Seasonal and inter-annual variability in the total number of observed grunts per day at site A during the 2013 – 2015 sampling periods (columns) and the predicted number of grunts per day (blue line) under the global model for grunt rate.
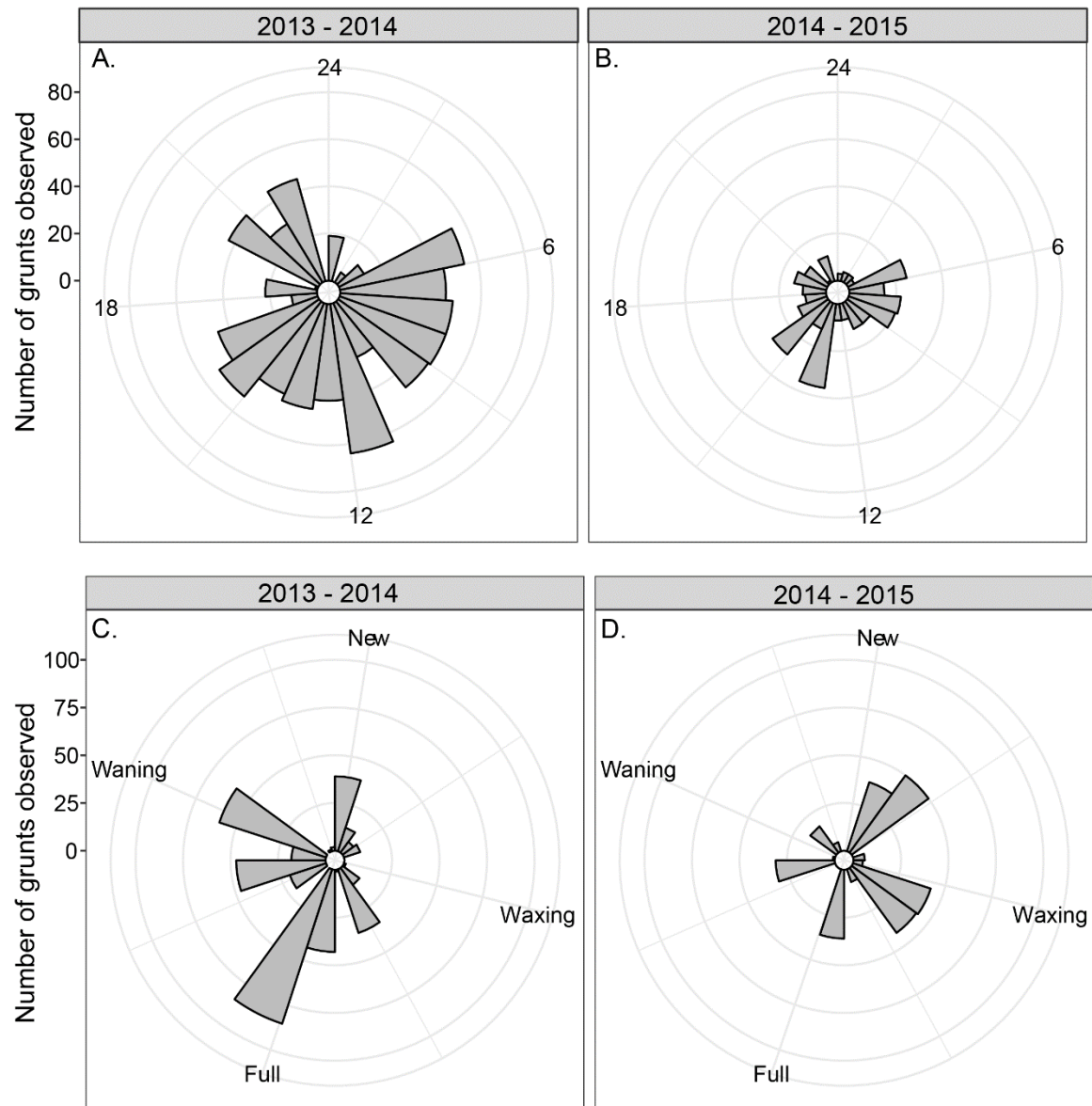
Figure 5. 4 Number of observed cod grunts at site A (A, B) per hour and (C, D) throughout the lunar cycle during each spawning season sampled.
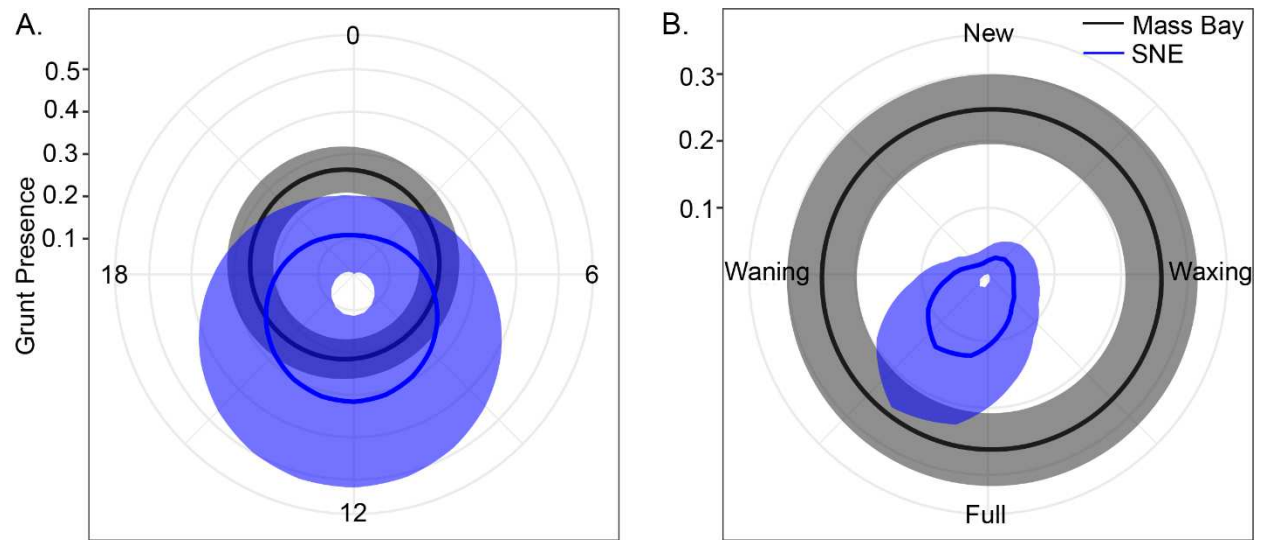
Figure 5. 5 Comparison of the estimated marginal mean effect of (A) diel and (B) lunar cycles on grunt presence at fixed stations between Massachusetts Bay and Southern New England. The shaded regions represent the 95% confidence interval of the estimates.
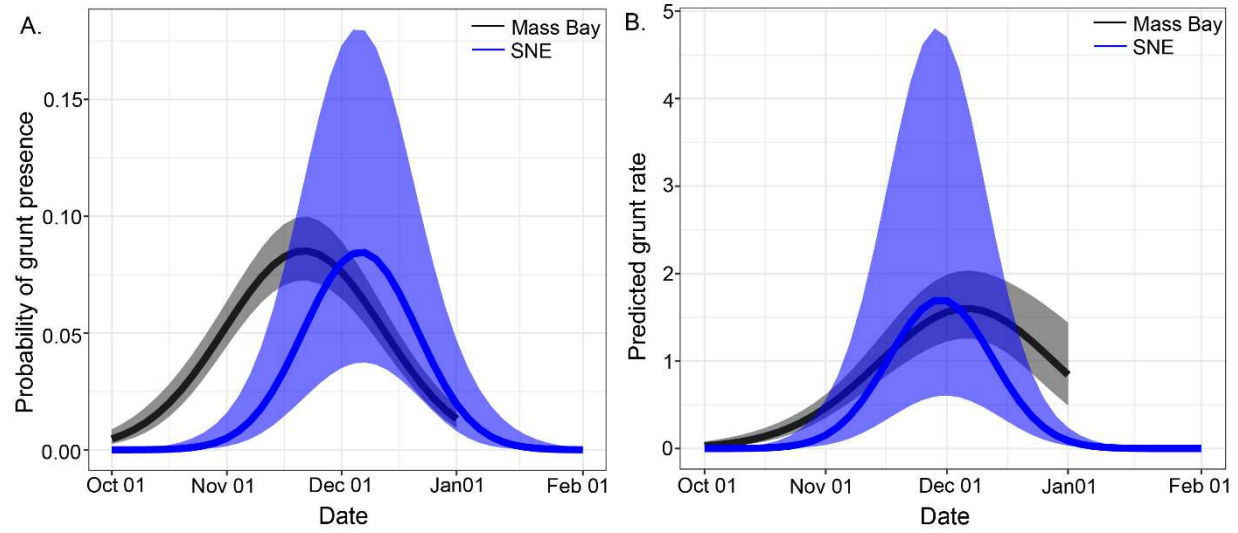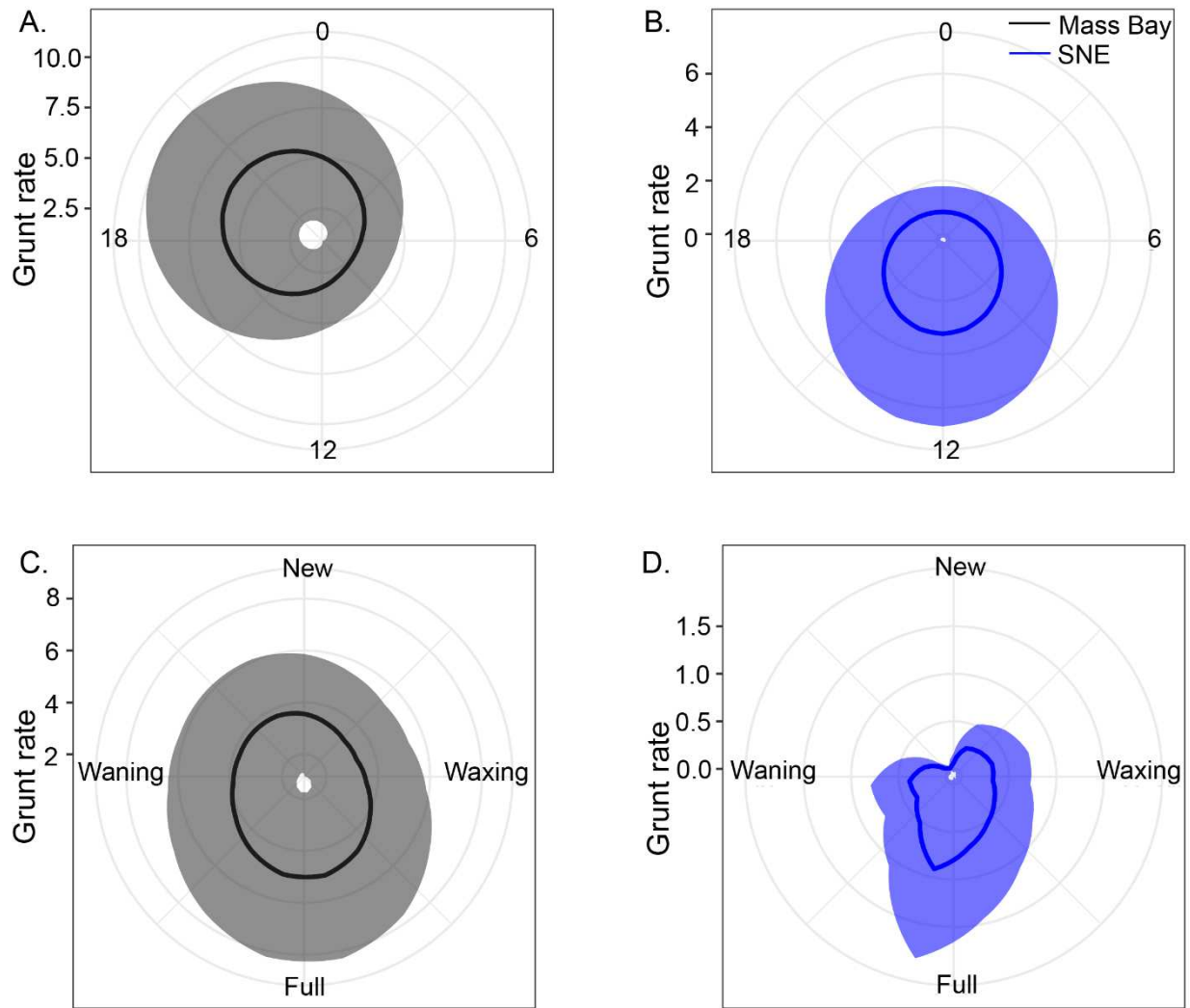
Figure 5. 6 Estimated marginal mean effect of calendar date on (A) grunt presence and (B) grunt rate at fixed stations in Massachusetts Bay and Southern New England. The shaded regions represent the 95% confidence interval of the estimates.

Figure 5. 7 Estimated marginal mean effects of (A) diel and (C) lunar cycles on grunt rate at fixed stations in Massachusetts Bay and (B) diel and (D) lunar cycles in Southern New England. Note the change in the y-axis scales. The shaded regions represent the 95% confidence interval of the estimates.

Table A2. 1 Sampling dates for data included in analyses. The gap in data used in January is due to a sampling error that resulted in skipped files and an incomplete daily timeseries. Data used for each deployment were held constant across all sites to ensure differences detected were not due to different sampling dates. The Aeolus was only sampled for the final three deployments after it was selected as a contingency site due to strong currents at the initial artificial reef.

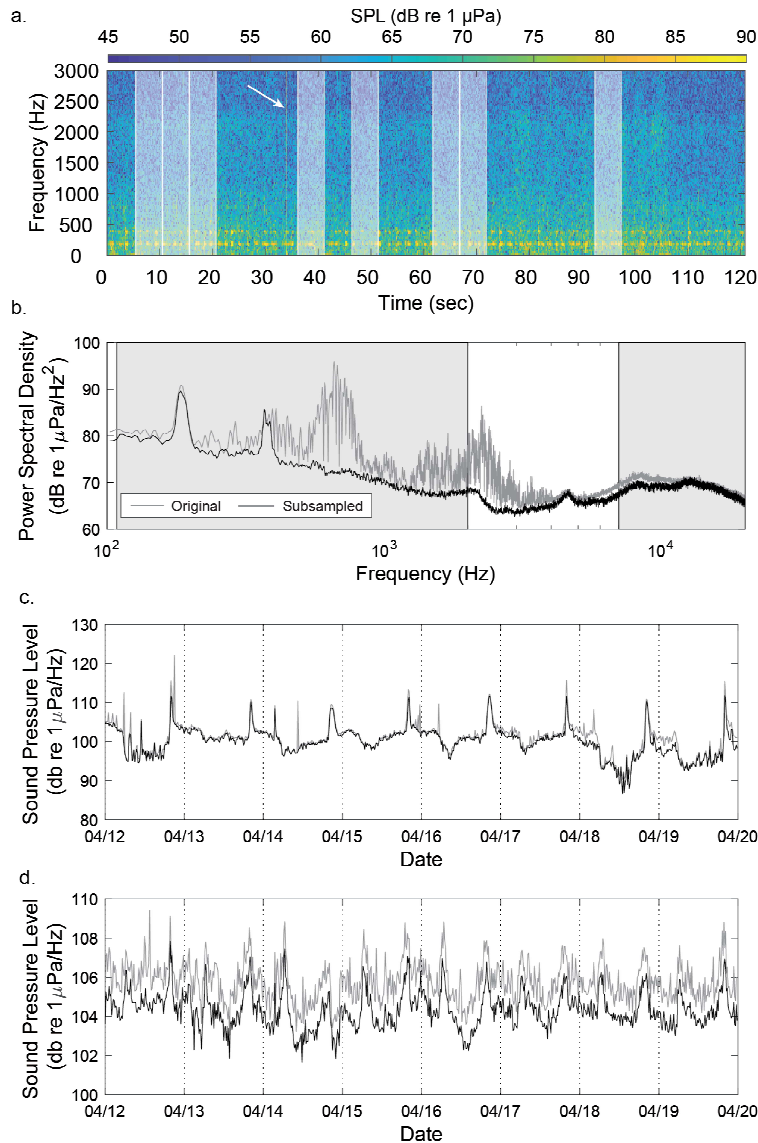|	**Nov 2015**	**Jan 2016**	**Apr 2016**	**Jun 2016**	**Aug 2016**
210 Rock	11/03 - 11/09	01/15; 01/18-01/22	04/12 - 04/19	06/10 - 06/16	08/17 - 08/22
West Rock	11/03 - 11/09	01/15; 01/18-01/22	04/12 - 04/19	06/10 - 06/16	08/17 - 08/22
Spar	11/03 - 11/09	01/15; 01/18-01/22	04/12 - 04/19	06/10 - 06/16	08/17 - 08/22
Aeolus	--	--	04/12 - 04/19	06/10 - 06/16	08/17 - 08/22

Figure A2. 1 Demonstration of the effect of a "fish bump" on the average power spectral density of a two-minute audio file and the effectiveness of the subsampling methodology to preserve biological signals and temporal patterns. (a) Spectrogram of a representative file recorded on 210 Rock in April 2016. The arrow points to an impulsive signal likely the result of an animal collision with the hydrophone. The shaded boxes indicate the eight quietest, five-second subsamples extracted to remove the effect of the fish bump. (b) Plot of power spectral density demonstrating that the subsampling methodology preserves the toadfish peaks while removing the noise due to the fish bump. The gray shaded boxes indicate the frequencies summarized in each frequency band (c) Time series of low-frequency SPL (0.1 – 2 kHz) for the original (gray) and subsampled (black) data. Spikes in the original data that are removed via subsampling are a result of fish bumps or boat noise. The subsampling methodology preserves the diurnal pattern in SPL while removing variability due to non-biological sounds that complicate ecological interpretation. (d) Time series of high frequency SPL (7 – 20 kHz) for the original (gray) and subsampled (black) data. The subsampling reduces the SPL of each file by an average of 1.5 dB but preserves the diurnal pattern while removing the spikes due to fish bumps.